

# LIBRARY Michigan State University

This is to certify that the

dissertation entitled

FUNDAMENTAL STUDIES OF THREE-COMPONENT RADICAL PHOTOINITIATORS

presented by

Kathryn Sirovatka Padon

has been accepted towards fulfillment of the requirements for

Ph. D. degree in \_\_\_\_\_\_\_\_ Engineering

Major professor

Date 4/20/00

### PLACE IN RETURN BOX to remove this checkout from your record. TO AVOID FINES return on or before date due. MAY BE RECALLED with earlier due date if requested.

DATE DUE	DATE DUE	DATE DUE
	<u></u>	

11/00 c/CIRC/DateDue.p65-p.14

## FUNDAMENTAL STUDIES OF THREE-COMPONENT RADICAL PHOTOINITIATORS

Ву

Kathryn Sirovatka Padon

#### **A DISSERTATION**

Submitted to
Michigan State University
in partial fulfillment of the requirements
for the degree of

**DOCTOR OF PHILOSOPHY** 

Department of Chemical Engineering

2000

#### **ABSTRACT**

### FUNDAMENTAL STUDIES OF THREE-COMPONENT RADICAL PHOTOINITIATORS

By

#### Kathryn Sirovatka Padon

Three-component systems, which contain a light-absorbing species (typically a dye), an electron donor (typically an amine), and a third component (usually an iodonium salt), have emerged as efficient visible-light sensitive photoinitiators. However, these systems are not well understood and a number of distinct mechanisms have been reported in the literature. In this work, photo-differential scanning calorimetry and *in situ*, time-resolved, laser-induced, steady-state fluorescence spectroscopy have been used to study the initiation mechanism of several three-component systems.

Most mechanistic studies were carried out on the model system methylene blue, N-methyldiethanolamine (MDEA) and diphenyliodonium chloride (DPI). This system is useful because the cationic nature of the methylene blue dye precludes direct reaction between the dye and the iodonium salt. Kinetic studies based upon photo-differential scanning calorimetry reveal a significant increase in polymerization rate with increasing concentration of either the amine or the iodonium salt. However, laser-induced fluorescence experiments show that while increasing the amine concentration dramatically increases the rate of dye fluorescence decay, increasing the DPI concentration actually slows consumption of the dye. We concluded that the primary photochemical reaction involves electron transfer from the amine to the dye. We suggest

that the iodonium salt reacts with the resulting dye-based radical (which is active only for termination) to regenerate the original dye and simultaneously produce a phenyl radical (active in initiation) derived from the diphenyliodonium salt.

When present, oxygen quenches the triplet state of the dye, leading to retardation of the reaction. Fluorescence monitoring was used to observe the methylene blue concentration in situ in a sealed reactor as the dye is consumed via photoreaction. In the sealed reactor, we observed a retardation period (attributed to the presence of oxygen) followed by rapid exponential decay of the methylene blue fluorescence after the oxygen was depleted. Based on the impact of the amine and iodonium concentrations on the fluorescence intensity and the duration of the retardation period, our proposed mechanism includes an oxygen-scavenging pathway in which the tertiary amine radicals formed in the primary photochemical process consume the oxygen via a cyclic reaction mechanism.

The dyes Eosin Y and Eosin Y, spirit soluble were chosen as model anionic and neutral dyes, respectively. In contrast to the cationic methylene blue dye, the eosin dyes are able to react directly with both the amine and the iodonium components. In fact, electron transfer from eosin to iodonium salt is several times faster than the eosin/MDEA interaction. In spite of this, photo-DSC indicates that the eosin/DPI interaction does not produce active radicals as efficiently as does the eosin/MDEA interaction.

The eosin systems do not show evidence of the iodonium-mediated regeneration of amine-bleached dye observed in the methylene blue system. However, evidence was observed for the reverse mechanism: amine-mediated regeneration of iodonium-bleached dye. As with methylene blue, the effect is twofold: an active amine radical replaces the presumably less active dye-based radical and the original eosin dye is regenerated.

#### **ACKNOWLEDGEMENTS**

Preparation of an extensive work such as a dissertation is never purely an individual effort. As such, I would like to acknowledge those who have made contributions to this work.

First and foremost is my advisor, Dr. Alec Scranton. His guidance in all steps of this research work, from concept to final written form, is gratefully acknowledged. I also appreciate the contributions of Dr. Tom Carter and Dr. Ruiping Huang, who provided invaluable technical assistance with the laser fluorescence bleaching experiments. I am also grateful to Joe Oxman and other members of the IUCRC on fundamentals and applications of photopolymerizations, who offered many useful suggestions and perhaps more importantly, through their interest, affirmed the usefulness of my work. An enormous thank you is due to Joe Oxman and Robert Fitzgerald of 3M, who, when the microporous polyethylene film used in the thin film laser experiments was discontinued, very generously located and sent me an ample supply. I also wish to thank Drs. Greg Baker, Martin Hawley, and Robert Ofoli for their service on my graduate committee. Finally, the contributions of my fellow lab group members (both past and present) cannot be underestimated: Kiran Baikerikar, Bernhard Drescher, Julie Jessop, Arvind Mathur, Vijay Narayanan, and Khanh Nguyen.

There are many others whose contributions were non-scientific but no less vital.

Chief among these is my husband Andy, whose unwavering support helped me through
many a tight spot. His seemingly inexhaustible tolerance for just one more trip to the

quilt store didn't hurt either! My parents, Jim and Marilyn Sirovatka, deserve several rounds of applause for their continued encouragement and love. It is a credit to them that I never thought being a girl who liked science and math was a weird thing. On the same note, thanks to all those teachers and professors who have shaped my life, especially Stan Czaplak, who still thinks I'm going to win a Nobel prize some day, and William Savage, in whose eighth grade class I discovered (to my shock and delight) that I was actually quite good at math and science.

#### **TABLE OF CONTENTS**

LI	ST O	F TABLES	ix
LI	ST O	F FIGURES	x
1.		RODUCTION TO THREE-COMPONENT SYSTEMS	
		Introduction	
	1.2.	UV Sensitive Free Radical Photoinitiators	
		1.2.1. Initiation via Photoscission	
		1.2.2. Bimolecular Initiation Processes	
		1.2.2.1. Hydrogen Abstraction	
		1.2.2.2. Electron Transfer	
		Motivation for Visible Light Initiation	
	1.4.	<b>3</b> · · · · · <b>3</b> · · · · · · · · · · · · · · · · · · ·	
		1.4.1. Cleavable and Bimolecular Systems	
		1.4.2. Three-Component Systems	
		1.4.2.1. Advantages of Three-Component Systems	
		1.4.2.2. Dyes for Three-Component Initiators	11
		1.4.2.3. Electron Donors for Three-Component Initiators	
		1.4.2.4. Compounds Used for the Third Component	
	1.5.	Mechanism of Three-Component Initiators	
		1.5.1. Parallel Reaction Hypothesis	
		1.5.2. Serial Reaction Hypothesis I	
		1.5.3. Serial-Parallel Reaction Hypothesis	21
		1.5.4. Serial Reaction Hypothesis II and Parallel Reaction Hypothesis II	23
		1.5.5. Cationic Polymerization	
	1.6.	, ,	
	1.7.	References	32
2	ORI	ECTIVES AND TECHNIQUES	36
	2.1.		36
	2.2.	· ·	
	2.2.	2.2.1. Differential Scanning Calorimetry	
		2.2.2. Steady State Fluorescence Monitoring	
2	A 10	IECHANISTIC INVESTIGATION OF THE THREE-COMPONEN	T
<b>J.</b>		DICAL PHOTOINITIATOR SYSTEM METHYLENE BLUE,	
	MET	THYLDIETHANOLAMINE, AND DIPHENYLIODONIU	M
		ORIDE	40
	3.1.	Introduction and Motivation	40
	3.2.	Three-Component Visible Light Photoinitiators	
		3.2.1. Reaction Mechanism	42
		3.2.2. System and Rationale.	
	3.3.	Experimental	47

		3.3.1. Materials.	47
		3.3.2. Photo-differential scanning calorimetry	47
		3.3.3. Time-resolved steady state fluorescence	
	3.4.	Results and Discussion	
		3.4.1. Photo-DSC	51
		3.4.2. Photobleaching Studies	53
		3.4.3. Discussion of Reaction Mechanism.	60
		3.4.3.1. Primary Photochemical Reaction	62
		3.4.3.2. Role of the Iodonium Salt	
		3.4.3.3. Influence of Iodonium Salt on the Termination Step	67
	3.5.	•	
	3.6.	References	72
4.	PHC	E EFFECT OF OXYGEN ON THE THREE-COMPONENT RADICAL DTOINITIATOR SYSTEM METHYLENE BLUE, N-METHYL THANOLAMINE, AND DIPHENYLIODONIUM CHLORIDE	<b>_</b>
		Introduction and Motivation	
	7.1.	4.1.1. Reaction Mechanism	
		4.1.2. Effect of Oxygen on the initiation reaction	
	42	Experimental Experimental	
	4.3.	•	
	7.5.	4.3.1. Thin Film Experiments	
		4.3.2. Capillary tube experiments	
	4.4.		
		References and Notes	
	٦.٥.	References and 140tes	, 1 00
5.	FUN	DAMENTAL STUDIES OF THREE-COMPONENT PHOTO	)-
•		TIATOR SYSTEMS CONTAINING EOSIN DYES	
		Introduction and Motivation	
	5.2.		
		5.2.1. Materials	
		5.2.2. Photo-Differential Scanning Calorimetry	
		5.2.3. Time-Resolved Steady-State Fluoresence Monitrring	
	5.3.	Results and Discussion	108
	0.5.	5.3.1. Photo-Differential Scanning Calorimetry	
		5.3.2. Time-Resolved Steady-State Fluorescence Monitoring	
		5.3.2.1. Mechanisms for Direct Reaction	
		5.3.2.2. Effect of Iodonium Concentration	
		5.3.2.3. Effect of Amine Concentration	
		5.3.2.4. Behavior of Eosin Y salt	
	5.4.	Summary and Conclusions	
	5.5.		136
	٥.٥.	1101V1V11V0 W1W 11V10U	
5.	CON	ICLUSIONS	.137
- •		Methylene Blue	
		Fosin Dyes	

7.	REC	COMMENDATIONS FOR FUTURE WORK	.142
	7.1.	Identification of the Active Radical Species	.142
		7.1.1. Electron Spin Resonance	
		7.1.2. End Group Analysis	
		7.1.2.1. Matrix-Assisted Laser Desorption Ionization Mass	
		Spectrometry	.143
		7.1.2.2. Nuclear Magnetic Resonance	.144
	7.2.	<del>_</del>	
	7.3.	Kinetic Studies	.146
	7.4.	Biological Applications Of Three-Component Systems	
	7.5.	• •	
		7.5.1. Cationic photoinitiation	
		7.5.2. Combination of two dyes plus amine	
	7.6.	References	
ΑF		DIX	
	<b>A</b> .1.	Concentration Effects of Methylene blue	.153
		A.1.1. Dimerization	.153
		A.1.2. Polymerization inhibitor	.153
		A.1.3. Photobleaching	.154
	A.2.	Ground State Complexes	.160
		A.2.1. Literature	.160
		A.2.2. Looking for Complexes	.161
	A.3.	Three-Component Systems Containing Camphorquinone	.161
		A.3.1. Motivation	
		A.3.2. DSC results.	
		A.3.3. Photobleaching	
	Δ Δ		

#### LIST OF TALBES

CHAPTER	
Table 1.1	Photoinitiators Used in Three-Component Systems
Table 1.2	Electron Donors Used in Three-Component Systems
Table 1.3	Third Components Used in Three-Component Systems
Table 1.4	Summary of Proposed Three-Component Mechanisms31
CHAPTER 5	
Table 5.1	Time to reach exotherm peak for eosin initiator systems
Table 5.2	Average photobleaching constants for component combinations 112

#### **LIST OF FIGURES**

#### **CHAPTER 1**

Figure 1.1	$\alpha$ -Photoscission process. Excitation light of the proper wavelength raises the photoinitiator to an excited state. After intersystem crossing to the triplet state, Norrish I cleavage occurs to produce an active benzoyl fragment and a residual fragment, which may or may not be active.
Figure 1.2	Gamma-cleavable photoinitiator. The benzoyl oxime ester family can undergo both alpha cleavage, as illustrated in Figure 1.1, and gamma cleavage, as illustrated here
Figure 1.3	Examples of beta-cleavable photoinitiators
Figure 1.4	Bimolecular initiation reactions: (A): Hydrogen abstraction reaction. The excited triplet state photoinitiator abstracts a hydrogen atom from a hydrogen donor DH to form an initiating donor radical and a ketyl radical. (B): Electron transfer reaction. The excited triplet state photoinitiator forms an exciplex with an electron donor (an amine is illustrated) and an electron is transferred. Subsequent proton transfer balances the charges and results in initiating amine radical and a ketyl radical.
Figure 1.5	Interaction of ketocoumarin dye and iodonium salt. Excited triplet ketocoumarin, 3KC, interacts with iodonium cation to produce the ketocoumarin cation-radical and an iodonium radical. The iodonium radical decomposes into neutral phenyl iodide and a phenyl radical, which may initiate polymerization.
Figure 1.6	Interaction of ketyl radical derived from ketocoumarin with iodonium salt. After excited ketocoumarin dye KC reacts with an electron donor such as an amine, a ketyl radical (KC-H•) is formed. (See Figure 1.4b). This radical is theorized to be oxidized by the iodonium cation, forming phenyl iodide, a phenyl radical, a proton, and regenerating the original dye
CHAPTER 3	
Figure 3.1	Three-component initiation system used

Figure 3.2	Normalized absorbance spectrum of the three-component system. All components were dissolved in methanol. Spectra were normalized to a peak absorbance of 1 for ease of comparison
Figure 3.3	Thin film fluorescence monitoring apparatus. The laser beam illuminates the thin film from below. The fluorescence is collected above the sample and routed to the spectrometer. A nitrogen purge port allows control of the atmosphere, while a recirculating water bath moderates the temperature.
Figure 3.4	Effect of each component on photopolymerization rate as measured by DSC. Each component plays an important role in the photopolymerization reaction. [MB] = $0.00011$ M, [MDEA] = $0.013$ M, [DPI] = $0.001$ M, all in neat HEMA. $I_a = 4$ mW/cm², $T = 50$ °C. Each curve is obtained by averaging three independent experiments. The initial overshoot in reaction rate observed for the two fastest reactions is believed to be an instrumental artifact arising from the relatively sluggish response time (~ 3 seconds) of the DSC technique 52
Figure 3.5	Effect of MDEA concentration on photopolymerization rate as measured by DSC. The photopolymerization rate increases dramatically as the amine concentration is increased. [DPI] = $0.001$ M, [MB] = $0.00011$ M, all in neat HEMA. $I_a = 4$ mW/cm <sup>2</sup> , $T = 50$ °C 54
Figure 3.6	Effect of DPI concentration on photopolymerization rate as measured by DSC. The rate of photopolymerization rises dramatically as the DPI concentration is increased. MDEA = $0.013$ M, MB = $0.00011$ M, $I_a = 4$ mW/cm <sup>2</sup> , $T = 50$ °C.
Figure 3.7	Methylene blue fluorescence intensity as a function of illumination time. [MB] = 0.00011 M, [MDEA] = 0.012 M, [DPI] = 0.0010 M. I <sub>a</sub> at 647.1 nm = 40 mW/cm <sup>2</sup> , T = 25°C. (A). The steady state dye fluorescence is monitored by acquiring a fluorescence spectrum every 400 msec. (B). The three-dimensional plot is sliced parallel to the time axis to yield a single fluorescence vs. time curve. The fit to an exponential decay is illustrated. In the experiments reported here, the maximum fluorescence was observed at 724 nm. The fluorescence peak of MB occurs at ~687 nm, but this wavelength is attenuated by the subtractive-dispersive filter stage of the spectrometer
Figure 3.8	Decay of methylene blue steady-state fluorescence. Methylene blue undergoes slow decay upon illumination, both alone (MB) and in the presence of diphenyliodonium chloride (MB + DPI). The addition of N-methyldiethanolamine (MDEA) to the system causes rapid consumption of methylene blue. [MB] = 0.00011 M, [MDEA] = 0.013 M, [DPI] = 0.0010 M. Curves shown are the average of three trials. I <sub>a</sub> at 647.1 nm = 40 mW/cm <sup>2</sup> , T=25°C

Figure 3.9	Effect of MDEA concentration on characteristic decay time. Increasing amine concentration produces a very dramatic decline in the characteristic exponential decay constant associated with the fluorescence bleaching. Data shown represent the average of three trials. The error bars represent one standard deviation. [MB] = 0.00011 M, [DPI] = 0.001 M. I <sub>a</sub> at 647.1 nm = 40 mW/cm <sup>2</sup> , T=25°C 61
Figure 3.10	Primary photoreaction occurs between excited methylene blue and amine. Electron transfer from amine to dye is immediately followed by proton transfer from amine to chloride ion, resulting in a neutral, bleached MB radical, an MDEA radical, and HCl
Figure 3.11	Effect of MDEA concentration on predicted long time fluorescence. The parameter y0 in the exponential fit of the fluorescence decay reflects the predicted asymptotic or long time value of the fluorescence. As the MDEA concentration is increased, this parameter decreases due to consumption of the dye via electron transfer reaction with MDEA. Data shown represent the average of three trials. The error bars represent one standard deviation. [MB] = 0.00011 M, [DPI] = 0.001 M. I <sub>a</sub> at 647.1 nm = 40 mW/cm <sup>2</sup> , T=25°C.
Figure 3.12	Effect of DPI concentration on $t_1$ , the characteristic decay time for methylene blue fluorescence. Increasing DPI concentration produces a slight but clear increase in the characteristic decay time, indicating a slower rate of decay. Data shown represent the average of three trials. The error bars represent one standard deviation. [MDEA] = 0.013 M, [MB] = 0.00011 M. $I_a$ at 647.1 nm = 40 mW/cm <sup>2</sup> , T=25°C65
Figure 3.13	Mechanistic Role of Iodonium Salt. The iodonium salt abstracts an electron from the bleached methylene blue neutral radical. The resulting methylene blue cation abstracts the chloride counterion to regenerate the original dye. The iodonium radical fragments to produce an active, initiating phenyl radical along with a phenyl iodide molecule.
Figure 3.14	Effect of DPI concentration on predicted long time fluorescence. The parameter y0 in the exponential fit of the fluorescence decay reflects the predicted asymptotic or long time value of the fluorescence. As the DPI concentration is increased, this parameter rises due to regeneration of the MB dye. Data shown represent the average of three trials. The error bars represent one standard deviation. [MDEA] = 0.013 M, [MB] = 0.00011 M. I <sub>a</sub> at 647.1 nm = 40 mW/cm <sup>2</sup> , T=25°C.
Figure 3.15	Dark polymerization exotherms for various DPI concentrations. Increasing DPI slows termination of the polymerization reaction. [MB] = 0.00010 M, [MDEA] = 0.013 M in EGDMA/HEMA 8:1 mass

	ratio. T = 25°C, I <sub>a</sub> = 0.3 mW/cm <sup>2</sup> . Each curve is the average of three replicate trials
Figure 3.16	Reaction mechanism for the three-component system MB/MDEA/DPI71
CHAPTER 4	
Figure 4.1	Reaction mechanism for the system methylene blue (MB), N-methyldiethanolamine (MDEA), and diphenyliodonium chloride (DPI)
Figure 4.2	Steady state fluorescence monitoring. (A). The steady state dye fluorescence is monitored by taking a fluorescence spectrum approximately every 700 msec. (B). The three-dimensional plot is sliced parallel to the time axis to yield a single fluorescence vs. time curve. The fit to an exponential decay is illustrated. For the representative data shown here, the concentrations of methylene blue, N-methyldiethanolamine, and diphenyliodonium chloride were 0.00011 M, 0.013 M, and 0.0010 M, respectively. The reaction temperature was 50°C and the capillary cell geometry was used
Figure 4.3	Characteristic decay constant of methylene blue fluorescence as a function of the percentage air. (The balance of the atmosphere is nitrogen.) The photobleaching rate is reduced (the decay time is increased) as the oxygen concentration is increased, suggesting a significant role for the methylene blue triplet state in the photobleaching reaction. Thin film geometry, [MB] = 0.00011 M, [MDEA] = 0.012 M, [DPI] = 0.0010 M. I <sub>a</sub> at 647.1 nm = 40 mW/cm <sup>2</sup> , T = 25°C. Error bars represent one standard deviation
Figure 4.4	Effect of each component on decay of methylene blue steady state fluorescence in 20% air atmosphere. Thin film geometry, [MB] = 0.00011 M, [MDEA] = 0.012 M, [DPI] = 0.0010 M. I <sub>a</sub> at 647.1 nm = 40 mW/cm <sup>2</sup> , T = 25°C. Each curve is the average of multiple trials 84
Figure 4.5	Decay of methylene blue fluorescence in the presence of amine and iodonium salt. Methylene blue alone (MB), and methylene blue with diphenyliodonium chloride (DPI) do not show any decay in fluorescence over 250 seconds. The addition of N-methyldiethanolamine (MDEA) to the system produces rapid consumption of methylene blue. Capillary geometry, methylene blue 0.00011 M, N-methyldiethanolamine 0.013 M, diphenyliodonium chloride 0.0010 M, 50°C
Figure 4.6	Effect of amine concentration on rate of methylene blue

	dramatic increase in the rate of photobleaching. Capillary geometry, [DPI] = 0.001 M, [MB] = 0.00011 M, 50°C
Figiure 4.7	Effect of MDEA concentration on characteristic decay time. Increasing amine concentration produces a very dramatic decline in the exponential decay constant associated with the fluorescence bleaching. Capillary geometry, [MB] = 0.00011 M, [DPI] = 0.001 M 89
Figure 4.8	Effect of DPI concentration on $t_1$ , the characteristic decay time for methylene blue fluorescence. Increasing DPI concentration produces a clear decrease in the characteristic decay time, indicating a faster rate of decay. The error bars shown represent one standard deviation. Capillary geometry, [MDEA] = 0.013 M, [MB] = 0.00011 M91
Figure 4.9	Effect of DPI concentration on $x_0$ , a measure of the latent time before fluorescence decay. Increasing amounts of DPI cause the decay to begin slightly earlier. The error bars shown represent one standard deviation. The overall trend is not significantly affected by temperature. Capillary geometry, [MDEA] = 0.013 M, [MB] = 0.00011 M.
Figure 4.10	Effect of DPI concentration on rate of photobleaching. The arrow indicates the direction of generally increasing DPI concentration. Capillary geometry, 50°C, [MDEA] = 0.013 M, [MB] = 0.00011 M93
Figure 4.11	Proposed oxygen-scavenging mechanism. The tertiary amine radical formed from reaction with the methylene blue initiates a cyclic electron transfer/proton transfer reaction which consumes molecular oxygen.
Figure 4.12	Effect of MDEA concentration on retardation time. Decreasing the MDEA concentration leads to an enormous increase in the retardation time associated with the MB photobleaching reaction, as measured by the timeshift factor $x_0$ . Capillary geometry, [MB] = 0.00011 M, [DPI] = 0.001 M.
Figure 4.13	Effect of oxygen on the proposed reaction mechanism for the three-component system MB/MDEA/DPI
CHAPTER 5	<b>;</b>
Figure 5.1	Eosin dyes
Figure 5.2	Electron donor and third component of photoinitiation system 103
Figure 5.3	Absorbance spectrum of Eosin Y. 1 × 10 <sup>-5</sup> M Eosin Y in HEMA 105

Figure 5.4	Decay of Eosin Y, spirit soluble steady-state fluorescence. [EYss] = 0.0001 M, [MDEA] = 0.012 M, [DPI] = 0.0010 M, all in HEMA, T = 25°C, I <sub>a</sub> = 50 mW/cm <sup>2</sup> . Long observation time. Each curve represents the average of three trials
Figure 5.5	Decay of Eosin Y, spirit soluble steady-state fluorescence. [EYss] = 0.0001 M, [MDEA] = 0.012 M, [DPI] = 0.0010 M, all in HEMA, T = 25°C, I <sub>a</sub> = 50 mW/cm <sup>2</sup> . Short observation time. Each curve represents the average of three trials.
Figure 5.6	Proposed direct reaction between Eosin Y, spirit soluble and MDEA 117
Figure 5.7	Formation of leuco dye
Figure 5.8	Proposed direct reaction between Eosin Y, spirit soluble and diphenyliodonium chloride
Figure 5.9	Effect of DPI concentration on Eosin Y, spirit soluble photobleaching. The rate of photobleaching increases as DPI concentration is increased. [EYss] = 0.0001 M, [MDEA] = 0.012 M, all in HEMA, T = 25°C, I <sub>a</sub> = 50 mW/cm <sup>2</sup> . Short observation time
Figure 5.10	Effect of DPI concentration on Eosin Y, spirit soluble photobleaching. At high DPI concentrations, the photobleaching profile exhibits the characteristics of the EYss/DPI reaction, whereas at low DPI concentrations, the profile has the characteristics of the EYss/MDEA reaction. Both photobleaching mechanisms are apparent at intermediate DPI concentrations. [EYss] = 0.0001 M, [MDEA] = 0.012 M, all in HEMA, 25°C, I <sub>a</sub> = 50 mW/cm <sup>2</sup> . Long observation time
Figure 5.11	Long time constant (EYss/MDEA reaction) versus DPI concentration. The time constant for the EYss/MDEA reaction is not affected by the DPI concentration, indicating that iodonium-mediated dye regeneration does not occur in this system. [EYss] = 0.0001 M, [MDEA] = 0.012 M, all in HEMA, 25°C, I <sub>a</sub> = 50 mW/cm <sup>2</sup> . Long observation time. Error bars represent one standard deviation
Figure 5.12	Effect of MDEA on Eosin Y, spirit soluble photobleaching. [EYss] = 0.0001 M, [DPI] = 0.0010 M, all in HEMA, 25°C, I <sub>a</sub> = 50 mW/cm <sup>2</sup> . Each curve represents the average of three trials
Figure 5.13	Effect of MDEA on photobleaching of Eosin Y, spirit soluble. Increasing MDEA concentration has a retarding effect on the rapid EYss/DPI reaction. [EYss] = 0.0001 M, [DPI] = 0.0010 M, all in HEMA, 25°C, I <sub>a</sub> = 50 mW/cm <sup>2</sup> . Short observation time. Each curve represents the average of three trials

Figure 5.14	Proposed amine-mediated dye regeneration scheme
Figure 5.15	Effect of MDEA concentration on Eosin Y photobleaching. [EY] = 0.0001 M, [DPI] = 0.0013 M, all in HEMA, 25°C, I <sub>a</sub> = 50 mW/cm <sup>2</sup> . Each curve represents the average of three trials
Figure 5.16	Comparison of Eosin Y and Eosin Y, spirit soluble photobleaching by DPI. [EY] = [EYss] = 0.0010 M, [DPI] = 0.001 M, all in HEMA, 25°C, I <sub>a</sub> = 50 mW/cm <sup>2</sup> . No MDEA is present. Short observation time. Each curve represents the average of three trials
Figure 5.17	Effect of MDEA concentration on Eosin Y photobleaching. MDEA does not regenerate EY as efficiently as EYss. [EY] = 0.0001 M, [DPI] = 0.0013 M, all in HEMA, 25°C, I <sub>a</sub> = 50 mW/cm <sup>2</sup> . Short observation time. Each curve represents the average of three trials 133
Figure 5.18	Summary of eosin reactions
CHAPTER 6	
Figure 6.1 Figure 6.2	Proposed reaction mechanism for the three-component system MB/MDEA/DPI. The amine and phenyl radicals are active for initiation; the MB radicals is a terminator
APPENDIX	
Figure A.1	Molar absorptivity of methylene blue monomer and dimer peaks as a function of concentration
Figure A.2	Polymerization exotherm for sample with high methylene blue concentration. [MB] = 0.0010 M, [MDEA] = 0.0018 M, [DPI] = 0.0010 M. T = 35 °C
Figure A.3	Photobleaching of methylene blue at high dye concentration. [MB] = $0.001$ M, [MDEA] = $0.0018$ M, [DPI] = $0.001$ M, $I_a = \sim 5.3$ W/cm <sup>2</sup> , T= $25$ °C, capillary geometry as described in Chapter 4
Figure A.4	Effect of amine concentration on pre-bleaching fluorescence peak.  [MB] = 0.001 M, [DPI] = 0.001 M, I <sub>a</sub> = ~5.3 W/cm <sup>2</sup> , T= 25 °C, capillary geometry as described in Chapter 4
Figure A.5	Camphorquinone
Figure A.6	Absorbance spectrum for camphorquinone. 0.051 wt.% in methanol 163
Figure A.7	Polymerization exotherm for camphorquinone/N-methyldiethanol-amine/diphenyliodonium chloride system. [CQ] = 0.0012 M, [MDEA] = 0.013 M, [DPI] = 0.001 M, T = 50 °C, I <sub>a</sub> ~ 27 mW/cm <sup>2</sup>

Figure A.8 Camphorquinone fluorescence bleaching. [CQ] = 0.0012 M, [MDEA] = 0.013 M, [DPI] = 0.001 M, T = 25 °C,  $I_a \sim 800 \text{ mW/cm}^2$ ......166

#### CHAPTER 1

#### INTRODUCTION TO THREE-COMPONENT SYSTEMS

#### 1.1. Introduction

Photopolymerization has gained prominence as an inexpensive, efficient, and environmentally friendly means to produce polymeric films and even thick parts. Photopolymers are used to produce a variety of products with greatly reduced production and capital costs as compared to traditional thermal polymerization.

The continuing growth of the photocuring market can be attributed to the significant advantages offered by photopolymerization compared to traditional thermal polymerization methods. In photocuring, light rather than heat is used to produce active centers which initiate a chain polymerization. The use of light affords great temporal and spatial control over the polymerization, since the light can be directed to a location of interest and shuttered at will. For industrial processes, the ease of control provides "cure on demand" which eliminates problems of premature reaction and waste which can occur with thermally initiated reactions. Since photocure is typically rapid, even at room temperature, it may be used with heat-sensitive substrates without risk of thermal deformation.<sup>1</sup>

Photopolymerizations also offer tremendous environmental advantages. For instance, photocurable compositions are typically solvent free, so they do not contribute to emissions of volatile organic compounds. In addition, photopolymerizations consume only a fraction of the energy typically required by thermally initiated polymerizations,

resulting in both economic and environmental benefits.

Radiation curing first gained prominence as an inexpensive, non-polluting means for producing coatings, varnishes, and paints for diverse substrates including wood, plastic, and metal. Recently, photocuring has become popular for imaging applications. For example, photocuring is the method of choice for production of printing plates and is used extensively in the microelectronics and optics industries. Recent research has broadened the applicability of photocuring from the usual thin film applications to thick section cure, opening a range of previously untouched applications.

This chapter briefly discusses various radical photoinitiators and then focuses on recent advances in the understanding of a relatively new class of radical photoinitiators: three-component photoinitiator systems sensitive to visible light. Although these initiator systems have appeared extensively in the patent literature in the past ten years, comparatively little research on these systems has been reported in the scientific literature. For this reason, references to the patent literature will be only representative, while the review of the scientific literature will be more exhaustive.

#### 1.2. UV Sensitive Free Radical Photoinitiators

Photopolymerization is very versatile since essentially any monomer can be photopolymerized. Light has been used to initiate free radical, cationic, anionic, and charge transfer polymerizations. However, radically polymerizable monomers (primarily acrylates) have been used most extensively in photocuring schemes, primarily because of the wide availability of initiator systems and the ease with which acrylates can be

functionalized at the ester moiety.

Radical photoinitiation can proceed by one of two basic mechanisms. In both mechanisms, the photoinitiator molecule is raised to an excited electronic state by absorption of light. In the first mechanism, the excited state molecule undergoes homolytic cleavage to produce two radicals. The second mechanism is somewhat more complicated, since the excited state molecule undergoes a bimolecular reaction with a coinitiator molecule to produce radicals. Both mechanisms are discussed in further detail below.

#### 1.2.1. Initiation via Photoscission

The most common photoscission reaction is termed  $\alpha$ -cleavage or Norrish I photoscission. As illustrated in Figure 1.1, in this type of reaction, the photoinitiator is excited by absorption of ultraviolet light and rapid intersystem crossing to the triplet state. In the triplet state, the bond alpha to the carbonyl group is cleaved, producing an active benzoyl radical fragment and another fragment, which may or may not be active in the initiation reaction. The efficiency of the cleavage reaction is determined by the presence of heteroatoms. Carbon-sulfur bonds and carbon-phosphorus bonds such as those in benzoyl phosphine oxides are easily cleaved. In addition, the presence of oxygen or nitrogen on the alpha carbon tends to stabilize the transition state and promote cleavage.<sup>3</sup> Some common classes of  $\alpha$ -cleavable photoinitiators possessing this characteristic include benzoin ethers, dialkoxyacteophenones, hydroxy alkyl ketones, benzoyl oxime esters, amino ketones, and morpholino ketones. These molecules are all built on the benzoyl chromophore, which has an absorption in the UV region of the

spectrum (approximately 150 to 400 nm.)

Some  $\alpha$ -cleavable photoinitiators can also undergo gamma cleavage. In this process, the bond gamma to the carbonyl group is cleaved. One such class is the benzoyl oxime ester family, as illustrated in Figure 1.2.<sup>3</sup>

A third class of photoscission reaction is beta cleavage, which can occur on ketones possessing a sulfur atom, a sulfonyl or oxysulfonyl group<sup>1,3</sup> or a halogen atom<sup>1</sup> attached to the beta carbon. This type of cleavage is illustrated in Figure 1.3.

#### 1.2.2. Bimolecular Initiation Processes

A second means of photoinitiation is a bimolecular reaction involving either hydrogen abstraction or electron transfer. These systems require the presence of a coinitiator, which is typically a hydrogen donor such as an alcohol, a thiol, or tetrahydrofuran, or an electron donor such as an amine. The reactions are illustrated schematically in Figure 1.4.

#### 1.2.2.1. Hydrogen Abstraction

Generally, only the triplet state of the photoinitiator participates in the hydrogen abstraction reaction.<sup>3</sup> The photoinitiator removes a hydrogen atom from the donor, forming two radicals. In this reaction, the radical produced on the hydrogen donor is the initiating species, while the photoinitiator residue participates only in the termination process.<sup>1,4</sup> This reaction mechanism is not very common, but examples of photoinitiators which can react via this pathway include the benzophenone and thioxanthone families.

Figure 1.1:  $\alpha$ -Photoscission process. Excitation light of the proper wavelength raises the photoinitiator to an excited state. After intersystem crossing to the triplet state, Norrish I cleavage occurs to produce an active benzoyl fragment and a residual fragment, which may or may not be active.

Figure 1.2: Gamma-cleavable photoinitiator. The benzoyl oxime ester family can undergo both alpha cleavage, as illustrated in Figure 1.1, and gamma cleavage, as illustrated here.

Figure 1.3: Examples of beta-cleavable photoinitiators

#### 1.2.2.2. Electron Transfer

Electron transfer is a far more efficient pathway for bimolecular photoinitiation. In this type of reaction, the triplet state photoinitiator forms an exciplex with an electron donor, which is typically an amine. An electron is transferred from the amine to the photoinitiator, forming charged radicals. Subsequent proton transfer from the amine to the photoinitiator forms neutral amine and ketyl radicals. The amine radical is active towards initiation, while again the ketyl radical participates only in the termination reaction. The end result of the electron transfer reaction is the same as hydrogen abstraction, but the mechanism is distinctly different.

Some common photoinitiators<sup>1,3</sup> which react via the electron transfer mechanism include benzophenones, thioxanthones, benzil derivatives, ketocoumarins, xanthones, and camphorquinone. These photoinitiators have a broad range of absorption maxima, so the wavelength sensitivity of the initiating system can be adjusted somewhat by choice of photoinitiator.

Figure 1.4: Bimolecular initiation reactions: (A): Hydrogen abstraction reaction. The excited triplet state photoinitiator abstracts a hydrogen atom from a hydrogen donor DH to form an initiating donor radical and a ketyl radical. (B): Electron transfer reaction. The excited triplet state photoinitiator forms an exciplex with an electron donor (a) amine is illustrated) and an electron is transferred. Subsequent proton transfer balances the charges and results in initiating amine radical and a ketyl radical.

#### 1.3. Motivation for Visible Light Initiation

As previously mentioned, most cleavable radical photoinitiators are based on the benzoyl chromophore and therefore require ultraviolet light to produce radicals. However, lamps and lasers which emit ultraviolet radiation are significantly more expensive than the corresponding sources of visible light. Furthermore, white light is readily available from commercial sources and of course the sun. These sources provide far more photons in the visible range than the ultraviolet range. In addition, ultraviolet light is undesirable for many applications. For instance, in biological applications, visible light is preferable due to the damaging effects of UV radiation on living cells.

One application which has driven the development of visible light photoinitiators is the production of photopolymer plates, especially master printing plates.<sup>5-11</sup> Visible light photoinitiators are not suitable for microlithography for production of electronic devices since this application requires submicron feature sizes (and therefore is based upon deep UV light). However, visible initiators are ideal for printing plates and other larger-feature lithographic applications. Indeed, the ready availability and low cost of visible lasers and other light sources has made visible initiating systems very attractive for use in photopolymer plates.

Biological applications, such as dental composites and bone cements, have also motivated the development of visible light photoinitiators. As previously mentioned, visible light is required for *in situ* cure in biological systems due to the damaging effects of ultraviolet light on cells. For example, a camphorquinone / ethyl-4-N,N-methylaminobenzoate system, active at 470-490 nm, has been used in the development of a degradable

material for orthopedic implants.<sup>12</sup> Camphorquinone was also the basis for a new dental composite system which used N-phenylglycine and derivatives as the electron donor.<sup>13</sup>

While the above discussion is far from a comprehensive review of emerging applications for visible-light photoinitiators, the examples cited do make clear the importance of visible-light initiators and the consequent need for research in this area.

#### 1.4. Current Visible Light Initiators

#### 1.4.1. Cleavable and Bimolecular Systems

In the past, the need for visible light radical photoinitiators has been addressed primarily by using bimolecular initiator systems. As previously mentioned, electron transfer bimolecular initiators, which use a light absorbing photoinitiator and an amine to produce active radicals, can be tailored to a specific wavelength range by choice of the photoinitiator. Many dyes and other compounds absorbing in the visible range have been used as the photoinitiator in this type of system, including camphorquinone, thioxanthone derivatives, and ketocoumarin derivatives.<sup>1</sup> A large number of papers have been published on this topic and the mechanism is fairly well understood; for reviews, see references 1, 3, and 14-17. Other approaches to visible light photoinitiation involve ironarene complexes and titanocene derivatives.<sup>1,15</sup> Some new type I (cleavable) systems with absorption maxima beyond 300 nm have also been developed.<sup>15</sup>

#### 1.4.2. Three-Component Systems

In the last decade, three-component photoinitiation systems have emerged as an improvement over two-component electron transfer initiating systems. These systems consist of a light absorbing moiety which is typically a dye, an electron donor which is almost always an amine, and a third component which is usually an iodonium salt. These three-component systems have been consistently found to be faster and more efficient than their two-component counterparts. 8,18,19 Furthermore, the initiator sensitivity, as measured by the energy required to complete the cure of an arbitrary standard system, is significantly better for the three-component systems than for the corresponding two component systems. 9

#### 1.4.2.1. Advantages of Three-Component Systems

In addition to the advantages of enhanced cure rate and higher sensitivity mentioned above, three-component systems have some other significant features which make them quite interesting. For example, a single combination of electron donor and iodonium salt can be used with a variety of different dyes thereby providing tremendous flexibility in selection of the initiating wavelength. In addition, because the dyes in these systems typically undergo photobleaching during the reaction, of cure of relatively thick sections is possible. Finally, some evidence suggests that the same initiating systems may be effective for initiation of cationic polymerizations as well as radical polymerizations.

#### 1.4.2.2. Dyes for Three-Component Initiators

A variety of three-component systems have been reported in the literature to date. Because the choice of dye allows selection of the region of the spectrum to which the initiating system is sensitive, the greatest variation has been in the choice of dye used. Many of the same photoinitiators used for two component electron transfer initiation schemes may also be used in three-component initiation systems. A selection of dyes that have been used in three-component initiator systems is illustrated in Table 1.1. These compounds include ketones such as benzil, benzophenone, and camphorquinone, <sup>19,23-27</sup> xanthenes such as eosin, <sup>10,19,21,28,29</sup> thioxanthenes, <sup>8,10,11,26,30</sup> xanthones and thioxanthones, <sup>19,23,24,26,31,32</sup> coumarins and ketocoumarins, <sup>8,19,24,26,28,33</sup> thiazines, <sup>10,19-21</sup> and merocyanines. <sup>8,19,26</sup>

#### 1.4.2.3. Electron Donors for Three-Component Initiators

The second component in three-component initiators, as in their two-component counterparts, is an electron donor. A variety of donors that have been reported in the literature are illustrated in Table 1.2. As a general criterion for selection of an electron donor, Oxman *et al.*<sup>19</sup> report that the oxidation potential of the donor should lie between zero and 1.32 volts relative to a saturated calomel electrode.

In most three-component systems reported to date, the electron donor is a tertiary amine such as N-methyldiethanolamine<sup>9,23-25</sup> or triethylamine.<sup>18</sup> Because of the high toxicity of alkyl amines, aromatic amines such as N-phenylglycine<sup>8,9,13</sup> have also been used. Although amines are by far the most common electron donors for three-component initiators, a number of other compounds have also been reported, primarily in the patent

systems. <sup>19,20</sup> Other reported electron donors for three-component initiators include amides, <sup>19</sup> ethers, <sup>19</sup> ferrocene <sup>19</sup> and other metallocenes, <sup>6</sup> and ureas. <sup>10,19</sup> For the mechanistic studies reported below, this chapter will focus on amine electron donors.

#### 1.4.2.4. Compounds Used for the Third Component

The third component in these initiator systems is almost always an iodonium salt. Diphenyliodonium chloride (see Table 1.3) is by far the most common third component,  $^{8,9,11,18-20,24}$  but iodonium salts with other less nucleophilic counterions such as  $AsF_6^{-,19,28}$   $PF_6^{-,19,21}$   $SbF_6^{-,19,21}$   $BF_4^{-,19,30}$   $Br_7^{-,19}$   $\Gamma_7^{-,19}$   $C_6H_5SO_3^{-,19}$  and  $SbF_5OH_7^{-,19}$  have also been used. While the unsubstituted diphenyliodonium salt is the most common compound used for these initiators, substituted iodonium cations have also been used.  $^{21}$ 

The mechanistic studies reviewed here focus primarily on iodonium salts as the third component since they are by far the most common. Because the precise role of the third component is not well understood, it is difficult to develop a general criterion for its selection. However, in addition to the iodonium salts, a few other compounds have been reported in the literature. For example, researchers from France and Japan have replaced the iodonium salt with bromo-compounds<sup>11,23,25</sup> to obtain enhanced thermal stability. In addition, two recent studies use iron-arene complexes as the third component.<sup>34,35</sup> Examples of these compounds are illustrated in Table 1.3.

Table 1.1: Photoinitiators Used in Three-Component Systems

Photoinitiator	Structure	References
class		
Benzil (a ketone)		19, 23, 24, 25, 26, 27
Benzophenone (a ketone)	$R_1$ $C$	19, 23, 24, 25, 26, 27
Camphorquinone (a ketone)	H <sub>3</sub> C CH <sub>3</sub>	19, 23, 24, 25, 26, 27
Xanthene		10, 19, 21, 28, 29
Thioxanthene	S	8, 10, 11, 26, 30
Xanthone		19, 23, 24, 26, 31, 32
Thioxanthone	$R_1$ $R_2$	19, 23, 24, 26, 31, 32
Ketocoumarin	O O R	8, 19, 24, 26, 28, 33
Thiazine		10, 19, 20, 21

Table 1.1 (continued)

Photoinitiator class	Structure	References
Merocyanine	S CH-CH-CH-CH-CH-CH-CH-CH-CH-CH-CH-CH-CH-C	8, 19, 26

Table 1.2: Electron Donors Used in Three-Component Systems

Electron Donor	Structure	References
N- methyldiethanolamine	CH <sub>2</sub> CH <sub>2</sub> OH H <sub>3</sub> C-N CH <sub>2</sub> CH <sub>2</sub> OH	9, 23, 24, 25
N-phenylglycine	H., HO <sub>2</sub> CH <sub>2</sub> C	8, 9, 13
Sodium toluene sulfinate	H <sub>3</sub> C—SO <sub>2</sub>	19, 20
N,N-dimethylacetamide (an amide)	O CH₃ CH₃CN CH₃	19
4,4-dimethoxybiphenyl (an ether)	H <sub>3</sub> CO————————————————————————————————————	19
N,N-dimethylurea (a urea)	H <sub>3</sub> C O NCNH <sub>2</sub> H <sub>3</sub> C	10, 19
Ferrocene	F. C.	19

Table 1.3: Third Components Used in Three-Component Systems

Third Component	Structure	References
Diphenyliodonium chloride		8, 9, 11, 18, 19, 20, 24
2,2,2,- tribromoacetophenone (a bromo compound)	C-CBr <sub>3</sub>	11, 23, 25
Iron arene complex	Fe <sup>+</sup> PF <sub>6</sub> <sup>-</sup>	34, 34

## 1.5. Mechanism of Three-Component Initiators

Although many three-component systems have been identified, only a few research groups have attempted to elucidate the mechanism by which active centers are produced. The mechanisms which have been proposed can be loosely grouped into two general classes: 1) parallel reactions in which two component pairs react independently and 2) serial reactions in which two of the three components first react with one another and the third component then reacts with the products of the first reaction.

In all of the proposed mechanisms, the dye functions as the light absorber and therefore begins the photochemical reaction. (In one mechanism a charge transfer complex also absorbs visible light; this will be discussed below.) In the excited photophysical state, the dye participates in an electron transfer reaction in which it is either oxidized (by the iodonium salt) or reduced (by the electron donor).

The role of the electron donor component (an amine in the following discussion) is to reduce another component, which may subsequently accept a proton from the amine as well. This reaction always follows the light absorption step, either directly (if, for example the photoexcited dyes accepts an electron), or indirectly (if the amine reduces a previously oxidized dye radical).

The role of the third component (an iodonium salt in the following discussion) is always to accept an electron, although the postulated source of the electron varies among the proposed mechanisms.

The following discussion provides a review of five distinct mechanisms proposed to date for three-component initiator systems. Because these systems have emerged only

recently, they have received relatively little investigation, and there is currently no consensus on the mechanisms whereby they produce active centers. The fact that so many different mechanisms have been derived suggests that the mechanism may indeed vary depending on the precise choices of each of the three components, the monomer selected, and any solvent present.

#### 1.5.1. Parallel Reaction Hypothesis

In a relatively early study (1990), He and Wang used kinetic arguments to support a proposed "binary" mechanism in which the component pairs (dye/amine and amine/iodonium salt) react independently. This hypothesis was based upon their observations in an earlier paper, the in which a two component system containing diphenyliodonium chloride and triethylamine was observed to form a charge-transfer complex with an absorption peak centered around 500 nm. Illumination of this charge transfer peak was effective for initiating polymerization of methyl methacrylate. The authors proposed that the reaction proceeds by electron transfer from the amine to the iodonium salt within the excited complex, to form an amine-based cation-radical and a diphenyliodonium radical. The onium-based radical is believed to dissociate to form an active phenyl radical and a phenyl iodide molecule. The authors did not identify which of the two radical species initiates the polymerization.

In an effort to increase the sensitivity of the of the two component amine/iodonium system to ultraviolet radiation, the authors added benzophenone to the system.<sup>18</sup> They propose that the resulting three-component system reacts via two separate pathways: the amine is photo-oxidized by the onium salt via the charge transfer

complex studied in their earlier paper, and the amine is also photo-oxidized by benzophenone in the known bimolecular electron transfer initiation scheme.

The proposed reaction mechanism relies on formation of a charge transfer complex between the amine and the iodonium salt. For systems in which such a complex is not observed, the mechanism is not generally applicable. In the system they studied, He and Wang found that the charge-transfer complex requires polar solvents (they used CH<sub>3</sub>CN and water in a 14:1 ratio by volume) to promote its formation. For example, the intensity of the absorption band associated with the complex decreased as the methylmethacrylate monomer concentration was increased. In fact, the polymerization rate decreased when the methylmethacrylate concentration exceeded about four molar.

## 1.5.2. Serial Reaction Hypothesis I

In a later paper (1995), He, Li, Wang, and Wang studied the effect of triethylamine on the initiator eosin bis(diphenyliodonium) salt.<sup>37</sup> This novel photoinitiator included two diphenyliodonium cations with a doubly charged eosin dye anion as the counterion. Essentially, the authors concluded that the primary photoreaction occurred between the eosin dye and the iodonium cation. They suggested that the amine reduced the oxidized dye back to its original state.

In this study, the authors used a nonpolar solvent (1,4-dioxane); therefore, no iodonium-amine charge transfer complex was observed. However, the authors found that the amine did affect the absorption spectrum of the initiator. Although the absorption spectrum of eosin bis(diphenyliodonium) salt [Eo(IPh<sub>2</sub>)<sub>2</sub>] alone showed bands characteristic of contact ion pairs, after the amine was added, the spectrum showed a

band characteristic of solvent separated eosin/iodonium ion pairs. This result was attributed to insertion of the amine between the pairs of ions due to a weak interaction of the amine with the iodonium ion.

The authors arrived at their proposed reaction mechanism by first ruling out a parallel reaction mechanism in which the amine reduces the eosin and the iodonium oxidizes the eosin via intra-ion-pair electron transfer. This mechanism was ruled out based on the results of steady-state fluorescence quenching studies in which the diphenyliodonium chloride and triethylamine were used to quench sodium eosinate fluorescence. The quenching studies suggested that the overwhelming contribution to the initiation reaction is by the eosin-iodonium interaction, since its quenching constant is four times larger.

An enhancement in photopolymerization rate was nonetheless observed when triethylamine was added to the Eo(IPh<sub>2</sub>)<sub>2</sub> / methyl methacrylate system. Since the eosin-amine interaction is thought to be minimal, a different role for the amine is proposed. Based on the surprising observation that the eosin photobleaching rate decreases upon addition of amine (even though the polymerization rate increases), the authors propose the following serial mechanism: The eosin donates an electron to the iodonium via intra-ion-pair oxidative electron transfer. Then, the amine is thought to donate an electron to the resulting eosin radical to regenerate the original eosin ion while forming an amine radical. The end result is first, to increase the overall absorption of light due to eosin regeneration, and second, to produce amine-based radicals which are presumably more active than the eosin radicals.

Evidence cited for the proposed cyclic eosin regenerating scheme includes the

observation that the polymerization rate induced by this photoinitiator depends on  $Eo(IPh_2)_2$  in an unusual manner. The authors report  $R_p \propto [Eo(IPh_2)_2]^x$  where x increases with  $Eo(IPh_2)_2$  concentration (at constant amine concentration). This dependence of rate on a varying power of  $[Eo(IPh_2)_2]$  is attributed to the regeneration of the eosin, since, the authors reason, with an increase in  $[Eo(IPh_2)_2]$ , the electron transfer reaction of amine with eosin becomes more important.

The use of two initiator components as counterions for one another is a clever and interesting aspect of the paper. However, because of this novel aspect of the initiator system, the mechanistic studies may not generalize to other systems.

#### 1.5.3. Serial-Parallel Reaction Hypothesis

In another early study (1991), Harada and collaborators used electron spin resonance (ESR) to characterize the radical species produced by a three-component system consisting of a thioxanthene (TX) derivative as the dye, N-phenylglycine (NPG) as the amine, and diphenyliodonium tetrafluoroborate (DPI-BF<sub>4</sub>) as the onium salt.<sup>30</sup> They conclude that the excited thioxanthene dye accepts an electron from the amine as shown previously in the first step in Figure 1.4b, forming the thioxanthene anion-radical. They suggest that the subsequent proton transfer step which would form the neutral ketyl radical does not occur. Instead, the reduced dye donates an electron to the iodonium salt, regenerating the dye and producing an active phenyl radical.

Harada et al. observed an ESR signal that they attributed to the thioxanthene ketyl radical when a thioxanthene/N-phenylglycine solution was irradiated. Other combinations (TX/DPI-BF<sub>4</sub>, TX/NPG/DPI-BF<sub>4</sub>) did not produce the same ESR signals.

The identification of the experimentally observed radical as a thioxanthene ketyl radical is supported by the observation that the electrolytically generated thioxanthene radical anion (TX-\*) had a different signal from the experimentally observed ESR signal. Also, addition of NPG to the electrolytically generated TX-\* produced signals identical to those assigned to the ketyl radical. Harada *et al.* conclude that in the two-component TX/NPG system, the TX becomes electronically excited and accepts an electron from NPG, forming the thioxanthene radical anion and the amine radical cation. Subsequent proton transfer from NPG presumably forms the observed ketyl radical. (This is the mechanism illustrated previously in Figure 1.4b.)

The role of the iodonium salt in the three-component system was probed by adding both DPI-BF<sub>4</sub>/NPG and DPI-BF<sub>4</sub> alone to the electrolytically generated TX-\*. In both cases, the ESR signals disappeared. Furthermore, the thioxanthene absorption band was observed to fade rapidly upon photoirradiation for the TX/NPG system, but fade more slowly for the TX/NPG/DPI-BF<sub>4</sub> system. Harada *et al.* interpreted this to mean that in the three-component system, the iodonium salt accepts an electron from the TX-\* (whether photochemically or electrolytically generated) to form neutral TX and DPI-BF<sub>4</sub> radical anion (which dissociates to phenyl iodide, phenyl radical, and BF<sub>4</sub>.) The fate of the NPG cation-radical is not clear from the experiments.

In an effort to identify the free radical species responsible for initiation, Harada and collaborators studied dark polymerization of acrylate monomers in the presence of electrolytically generated TX-°, TX-°/NPG (which yields the TX ketyl radical, as seen above), and TX-°/DPI-BF<sub>4</sub>. In these experiments, only the TX-°/DPI-BF<sub>4</sub> system led to polymerization. They conclude that the initiating species in three-component

polymerizations is neither the thioxanthene radical anion TX-\* nor the TX ketyl radical. They surmise that the phenyl radical produced by electron transfer from TX-\* to the iodonium salt must be the initiating species.

A role for the amine-based radical is suggested based on literature references rather than experimental evidence presented within the paper. The investigators suggest that the NPG cation-radical undergoes decarboxylation and loses a proton to the BF<sub>4</sub><sup>-</sup> to form an active, neutral phenylaminomethyl radical and HBF<sub>4</sub>. It is not clear why the amine radical was not observed by the ESR experiments.

In summary, the scheme proposed by Harada et al. can be classified as a serial-parallel reaction mechanism. The photo-excited thioxanthene reacts with the amine to yield the thioxanthene radical anion which in turn reacts with the iodonium salt to produce an active phenyl radical and regenerate neutral thioxanthene. The amine cation-radical donates a proton to the iodonium anion to form an active phenylaminomethyl radical.

## 1.5.4. Serial Reaction Hypothesis II and Parallel Reaction Hypothesis II

A team of investigators led by Jean-Pierre Fouassier has carried out the most extensive mechanistic studies of three-component initiator systems to date. In an extensive series of papers, these scientists have reported experimental results based primarily on steady-state fluorescence quenching studies and transient absorption spectroscopy which suggest a different serial reaction mechanism for three-component initiator systems. Briefly, the mechanism they favor involves electron transfer/proton transfer from the amine to the excited dye as in two component systems. For all the dyes

studied, the dye residue was a ketyl radical which is inactive towards initiation. The iodonium salt participates in a second reaction whereby it oxidizes this ketyl radical and prevents it from terminating the propagating polymer chain. This process regenerates the original dye and while also producing an active phenyl radical. These authors also present a second possible mechanism which involves simultaneous electron transfer from the amine to the dye as well as from the dye to the iodonium salt. This parallel mechanism is largely discounted in favor of the serial mechanism.

In two papers published in the early 1990's, Fouassier and coworkers studied three-component systems composed of a ketocoumarin dye, N-methyldiethanolamine (MDEA), and an iodonium salt. Transient absorption was used to study the triplet state of the ketocoumarins. The authors determined the triplet state quenching rate constants for various ketocoumarins in the presence of the amine or the iodonium salt and used the results to infer a reaction mechanism. Two reaction mechanisms were proposed, as shown in Figure 1.5 and Figure 1.6.

The first proposed mechanism involves parallel reactions. In the first reaction the dye and amine react by photoinduced electron transfer just as in two component systems (see Figure 1.4b). The increased polymerization efficiency of the three-component system arises from the second parallel reaction in which additional initiating phenyl radicals are produced by the reaction of the excited triplet state ketocoumarin with the iodonium cation as shown in Figure 1.5. Transient absorption experiments provided supporting evidence for this mechanism since a new, long lived, weakly absorbing species was observed during excitation of a two-component solution containing ketocoumarin and diphenyliodonium chloride. 9,28 This species was assumed to be the

ketocoumarin cation-radical. The authors observe, however, that despite high efficiency of the quenching reaction between iodonium and certain ketocoumarins, the polymerization is quite inefficient for these systems. They suggest that this proposed mechanism, while plausible, is an ineffective initiation route.<sup>28</sup>

A second postulated explanation for the increased polymerization efficiency of the ketocoumarin-amine-iodonium system is shown in Figure 1.6. This serial mechanism begins with the familiar reaction between the excited ketocoumarin and the amine (again see Figure 1.4b). This reaction produces an active amine radical, which may initiate polymerization, and a ketyl radical derived from the ketocoumarin, which is not active towards initiation but can terminate growing chains. The authors report observing a residual signal in their transient absorption experiments which they attribute to this ketyl radical.<sup>9,28</sup> The improvement in photoinitiation efficiency of the three-component system is attributed to interaction of the iodonium salt with this ketyl radical. The postulated reaction produces a molecule of phenyl iodide, a phenyl radical which may initiate polymerization, a proton, and, interestingly, regenerates the original ketocoumarin dye while eliminating the ketyl radical (which is a potential chain terminator). It is relevant to note that in later papers by the same authors, the photobleaching of the dye is reported to be slowed by addition of the third component (either an iodonium salt11 or a bromo compound<sup>23</sup>). These observations can be explained by the dye regeneration feature of the proposed mechanism.

$$3KC + \bigcirc \longrightarrow KC^{\bullet+} + \bigcirc \longrightarrow \bigcirc$$

$$\bigcirc \longrightarrow \bigcirc \longrightarrow \bigcirc \longrightarrow \bigcirc \longrightarrow \bigcirc$$

Figure 1.5: Interaction of ketocoumarin dye and iodonium salt. Excited triplet ketocoumarin, <sup>3</sup>KC, interacts with iodonium cation to produce the ketocoumarin cation-radical and an iodonium radical. The iodonium radical decomposes into neutral phenyl iodide and a phenyl radical, which may initiate polymerization.

$$KC-H^{\bullet} + \bigcirc \longrightarrow \bigcirc \longrightarrow + KC + H^{+}$$

Figure 1.6: Interaction of ketyl radical derived from ketocoumarin with iodonium salt. After excited ketocoumarin dye KC reacts with an electron donor such as an amine, a ketyl radical (KC-H') is formed. (See Figure 1.4b). This radical is theorized to be oxidized by the iodonium cation, forming phenyl iodide, a phenyl radical, a proton, and regenerating the original dye.

In another paper from Fouassier and collaborators, the three-component initiator system studied consisted of diphenyliodonium chloride, N-methyldiethanolamine, and an initiator selected either from the aromatic ketone family (benzil or benzophenone) or a thioxanthone dye (2,4-diethylthioxanthen-7-one).<sup>24</sup> Again the triplet state quenching was studied using transient absorption techniques, and the singlet state was not investigated. As with the ketocoumarins discussed above, the transient absorption experiments revealed a residual, non-decaying peak which was also attributed to a ketyl radical formed by electron transfer from the amine to the dye. The computed quenching efficiencies revealed some interesting trends. For benzophenone, the monomer made the greatest contribution to the triplet state quenching, suggesting that benzophenone would make a poor initiator. Photopolymerization results confirmed this hypothesis. In contrast, for benzil most of the triplet quenching was due to the amine. Finally, with the thioxanthone initiator, about half the quenching was due to the amine, but nearly 40% was attributed to the iodonium salt.

The authors suggest that the primary role of the iodonium salt is to quench the ketyl radicals, resulting in decreased termination of the growing polymer chains and production of additional initiating radicals, as shown in Figure 1.6. However, in the case of the thioxanthone, the authors acknowledge the possibility of some direct role for the iodonium salt due to the relatively high quenching efficiency noted above. Because of the relative positions of the energy levels, energy transfer mechanisms are ruled out. Therefore, electron transfer between the thioxanthone photoinitiator and the iodonium salt as illustrated in Figure 1.5 is proposed. The authors also note that energy transfer between the benzophenone triplet state and the iodonium salt is feasible.

Another three-component initiator study from Fouassier and collaborators involved a substituted thioxanthene dye with diphenyliodonium chloride and either Nmethyldiethanolamine or N-phenylglycine as the electron donor. In these experiments, the excited triplet state was studied using transient absorption, while steady state fluorescence quenching was used to study the singlet state. Using the rate constants determined by these methods, the authors conclude that for the thioxanthene studied, the triplet state is strongly quenched by the monomer, so it is relatively ineffective for photoinitiation. Based on singlet quenching efficiencies calculated using quenching constants derived from Stern-Volmer steady state fluorescence quenching experiments, the authors conclude that the singlet state of the thioxanthene dye is responsible for the photoinitiation process. They conclude, as in prior experiments, that the primary initiation route is electron transfer between amine and dye followed by oxidation of the ketyl radical dye residue by the iodonium salt. They note that the residual absorption observed in transient triplet absorption studies, previously attributed to the ketyl radical, is inhibited by the presence of iodonium salt. This seems to support the serial mechanism proposed. In further studies, the absorption spectra of the component pairs were studied in methanol solution. Irradiation of a solution containing the thioxanthene dye and Nphenylglycine resulted in bleaching of the thioxanthene, as evidenced by a decrease in the thioxanthene absorption band. However, when iodonium salt was added to the mixture, the decay was slower. The proposed mechanism is able to explain this phenomenon, since the dye-amine interactions consume the dye (causing the decline in absorption), and the iodonium salt theoretically oxidizes the ketyl radicals back to the original dye (tending to restore absorption).

The observation of a thioxanthene ketyl radical ESR signal by Harada, Takimoto, Noma, and Shirota, 30 as discussed previously in this chapter, is cited by Erddalane, Fouassier, Morlet-Savary, and Takimoto 11 as further evidence of the interaction of photoexcited thioxanthene with amine to produce an amine radical and a thioxanthene-derived ketyl radical. Based on fluorescence quenching experiments, they conclude that even though the interaction of iodonium salt with the thioxanthene radical anion TX-° can theoretically produce an initiating radical, for the particular system studied, the thioxanthene radical/iodonium interaction is much slower than the thioxanthene/amine interaction. Therefore, the primary role of the iodonium salt is suggested to be a scavenger of the ketyl radicals produced by TX/amine interaction.

#### 1.5.5. Cationic Polymerization

As mentioned earlier in this chapter, there have been some reports that the same dye-amine-iodonium three-component initiation systems used for radical polymerizations can also be used to initiate cationic photopolymerization<sup>21,22</sup> with only minor modifications. The same dyes and iodonium cations may be used in these systems, but aromatic amines are used instead of aliphatic amines because they are less basic. The aliphatic amines tend to terminate the cationic active centers. Also, the iodonium anion must be of low nucleophilicity to prevent termination of the propagating cationic center. Appropriate choices for the counterion include AsF<sub>6</sub>-, PF<sub>6</sub>-, and SbF<sub>6</sub>-. Based on studies of the various two-component systems, Bi and Neckers<sup>21,22</sup> suggest that the reaction mechanism begins with electron transfer from the dye to the iodonium salt (akin to Figure 1.5) followed by hydrogen abstraction from the amine to the phenyl radical produced

from the dye/iodonium electron transfer step. The amine radical is then postulated to be oxidized by another iodonium molecule to produce an  $\alpha$ -aminocarbocationic active center capable of initiating the polymerization. Because of efficient back electron transfer, electron transfer from the amine to the dye, as observed in the radical systems, is not expected to occur.

## 1.6. Summary of Proposed Mechanisms

A number of hypotheses have been presented in the literature to explain the enhanced photoinitiation ability of three-component systems as compared to their two-component counterparts. Table 1.4 summarizes the main proposals.

Table 1.4: Summary of Proposed Three-Component Mechanisms.

Mechanism †	Principal Investigators	References
Parallel mechanism:	He and Wang	18
Onium + Amine $\rightarrow$ [Complex] $\xrightarrow{hv}$ Amine $\stackrel{+e}{\rightarrow}$ + $\phi^{e}$ + onium fragments		
$Dye^* + Amine \rightarrow \underline{Amine}^e + Dye-H^e$		
Serial mechanism for eosin/diphenyliodonium salt:	He, Li, Wang,	37
$[Eo^2][I(\phi)_2]_2^* \to Eo^{-\bullet} + 2I\phi + 2\underline{\phi}^{\bullet}$	and Wang	
$Eo^{-\bullet} + Amine \rightarrow \underline{Amine}^{\bullet} + Eo^{2-} + H^{+}$		
Serial-Parallel Mechanism:	Harada et al.	30
Dye* + Amine → Dye-* + Amine**		
$\Rightarrow$ Dye- $^{\bullet}$ + Onium $\rightarrow$ Dye + $\phi^{\bullet}$ + onium		
fragments		
$\Rightarrow$ Amine $^{+\circ}$ + [An $^{-}$ ] $\rightarrow$ Amine $^{\circ}$ + An-H		
Serial Mechanism:	Fouassier et al.	9, 11, 24,
Dye* + Amine $\rightarrow$ Amine + Dye ketyl radical		28
Dye-H $^{\circ}$ + onium $\rightarrow$ Dye + $\phi^{\circ}$ + onium fragments		
Parallel Mechanism:	Fouassier et al.	9, 24
Dye* + Amine $\rightarrow$ Amine + Dye ketyl radical	The authors	
Dye* + Onium $\rightarrow$ Dye <sup>+</sup> + $\phi$ + onium fragments	believe this	
	mechanism is	
	less important	
	than the serial	
	mechanism.	

<sup>†</sup> Dye\* refers to photoexcited dye. Dye-H\* refers to ketyl radical. Active (initiating) radicals shown underlined.

#### 1.7. References

- 1. J.P. Fouassier, *Photoinitiation, Photopolymerization, and Photocuring*, Hanser-Gardner, Cincinnati (1995).
- 2. V. Narayanan and A. B. Scranton, "Photopolymerization of Composites," *Trends in Polymer Science*, 5, 415-419 (1997).
- 3. Fouassier, J. P., "Excited-State Reactivity in Radical Polymerisation Photoinitiators," in Radiation Curing in Polymer Science and Technology, Vol II: Photoinitiating Systems, J. P. Fouassier and J. F. Rabek (eds.), Elsevier, London, 1-61 (1993).
- 4. H. Block, A. Ledwith, and A. R. Taylor, "Polymerization of methyl methacrylate photosensitized by benzophenones," *Polymer*, 12, 271-288 (1971).
- 5. M. Kawabata, and Y. Takimoto, "Properties of Dye-sensitized Polymer Containing Pendant N-Phenylglycine Moiety," J. Photopolym. Sci. Tech., 3, 147-148 (1990).
- 6. H. Baumann, H.-J. Timpe, and H.-P. Herting, "Light induced polymer and polymerization reactions. 9. Initiation of photopolymerization by the initiator systems trisoxalatoferrate/arene onium salts," EP 684,522 A1 (1995).
- 7. M. Z. Ali, and S. C. Busman, "High Sensitivity Photopolymerizable Composition," US Patent 4.971.892 (1990).
- 8. M. Kawabata, M. Harada, and Y. Takimoto, "Photoinitiation Systems Comprised of Dyes and Radical Precusors," J. Photopolym. Sci. Tech., 1, 222-227 (1988).
- 9. J. P. Fouassier, D. Ruhlmann, B. Graff, Y. Takimoto, M. Kawabata, and M. Harada, "A New Three-Component System in Visible Laser Light Photo-Induced Polymerization," J. Imaging Sci. and Tech., 37, 208-210 (1993).
- 10. R. Zertani, and D. Mohr, "Photopolymerizable Mixture and Recording Material Produced Therefrom," U.S. Patent 5,229,253 (1993).
- 11. A. Erddalane, J. P. Fouassier, F. Morlet-Savary, and Y. Takimoto, "Efficiency and excited state processes in a three component system, based on thioxanthone derived dye/amine additive, useable in photopolymer plates," J. Polymer Sci., A: Polym. Chem., 34, 633-642 (1996).
- 12. K. S. Anseth, D. C. Svaldi, C. T. Laurencin, and R. Langer, "Photopolymerization of Novel Degradable Networks for Orthobedic Applications," in *Photopolymerization: Fundamentals and Applications*, A. B. Scranton, C. N.

- Bowman, and R. W. Peiffer (eds.), American Chemical Society, Washington DC, 189-202 (1997).
- 13. Z. Kucybala, M. Pietrzak, J. Paczkowski, L.-Å. Lindén, and J. Rabek, "Kinetic studies of a new photoinitiator hybrid system based on camphorquinone-N-phenylglycine derivatives for laser polymerization of dental restorative and stereolithographic (3D) formulations," *Polymer*, 37, 4585-4591 (1996)
- 14. H. J. Hageman, "Photoinitiation for Free Radical Polymerization," *Prog. Org. Coatings*, 13, 123-150 (1985).
- 15. R. S. Davidson, "The chemistry of photoinitiators—some recent developments," J. Photochem. Photobiol. A: Chem., 73, 81 (1993).
- 16. H.-J. Timpe, S. Jockusch, and K. Körner, "Dye Sensitised Photopolymerisation," Radiation Curing Science and Technology, Vol. II: Photoinitiating Systems, J. P. Fouassier and J. F. Rabek (eds.), Elsevier, London, 575-601 (1993).
- 17. K. Dietliker, "Photoinitiators for Pigmented Systems," Radiation Curing Science and Technology, Vol, II: Photoinitiating Systems, J. P. Fouassier and J. F. Rabek (eds.), Elsevier, London, 155-237 (1993).
- 18. J. He and E. Wang, "Photoinitiated polymerization by aryliodonium salt/benzopehnone/tertiary amine binary photosensitization system," *Chin. J. Polym. Sci.*, 8, 44-50 (1990).
- 19. J. D. Oxman, A. Ubel III, and E. G. Larson, "Coated Abrasive Binder Containing Ternary Photoinitiator System," U.S. Patent 4,735,632 (1988).
- 20. T. Lyubimova, S. Caglio, C. Gelfi, P. G. Righetti, and T. Rabilloud, "Photopolymerization of polyacrylamide gels with methylene blue," *Electrophoresis*, 14, 40-50 (1993).
- 21. Y. Bi and D.C. Neckers, "A visible light initiating system for free radical promoted cationic polymerization," *Macromolecules*, 27, 3683-3693 (1994).
- 22. Y. Bi and D.C. Neckers, "Photopolymerization of cyclohexene oxide a visible light initiating system and mechanistic investigations," Proc. RadTech, Orlando, Florida, 180-186 (1994).
- 23. J. P. Fouassier, A. Erddalane, F. Morlet-Savary, I. Sumiyoshi, M. Harada, and M. Kawabata, "Photoinitiation Processes of Radical Polymerization in the Presence of a Three-Component system based on Ketone-Amine-Bromo Compound," *Macromolecules* 27, 3349-3356 (1994).
- 24. J. P. Fouassier, D. Ruhlmann, Y. Takimoto, M. Harada, and M. Kawabata, "New Three-Component Initiation Systems in UV Curing: A Time-Resolved Laser-

- Spectroscopy Investigation," J. Polymer Sci. A: Polym. Chem. 31, 2245-2248 (1993).
- 25. M. Harada, M. Kawabata, and Y. Takimoto, "Photoinitiation Systems Containing Bromo Compounds," J. Photopolym. Sci. Tech., 2, 199-204 (1989).
- 26. M. Kawabata, M. Harada, and Y. Takimoto, "Photopolymerizable composition highly sensitive to visible light," US Patent 4,868,092 (1989).
- 27. T. Nakahara, K. Kusumoto, and S. Yuasa, "Photochemical polymerization catalysts for dental materials," JP 62, 22,804 (1987).
- 28. J. P. Fouassier and S. K. Wu, "Visible Laser Lights in Photoinduced Polymerization. VI. Thioxanthones and Ketocoumarins as Photoinitiators," J. Appl. Polm. Sci., 44, 1779-1786 (1992).
- 29. Y Tomura, and S. Tomono, "Visible ray-sensitive hardener compositions and manufacture of glass fiber-reinforced resins using them," JP 02 97,503 (1990).
- 30. M. Harada, Y. Takimoto, N. Noma, and Y. Shirota, "Mechanism of photoinitiation of a three component system containing thioxanthene dye," J. Photopolym. Sci. Tech., 4, 51-54 (1991).
- 31. M. Harada, "Photocurable composition," EP 382,209 (1990).
- 32. H. Tomioka, M. Harada, M. Kawabata, and Y. Takimoto, "Photopolymerizable Composition," Eur. Pat. Appl. EP 333,224 (1989).
- 33. H. Ito, T. Taguchi, Y. Imai, and Y. Morimitsu, "Ketocoumarin-containing photopolymerization initiator compositions and photopolymerizable resin compositions containing them," JP 03 71,704 (1991).
- 34. J. P. Fouassier, F. Morlet-Savary, K. Yamashita, and S. Imahashi, "The role of the dye/iron arene complex/amine system as a photoinitator for photopolymerization reactions," *Polymer*, 38, 1415-1421 (1997).
- 35. J. P. Fouassier, F. Morlet-Savary, K. Yamashita, and S. Imahashi, "Visible Light-induced Polymerization Reactions: The seven-role of the Electron Transfer Process in the Dye/Iron Arene Complex/Amine system," J. Appl. Polym. Sci., 62, 1877-1885 (1996).
- 36. J. He and E. Wang, "Radical Photopolymerization Using Aryliodonium Salt/ Tertiary Amine Complex System as the Photoinitiator," *Chin. J. Polym. Sci.*, 8, 36-43 (1990)

37. J.-H. He, M.-Z. Li, J.-X. Wang, and E.-J. Wang, "Synergetic effects of amines on the intra-ion-pair electron transfer dye photosensitization system Eo(IPh<sub>2</sub>)<sub>2</sub>," J. Photochem. Photobiol. A: Chem., 89, 229-234 (1995).

#### **CHAPTER 2**

## **OBJECTIVES AND TECHNIQUES**

## 2.1. Objectives of Research

The previous chapter illustrates that although there is a compelling motivation for the development and understanding of three-component initiator systems, these systems have received very limited study, especially in the United States, and are poorly understood. In fact, the relatively few papers that have been published on the topic offer conflicting explanations, in part because the mechanism appears to depend to some degree on the selection of the three components.

The broad objective of this research was to clearly identify the mechanistic pathway or pathways whereby three-component initiation systems produce active centers.

This broad objective was approached by completing the following specific goals:

- To investigate the effects of each component and its concentration on polymerization rate using complete reaction profiles obtained by differential scanning calorimetry
- 2. To investigate the effects of each component and its concentration on dye photobleaching during reaction, using steady state fluorescence techniques
- To investigate the complex effects of oxygen on dye photobleaching, using steady state fluorescence techniques
- 4. To investigate the effects of iodonium salts on the termination step of photopolymerization, using photo-differential scanning calorimetry

5. To investigate the effect of dye structure, particularly the dye charge, on initiation reactions

The first two objectives, taken together, provide a flexible method for characterizing the behavior of three-component systems. The differential scanning calorimetry experiments allow study of the photopolymerization reaction, whereas the fluorescence experiments focus on the primary photochemical reaction. Understanding the influence of oxygen, as outlined in the third objective, is a matter of practical importance, since industrial applications of photopolymerization are rarely carried out under a nitrogen blanket.

Finally, the last two objectives are targeted to clarify specific aspects of the initiation reaction. In one of the mechanisms proposed for the three-component initiator system, the enhanced photopolymerization rate attained with the three-component systems is explained on the basis of an effect of diphenyliodonium chloride on the termination step. By observing the effect of the iodonium salt on "dark cure," this hypothesis can be tested. Furthermore, most previous studies have used anionic and neutral dye molecules. This research compared the initiation behavior of methylene blue, a cationic dye, to that of anionic and neutral eosin dyes.

# 2.2. Experimental Techniques

The two primary experimental techniques selected for these studies are very flexible and provide a wealth of fundamental information. Each technique targets a

different aspect of the reaction and these techniques work well in concert to provide a comprehensive characterization of three-component initiator systems.

## 2.2.1. Differential Scanning Calorimetry

Photo-DSC was used in this research to observe the reaction rate for three-component systems at various concentrations of each of the three components. Also, any so-called "dark cure" can be monitored using this technique, since the sample can be illuminated to initiate the reaction and then the light may be shuttered to observe the dark reaction. This type of experiment allows measurement of the termination rate constant.

DSC is particularly useful for study of photoreactions because accurate measurements of the light intensity are readily obtained. By placing two graphite discs in the DSC sample and reference chambers and illuminating the sample while keeping the reference dark, the resulting exotherm is easily analyzed to yield the total luminescent power striking the sample. Combining this data with the known emission profiles for the illumination source (a 200 W Hg-Xe lamp in the experiments presented in this work) and the known absorption profile of the dye in use gives a good estimate of the total absorbable light striking the sample.

#### 2.2.2. Steady State Fluorescence Monitoring

Direct study of the initiation rate of a polymerization reaction is difficult compared to study of the polymerization rate. However, one method which has been shown to be useful is steady state fluorescence monitoring. In this method, the fluorescence signal of the initiator is monitored *in situ* during the polymerization

reaction. If the structure of the initiator is changed sufficiently to modify its fluorescence signal during the initiation reaction, observation of the steady state fluorescence provides a direct method for observing progress of the initiation reaction. In the experiments presented here, the initiator fluorescence is destroyed over the course of the reaction. Thus, the steady state fluorescence decay profile can be easily fit to an exponential function, allowing determination and comparison of the decay constants. This method is especially attractive because the same wavelength used to initiate the reaction is also used for monitoring the reaction.

#### **CHAPTER 3**

# A MECHANISTIC INVESTIGATION OF THE THREE-COMPONENT RADICAL PHOTOINITIATOR SYSTEM METHYLENE BLUE, N-METHYLDIETHANOLAMINE, AND DIPHENYLIODONIUM CHLORIDE

#### 3.1. Introduction and Motivation

The continuing growth in applications of photopolymerization can be attributed to the significant advantages offered by light-induced polymerization compared to traditional thermal polymerization methods. In photopolymerization, light rather than heat is used to produce the active centers (radicals or cations) which initiate a chain polymerization. The use of light affords great temporal and spatial control over the polymerization, since the light can be directed to a location of interest and shuttered at will. For industrial applications, this ease of control provides "cure on demand" which eliminates problems of premature reaction and waste which can occur with thermally initiated reactions. Since photopolymerization is typically rapid, even at room temperature, it may be used with heat-sensitive substrates without risk of thermal deformation. Photopolymerization also offers tremendous environmental advantages. For instance, photocurable compositions are typically solvent free, so they do not contribute emissions of volatile organic compounds. addition. to In photopolymerizations consume only a fraction of the energy typically required by

thermally initiated polymerizations, resulting in both economic and environmental benefits.<sup>1</sup>

Free radical photoinitiators, which produce active centers upon absorption of light, have traditionally been built around the benzoyl chromophore which absorbs light in the ultraviolet (UV) region of the spectrum. Some common classes of these photoinitiators include benzoin ethers, dialkoxyacteophenones, hydroxy alkyl ketones, benzoyl oxime esters, amino ketones, and morpholino ketones. These photoinitiators produce active centers efficiently by the well-known α-cleavage process when illuminated with UV light.<sup>2</sup> However, ultraviolet light is undesirable for many applications. For instance, in biological applications, visible light is preferable due to the damaging effects of UV radiation.<sup>3,4</sup> In addition, visible light-initiated cure is attractive because of the ready availability of inexpensive, reliable sources of photons in the visible region of the spectrum.

# 3.2. Three-Component Visible Light Photoinitiators

Until recently, the need for visible light radical photoinitiators has been addressed primarily by using bimolecular initiator systems. In these systems, active radicals are generally produced via electron transfer and subsequent proton transfer from an amine to an photo-excited molecule (the photoinitiator). Using this approach, the system can be tailored to a specific wavelength range by choice of the photoinitiator. In the last decade, three-component photoinitiation systems have emerged as an improvement over two-component electron transfer initiating systems. Like the two component systems, the

three-component initiators include a light absorbing moiety which is typically a dye and an electron donor which is almost always an amine. The third component is usually an iodonium salt. Three-component systems are extremely flexible since a wide variety of dyes may be used. As in the two-component systems, the selection of the dye determines the active wavelength; classes of dyes that have been reported for three-component systems include ketones, xanthenes, thioxanthenes, xanthones, thioxanthones, coumarins, ketocoumarins, thiazines, and merocyanines. These three-component systems have consistently been found to be faster, more efficient, and more sensitive than their two-component counterparts. 6-9

#### 3.2.1. Reaction Mechanism

Although many three-component systems have been identified, only a few research groups have attempted to elucidate the mechanism by which active centers are produced. A number of hypotheses have been presented in the literature to explain the enhanced photoinitiation ability of three-component systems as compared to their two-component counterparts, and the operative mechanism may depend upon the specific system under consideration. Some authors have suggested a serial mechanism whereby the amine and the dye react via the known bimolecular initiating scheme. The resulting amine-based radical is active for initiation, but the dye-based radical is a terminating radical. The third component, the onium salt, is thought to oxidize this inactive dye-based radical, regenerating the original dye and producing an active phenyl radical in the process. Alternatively, it has been suggested that pairs formed from the three components react independently. In one proposed mechanism, the amine and dye

undergo the previously described bimolecular initiation reaction, and the onium salt and the dye react via electron transfer to form a dye-based cation radical, a phenyl radical, and phenyl iodide.<sup>9,11</sup> In addition, several other proposed mechanisms have been published in the literature.<sup>7,13,14</sup> For a recent review, see reference 5.

## 3.2.2. System and Rationale

In this paper we present a series of fundamental studies of the initiation mechanism whereby a three-component radical photoinitiator system produces active centers. As illustrated in Figure 3.1, the system under investigation consists of a methylene blue dye (MB), N-methyldiethanolamine (MDEA) as the electron donor component, and diphenyliodonium chloride (DPI) as the third component. Diphenyliodonium chloride and N-methyldiethanolamine were chosen because they are essentially standard choices for three-component systems.<sup>6-11</sup> Methylene blue, however, has not been well studied and was selected due to its unique characteristics. For example, since methylene blue is a cationic dye, electrostatic repulsion precludes direct reaction with the iodonium cation. By effectively shutting down this reaction pathway, we were able to simplify the list of possible reaction mechanisms. Furthermore, the entire class of cationic dyes has not been well studied in three-component systems. The few mechanistic studies carried out in the past have used anionic and neutral dyes almost exclusively. In addition, methylene blue possesses its own reducing group (the amine groups on the thiazine ring structure) which may indeed make it "extra" effective in a three-component photoinitiator system. Finally, methylene blue is of extremely low

toxicity, making it an appealing choice for biological applications of three-component systems.<sup>15</sup>

The normalized absorption spectra of the three components in the initiating system are given in Figure 3.2. The spectra show that only the methylene blue component has any absorption in the visible region of the spectrum (the peak occurs at 656 nm.) The amine component absorbs only in the deep UV, and the iodonium salt's absorption barely stretches to about 350 nm.

The photopolymerizations were carried out using 2-hydroxyethyl methacrylate (HEMA) as the monomer. All experiments were in neat monomer; no solvents were used. HEMA is a natural choice for studies of three-component photoinitiators since it has good biocompatibility and is already used in applications such as controlled release devices and contact lenses. Furthermore, its relatively low volatility offers safety advantages over most other acrylate monomers.

Studies of the termination behavior of the three-component system MB/MDEA/DPI were carried out in 8:1 mixture of ethylene glycol dimethacrylate (EGDMA) and HEMA (mass ratio). EGDMA was chosen because it forms a highly crosslinked network during photopolymerization which limits diffusion of the long polymer chains and slows the termination reaction sufficiently to allow observation by DSC. Since methylene blue is not highly soluble in EGDMA, a small amount of HEMA was added to aid the dissolution of the dye.

Figure 3.1: Three-component initiation system used

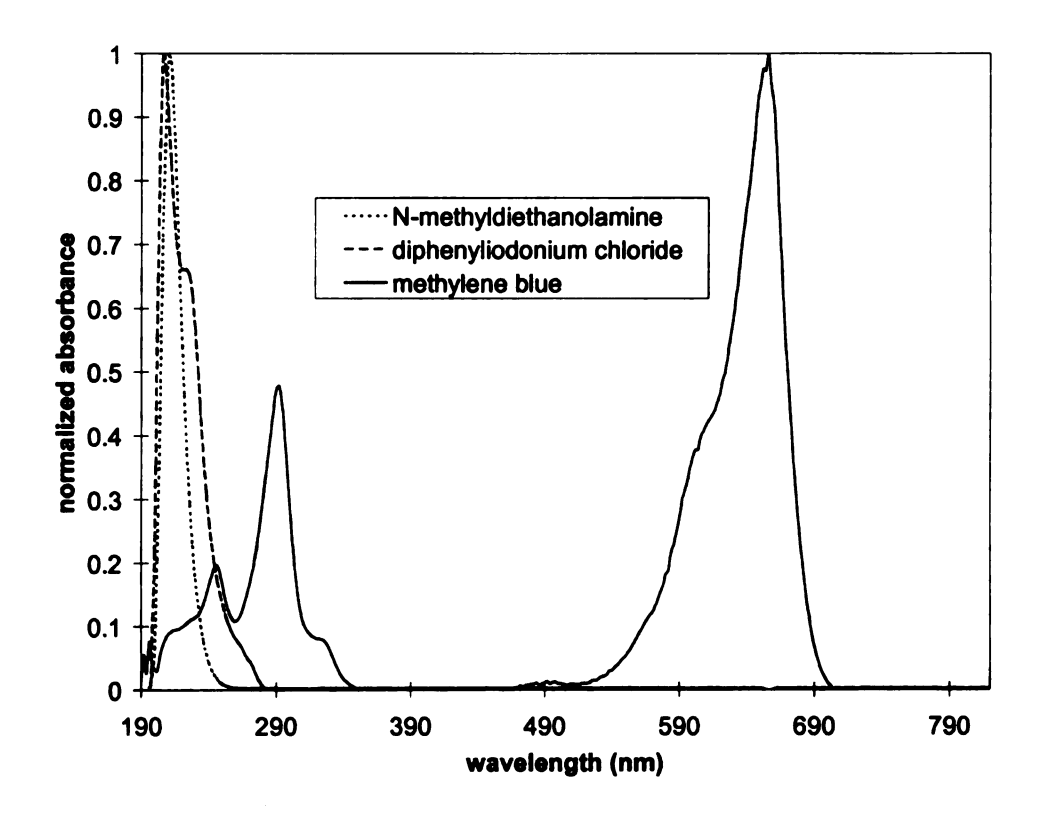


Figure 3.2: Normalized absorbance spectrum of the three-component system. All components were dissolved in methanol. Spectra were normalized to a peak absorbance of 1 for ease of comparison.

## 3.3. Experimental

#### 3.3.1. Materials

The monomers 2-hydroxyethylmethacrylate and ethylene glycol dimethacrylate were obtained from Aldrich. They were treated with DeHibit (from Polysciences) to remove hydroquinone inhibitor and filtered prior to use. Methylene blue was obtained from Aldrich, and N-methyldiethanolamine (MDEA) and diphenyliodonium chloride (DPI) were obtained from Fluka. All three components were used as received.

#### 3.3.2. Photo-differential scanning calorimetry

Photo-DSC was conducted using a Hewlett-Packard DSC 7 modified in-house for photo-experiments. The light source was a 200 W Oriel mercury-xenon lamp. The beam was passed through a water filter outfitted with a thermostatted recirculating jacket to reduce infrared radiation and limit sample heating. A glass cover on the DSC sample block was used to eliminate any ultraviolet-induced photoinitiation. The total radiant power incident on the sample was 63 mW/cm², as measured by graphite disc absorption. This measurement includes all visible region light, not all of which can be absorbed by the methylene blue photosensitive component. Comparison of the lamp's spectral characteristics with the absorbance profile of the methylene blue dye reveals that only about 6% of this total radiant intensity can be absorbed by the dye, for an effective incident power of approximately 4 mW/cm². This relatively low light intensity was used in order to produce a relatively slow reaction rate which can be accurately monitored using DSC. A nitrogen purge flowing at approximately 25 cm³/min was used in the DSC

to eliminate oxygen inhibition of the polymerization. Samples were degassed for a minimum of five minutes prior to illumination. The heat flow data collected by the DSC can be easily converted to the polymerization rate data reported in this contribution using the heat of polymerization, which is 49.8 kJ/mol for HEMA.<sup>18</sup>

This procedure was modified to gather information about the termination reaction by using the DSC to monitor the so-called "dark" polymerization which persists for a few minutes after a photoinitiated reaction is stopped prematurely by shuttering the light source. For these experiments, neutral density filters were used on the 200 W Hg-Xe lamp to reduce the effective absorbable light intensity to 0.3 mW/cm<sup>2</sup>. The samples were exposed to light for two minutes and then the dark cure was monitored for 2-4 minutes at 25°C. At the conditions used, the photopolymerization reaction is no more than 7% completed after two minutes of exposure (as determined from the fastest-curing sample). Using a low light intensity and a short exposure time ensures that termination step is not influenced by consumption of monomer.

#### 3.3.3. Time-resolved steady state fluorescence

The fluorescence monitoring experiments were performed using a Coherent Innova-90 Krypton ion laser (647.1 nm line) as the excitation source. A thin film sample cell geometry was used, as illustrated in Figure 3.3. The fluorescence was collected perpendicular to the sample film using a Spex Triplemate two stage triple monochromater equipped with a 1024-pixel OMA 4 liquid nitrogen cooled CCD detector. In order to exclude the laser line from the detection optics, wavelengths below 715 nm were severely attenuated using the spectrometer's subtractive-dispersive double-monochromater filter

stage. A thin microporous polyethylene film (3M IR sample card, qualitative PE type 61) was used to hold the sample flat. In order to control the film thickness, 2  $\mu$ L sample aliquots were measured with an Eppendorf pipette. In order to minimize the effects of component diffusion in and out of the illuminated region of the thin film, a relatively large spot on the film was illuminated, but data were sampled from only a portion of this region. To accomplish this, a lens was used to defocus the laser beam. The resulting illuminated spot was an ellipse with major and minor diameters of 3 mm and 1 mm respectively. Then, the entrance slit to the spectrometer was narrowed so that the fluorescence was collected from the center of the thin film sample.

The laser power output was approximately 25 mW (as measured by a Scientech 362 Power meter). Neutral density filters (OD = 1.4) were used to reduce the beam power to 1 mW, so the incident power was approximately 40 mW/cm<sup>2</sup>. The sample cell was attached to a recirculating bath in order to maintain a consistent sample temperature (25°C). A nitrogen purge was used to eliminate the effects of oxygen. Each experiment was run at least three times to verify results. Fifty complete fluorescence spectra in the wavelength range 700-850 nm were taken at time intervals chosen to capture the entire decay of the methylene blue fluorescence. The intervals used ranged from every 200 msec to every 4.6 seconds. The integration time was 167 msec in all cases.

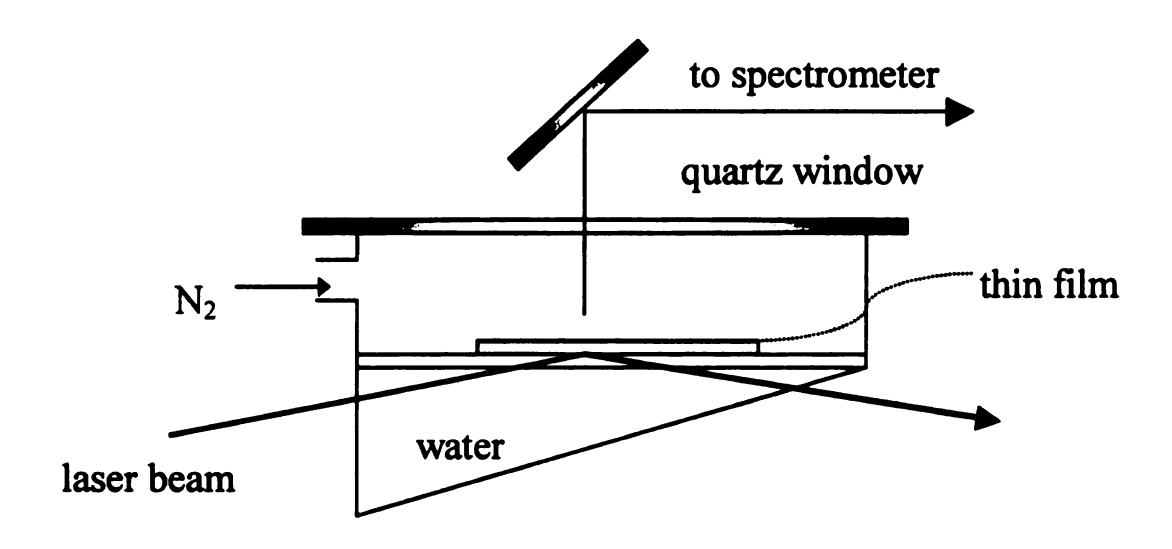


Figure 3.3: Thin film fluorescence monitoring apparatus. The laser beam illuminates the thin film from below. The fluorescence is collected above the sample and routed to the spectrometer. A nitrogen purge port allows control of the atmosphere, while a recirculating water bath moderates the temperature.

#### 3.4. Results and Discussion

#### 3.4.1. Photo-DSC

Figure 3.4 illustrates the effect of each initiator component on the photopolymerization rate as measured by DSC. The data illustrate that each component plays an important role in the photopolymerization reaction and showcase the advantages of three-component systems. As Figure 3.4 demonstrates, the maximum rate is observed when all three components are present (maximum rate 0.019 mol/L/s observed at 10.5 min). The two component system containing MDEA and MB exhibits the second fastest reaction rate (maximum rate 0.011 mol/L/s observed at 18 min), while a two-component system containing DPI and MB exhibits a relatively slow reaction (maximum rate 0.005 mol/L/s observed at 26 min. Finally, notice that methylene blue causes slow polymerization to occur, even in the absence of amine or iodonium salt. The mechanism of cure by methylene blue alone has not been investigated in this paper, but it is likely that the amine group present on the methylene blue structure (see Figure 3.1) acts as an electron donor to a second, photo-excited, MB molecule. The resulting radicals may then initiate polymerization. Early work on the photochemistry of dyes indeed indicates that photobleaching of MB could be attributed to the amine group in the absence of other reducing agents. 19

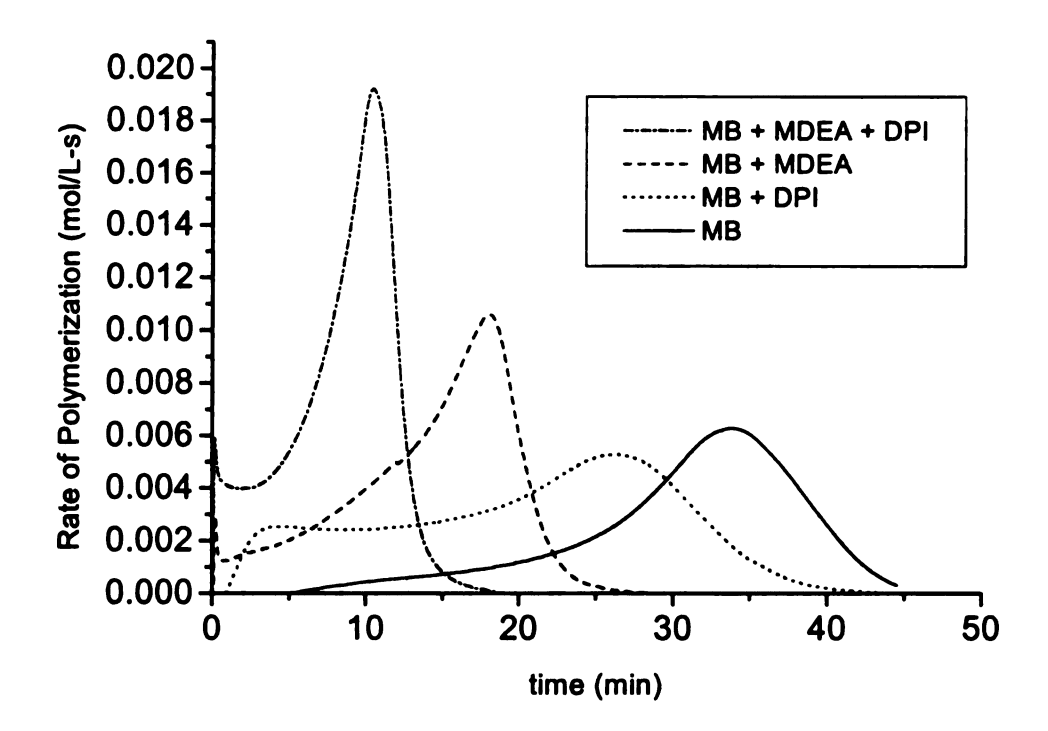


Figure 3.4: Effect of each component on photopolymerization rate as measured by DSC. Each component plays an important role in the photopolymerization reaction. [MB] = 0.00011 M, [MDEA] = 0.013 M, [DPI] = 0.001 M, all in neat HEMA.  $I_a = 4$  mW/cm<sup>2</sup>, T = 50°C. Each curve is obtained by averaging three independent experiments. The initial overshoot in reaction rate observed for the two fastest reactions is believed to be an instrumental artifact arising from the relatively sluggish response time (~ 3 seconds) of the DSC technique.

The data in Figure 3.4 clearly indicate that the presence of all three components is necessary to obtain the maximum polymerization rate. Next a more detailed series of studies on the three-component system was performed to investigate the effects of the concentrations of DPI and MDEA on the observed polymerization rate. Figure 3.5 demonstrates that the concentration of MDEA has a dramatic impact on the rate of photopolymerization. With the concentrations of MB and DPI held constant, as the MDEA concentration is increased from zero to 0.051 molar, the maximum polymerization rate was observed to increase from 0.005 to 0.024 mol/L/s. Similarly, as illustrated in Figure 3.6, the reaction rate also increases dramatically with increasing DPI concentration. With the concentrations of MB and MDEA held constant, as the DPI concentration is increased from zero to 0.0049 molar, the maximum polymerization rate was observed to increase from 0.010 to 0.025 mol/L/s.

### 3.4.2. Photobleaching Studies

The DSC experiments clearly indicate that each of the three components is important to the photocuring reaction. In order to learn how the amine and iodonium salt affect the consumption of the photosensitive component (methylene blue), we used steady state fluorescence monitoring experiments to observe the reduction of the methylene blue steady-state fluorescence as a function of the illumination time. The fluorescence signal is directly proportional to the ground state methylene blue concentration. Therefore, as the dye is consumed during the photoinitiation reaction, observation of the fluorescence signal provides a direct measure of the extent of the photoinitiation reaction.

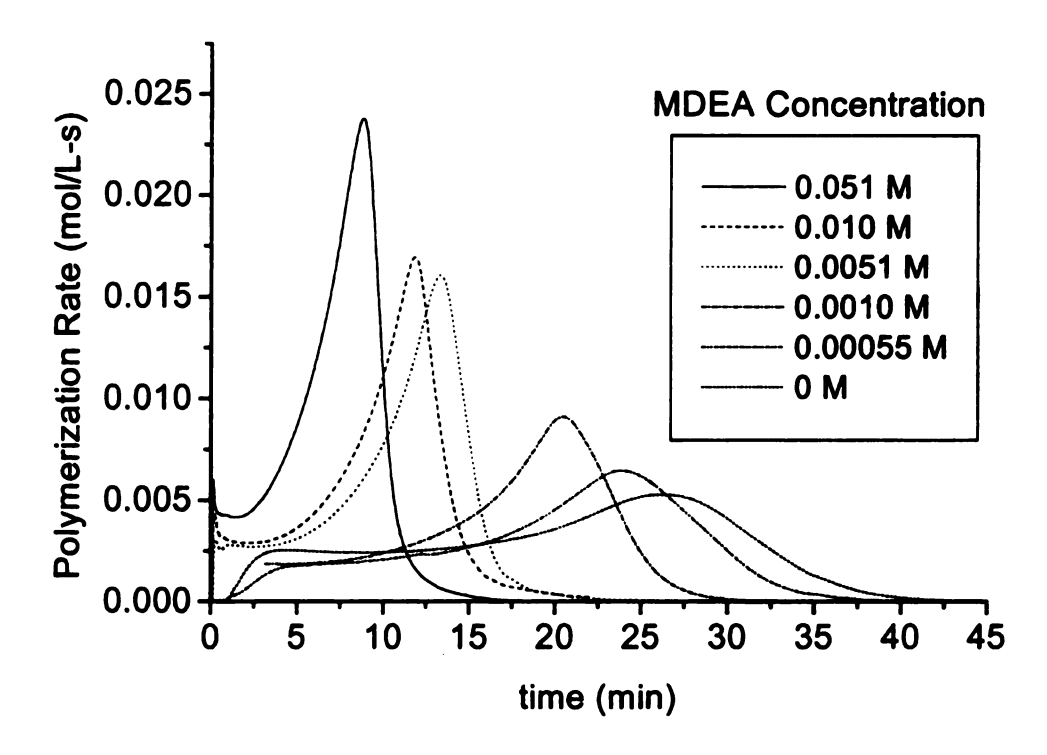


Figure 3.5: Effect of MDEA concentration on photopolymerization rate as measured by DSC. The photopolymerization rate increases dramatically as the amine concentration is increased. [DPI] = 0.001 M, [MB] = 0.00011 M, all in neat HEMA.  $I_a = 4 \text{ mW/cm}^2$ ,  $T = 50^{\circ}\text{C}$ .

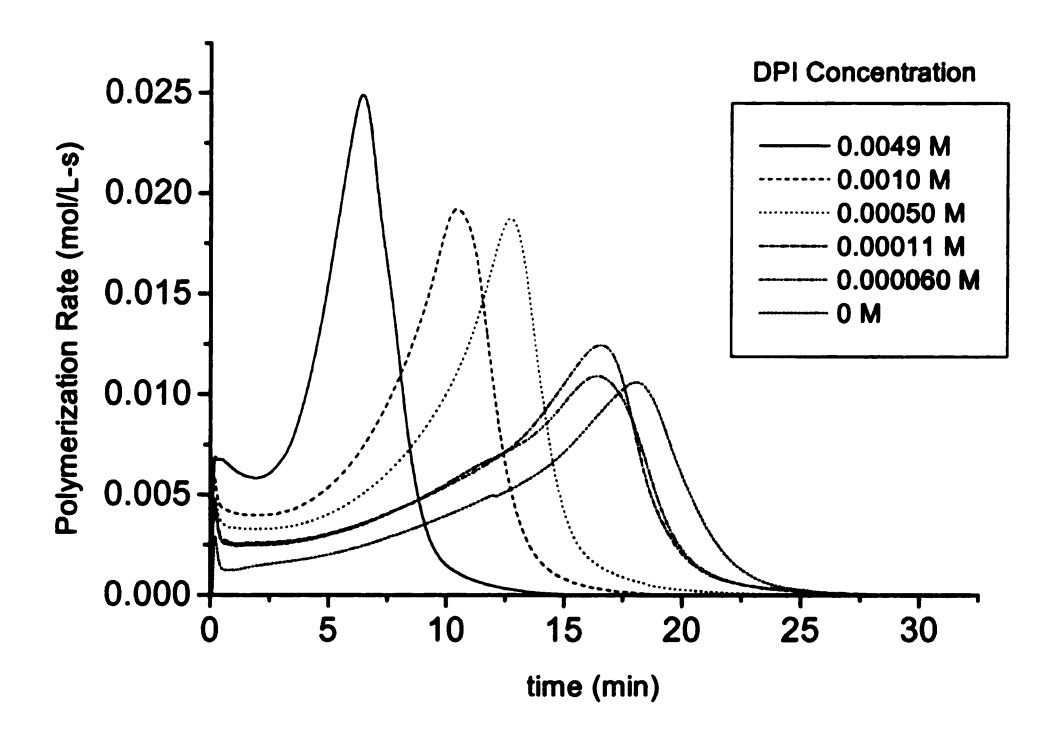
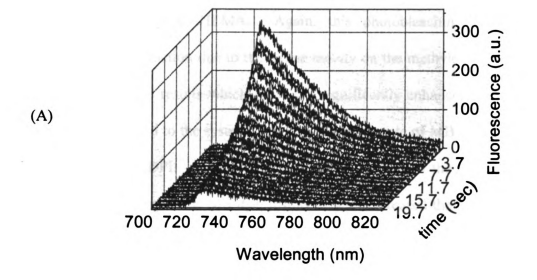


Figure 3.6: Effect of DPI concentration on photopolymerization rate as measured by DSC. The rate of photopolymerization rises dramatically as the DPI concentration is increased. MDEA = 0.013 M, MB = 0.00011 M,  $I_a = 4$  mW/cm<sup>2</sup>, T = 50°C.

As shown in Figure 3.7, a series of fifty complete fluorescence spectra was taken at time intervals (200 msec in this case) chosen to capture the entire decay of the dye florescence. Slicing this three-dimensional spectrum at the peak of the fluorescence (~724 nm in this case) produces a trace corresponding to the decay of the fluorescence intensity as a function of illumination time. To reduce the impact of noise in the fluorescence spectra, five points at the fluorescence peak were averaged to produce the final fluorescence vs. time trace. The decay of the fluorescence peak was fit to a first order exponential function as shown in Equation 3.1. As illustrated in the figure, the curve is well described by an exponential decay.

$$y = A_1 \exp\left[-\frac{x}{t_1}\right] + y_0$$
 Equation 3.1



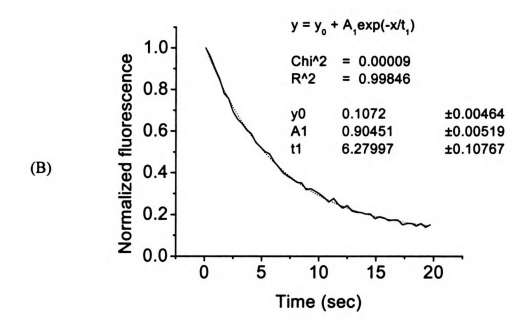


Figure 3.7: Methylene blue fluorescence intensity as a function of illumination time. [MB] = 0.00011 M, [MDE] = 0.012 M, [DPI] = 0.0010 M. I<sub>a</sub> at 647.1 nm = 40 mW/cm<sup>2</sup>, T = 25°C. (A). The steady state dye fluorescence is monitored by acquiring a fluorescence spectrum every 400 msec. (B). The three-dimensional plot is sliced parallel to the time axis to yield a single fluorescence vs. time curve. The fit to an exponential decay is illustrated. In the experiments reported here, the maximum fluorescence was observed at 724 nm. The fluorescence peak of MB occurs at ~687 nm, but this wavelength is attenuated by the subtractive-dispersive filter stage of the spectrometer.

Figure 3.8 illustrates the effect of each of the three components on the photobleaching rate. Notice that a system containing methylene blue alone undergoes slow photobleaching in HEMA. Again, this photobleaching likely arises from bimolecular self-reduction due to the amine moiety on the methylene blue. However, in contrast to the DSC results which showed a significantly enhanced polymerization rate when DPI was added to the system, the photobleaching rate of MB is virtually unaffected by the addition of DPI. As expected, addition of MDEA to the MB system results in faster photobleaching of the MB dye, just as MDEA increased the polymerization rate in the DSC experiments. However, the most surprising result is the observation that when all three components are present in the system (MB/MDEA/DPI), the photobleaching rate is slower than that observed when only MB and MDEA are present. In contrast, recall from the DSC experiments that the photopolymerization rate is maximized when all three components are present. Therefore DPI inhibits the consumption of the methylene blue dye, but increases the rate of photopolymerization.

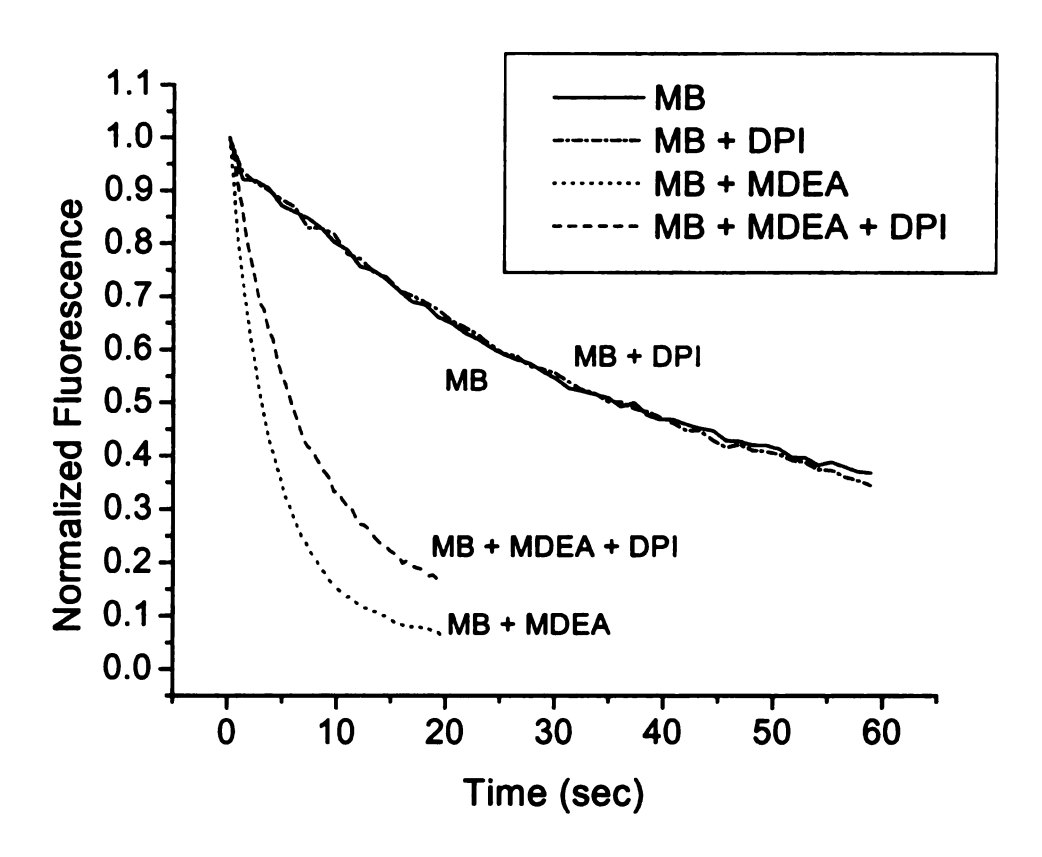


Figure 3.8: Decay of methylene blue steady-state fluorescence. Methylene blue undergoes slow decay upon illumination, both alone (MB) and in the presence of diphenyliodonium chloride (MB + DPI). The addition of N-methyldiethanolamine (MDEA) to the system causes rapid consumption of methylene blue. [MB] = 0.00011 M, [MDEA] = 0.013 M, [DPI] = 0.0010 M. Curves shown are the average of three trials. I<sub>a</sub> at 647.1 nm = 40 mW/cm<sup>2</sup>, T=25°C

### 3.4.3. Discussion of Reaction Mechanism

The experimental results shown in the previous section provide insight into the mechanism by which active centers are produced. For example, the dramatic impact of the MDEA concentration on the dye photobleaching rate suggests that the primary photoreaction occurs between the MB dye and the MDEA. As an illustration of this effect, Figure 3.9 shows how the characteristic fluorescence decay time (t<sub>1</sub> in Equation 1) depends upon the amine concentration. The figure illustrates that the decay constant decreases rapidly with increasing amine concentration (up to 100 times the dye concentration). The sensitivity of the decay time to the amine concentration decreases when an even greater excess as amine is present. The photobleaching results suggest a completely different role for the iodonium salt since the DPI actually inhibits the consumption of MB. This indicates that the DPI does not participate directly in the photo-induced reaction.

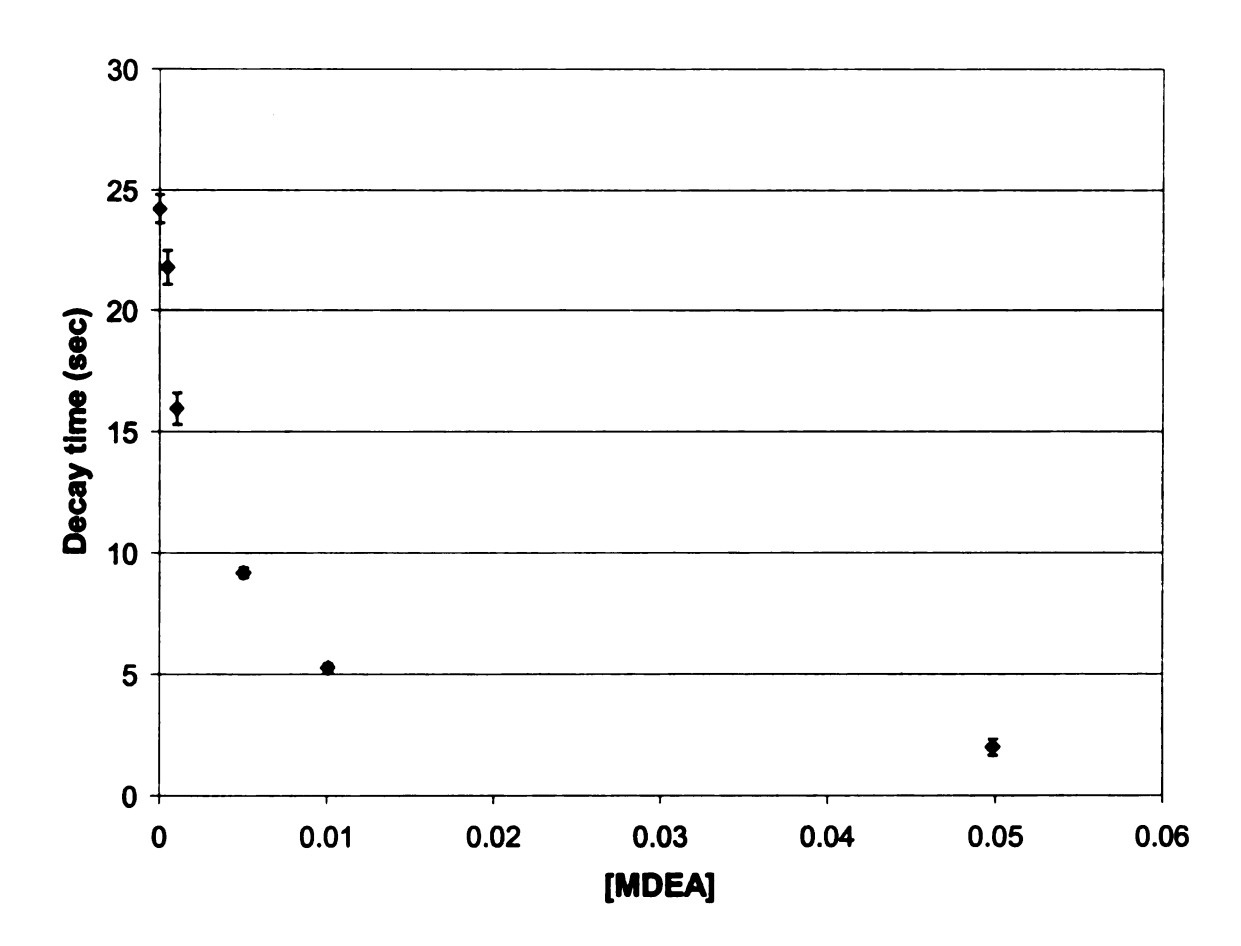


Figure 3.9: Effect of MDEA concentration on characteristic decay time. Increasing amine concentration produces a very dramatic decline in the characteristic exponential decay constant associated with the fluorescence bleaching. Data shown represent the average of three trials. The error bars represent one standard deviation. [MB] = 0.00011 M, [DPI] = 0.001 M. I<sub>a</sub> at 647.1 nm = 40 mW/cm<sup>2</sup>, T=25°C.

### 3.4.3.1. Primary Photochemical Reaction

Based upon our experimental results, we suggest that the primary photobleaching mechanism proceeds as illustrated in Figure 3.10. In the figure methylene blue is shown with a chloride counterion, which is the form that was used in these experiments. In the first step of the mechanism the methylene blue becomes excited by absorption of light of the appropriate wavelength. The photoexcited methylene blue molecule, denoted with a star in the figure, encounters an amine molecule and accepts an electron from the amine, forming a positively charged amine moiety and a neutral methylene blue dye moiety while leaving the chloride anion unchanged. In the next step, the amine loses a proton to the chloride ion to produce hydrogen chloride and a neutral tertiary amine radical, which is active for initiation. The neutral methylene blue radical is presumably not active for initiation, but is able to terminate the growing polymer chains, as is the case in other well known electron transfer/proton transfer reactions.<sup>20,21</sup> However, notice that this reaction mechanism is slightly different from the well-known electron transfer/proton-transfer reaction because the dye is cationic. In most other mechanistic studies, the dye has been neutral or anionic. The electron transfer reaction would therefore form a negatively charged dye moiety, and subsequent proton transfer from amine to dye would be needed to balance the charges. In this case, the MB dve moiety is neutral after the electron transfer reaction, and we suggest that the amine's proton is intercepted by the negatively charged chloride counterion.

The postulated role of the amine as the component responsible for the photobleaching of the dye is further supported by Figure 3.11, which illustrates how the asymptotic value (at long times) of the fluorescence intensity decreases as the MDEA

concentration is increased. This occurs because the amine chemically consumes the dye in the photoinduced reaction.

Since the primary photoreaction occurs between the methylene blue and the amine, the photobleaching reaction is extremely sensitive to the amine concentration, as Figure 3.9 illustrated. In contrast, the DPI concentration has a less dramatic effect on the rate of photobleaching. Recall that Figure 3.8 showed how the addition of DPI to the MB/ MDEA system actually caused the photobleaching rate to decline. Figure 3.12, which is a plot of decay time as a function of the DPI concentration, further illustrates this phenomenon. As shown, the characteristic decay time for the methylene blue fluorescence increases slightly when the DPI concentration is increased over the range 0 M to 0.005 M. This behavior is surprising because DPI has already been shown to increase the rate of photocuring (Figure 3.6).

Figure 3.10: Primary photoreaction occurs between excited methylene blue and amine. Electron transfer from amine to dye is immediately followed by proton transfer from amine to chloride ion, resulting in a neutral, bleached MB radical, an MDEA radical, and HCl.

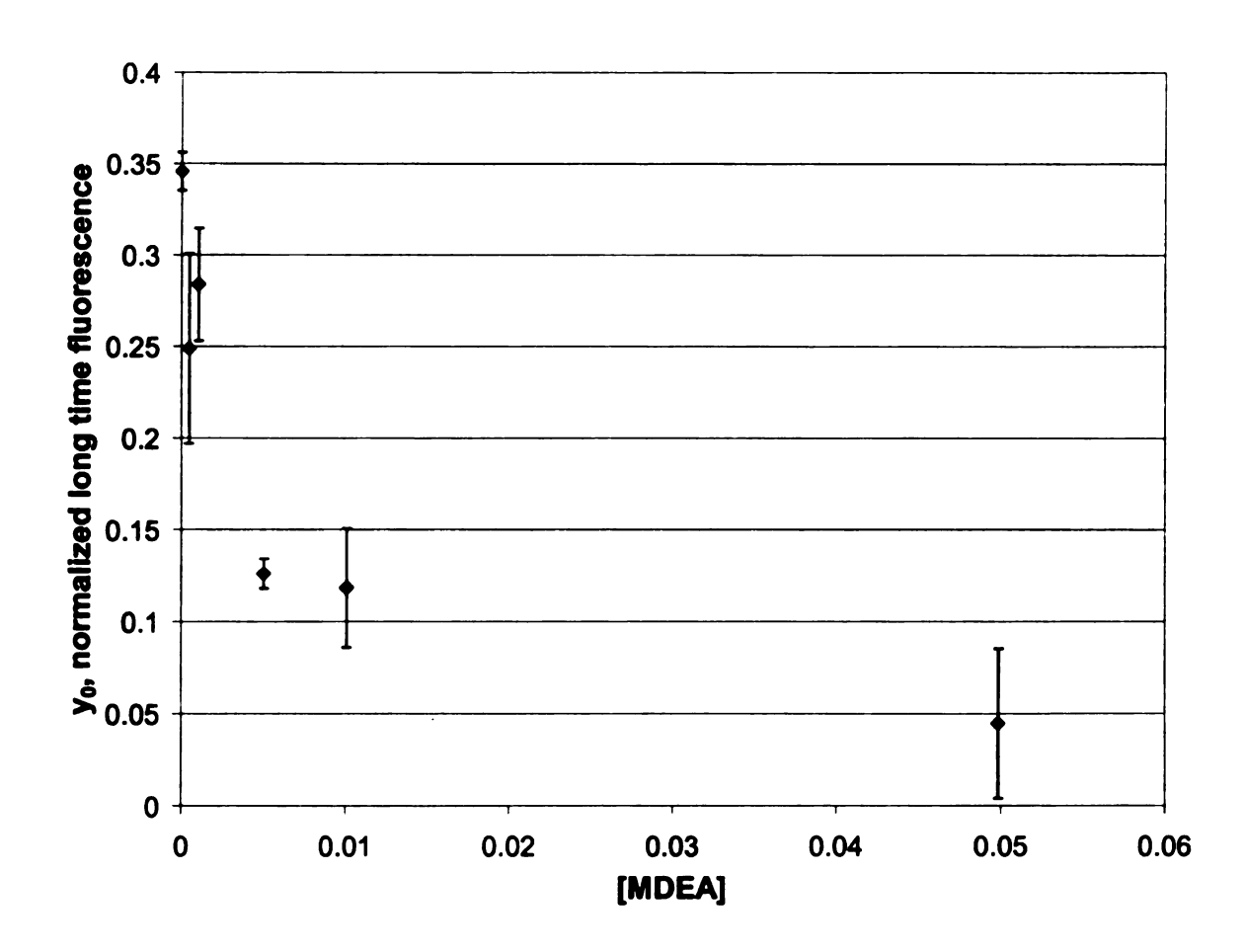


Figure 3.11: Effect of MDEA concentration on predicted long time fluorescence. The parameter  $y_0$  in the exponential fit of the fluorescence decay reflects the predicted asymptotic or long time value of the fluorescence. As the MDEA concentration is increased, this parameter decreases due to consumption of the dye via electron transfer reaction with MDEA. Data shown represent the average of three trials. The error bars represent one standard deviation. [MB] = 0.00011 M, [DPI] = 0.001 M. I<sub>a</sub> at 647.1 nm =  $40 \text{ mW/cm}^2$ , T=25°C.

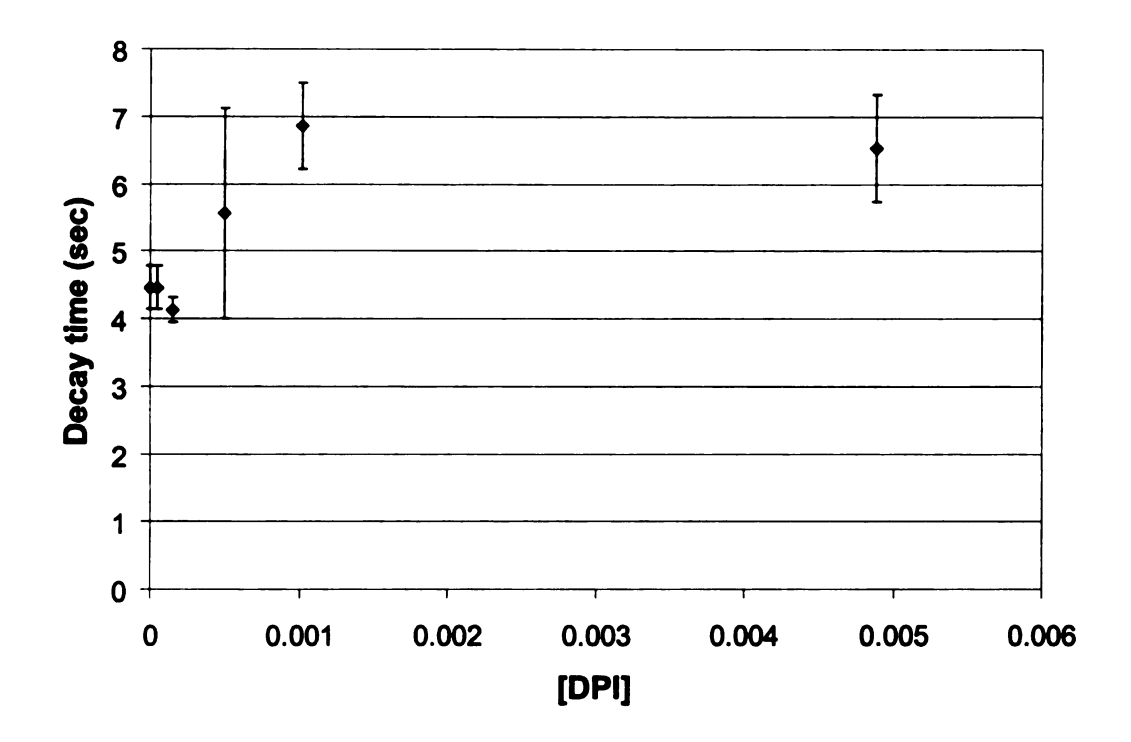


Figure 3.12: Effect of DPI concentration on  $t_1$ , the characteristic decay time for methylene blue fluorescence. Increasing DPI concentration produces a slight but clear increase in the characteristic decay time, indicating a slower rate of decay. Data shown represent the average of three trials. The error bars represent one standard deviation. [MDEA] = 0.013 M, [MB] = 0.00011 M.  $I_a$  at 647.1 nm = 40 mW/cm<sup>2</sup>, T=25°C.

### 3.4.3.2. Role of the Iodonium Salt

The influence of the onium salt concentration on the photoinitiation reaction (causing a slight decrease in photobleaching rate yet dramatically increasing the cure rate) can be explained by the role for the iodonium salt proposed in mechanism illustrated in Figure 3.13. The reaction involves electron transfer from the dye radical moiety (previously produced in the primary photoreaction between the amine and the dye) to the This reaction regenerates the original dye and produces a iodonium salt. diphenyliodonium radical which rapidly fragments into a molecule of phenyl iodide and a phenyl radical. The enhanced reaction rate observed in the presence of the iodonium is explained in part by the fact that the phenyl radical, unlike the methylene blue radical it replaces, is active for initiation. In this way a methylene blue radical that is active only in termination is effectively replaced by a phenyl radical that is active in initiation. In addition, since the ground state methylene blue dye is regenerated in this reaction, the initiation rate will be enhanced further. Finally note that since the electron transfer reaction effectively results in the transfer of the positive charge from the iodonium salt to the methylene blue, the chloride counterion will also be transferred. The mechanism shown in Figure 3.13 is consistent with results reported for different dyes by Fouassier and collaborators. 9-12 These investigators reported that an iodonium salt can interact with the dye-based radical (a ketyl radical in their case), re-oxidizing it back to its original state. In summary, the DPI thus plays a double role: it replaces an inactive, terminating radical with an active, initiating radical, and it regenerates the methylene blue dye, a component of the original initiating system.

$$MB^{\bullet}$$
 +  $O$  +  $O$  +  $O$  +  $O$  +  $O$ 

Figure 3.13: Mechanistic Role of Iodonium Salt. The iodonium salt abstracts an electron from the bleached methylene blue neutral radical. The resulting methylene blue cation abstracts the chloride counterion to regenerate the original dye. The iodonium radical fragments to produce an active, initiating phenyl radical along with a phenyl iodide molecule.

The photobleaching results are consistent with the mechanism proposed in Figure 3.13. Recall that as the DPI concentration was increased the photobleaching rate was observed to decrease. The dye-regeneration activity of the DPI explains this result. Since the presence of DPI causes dye molecules to be effectively "unbleached," the net rate of bleaching observed will be slower for samples with higher DPI concentrations. Furthermore, the presence of increasing DPI also causes the overall amount of bleaching to decrease, again due to regeneration of the dye. This is illustrated in Figure 3.14 which is a plot of asymptotic (long time) fluorescence intensity as a function of DPI concentration.

### 3.4.3.3. Influence of Iodonium Salt on the Termination Step

The mechanistic role for the iodonium salt proposed in Figure 3.13 has two primary implications: first, an effect on the photobleaching behavior of the methylene blue dye caused by regeneration of the dye, as confirmed above, and second, an effect on the termination step of the photopolymerization caused by consumption of the dye radical. As discussed in section 3.4.3.1, the methylene blue radical formed from reaction with the MDEA is not active for initiation, although it can terminate the growing polymer

chains. Since DPI is thought to consume the MB radical, increasing the DPI concentration should result in a reduction in the termination rate. The dark cure exotherms in Figure 3.15 confirm that this is indeed the case. Samples with higher DPI concentrations exhibit greater and more persistent levels of dark cure than samples with lower (or zero) DPI concentration, indicating that termination is reduced in the samples with higher DPI concentration.

Notice also that the initial rate when the dark cure experiment begins (when the light source is shuttered) is higher for samples with higher DPI concentrations. This is a natural effect of the increase in photopolymerization rate with increasing DPI concentration. However, the observed effect on the termination step cannot be attributed to hindered diffusion of growing chains arising from a higher degree of crosslinking for the samples with higher DPI concentrations because the overall conversion is quite low for these samples (the sample with the highest DPI concentration reaches only 7% of its final conversion during the first two minutes of exposure.) For this reason, variation in degree of crosslinking is expected to be minimal and should not significantly affect the termination step. The primary cause of the variation in the rate of termination illustrated in Figure 3.15 is the consumption of terminating MB radicals via reaction with DPI.

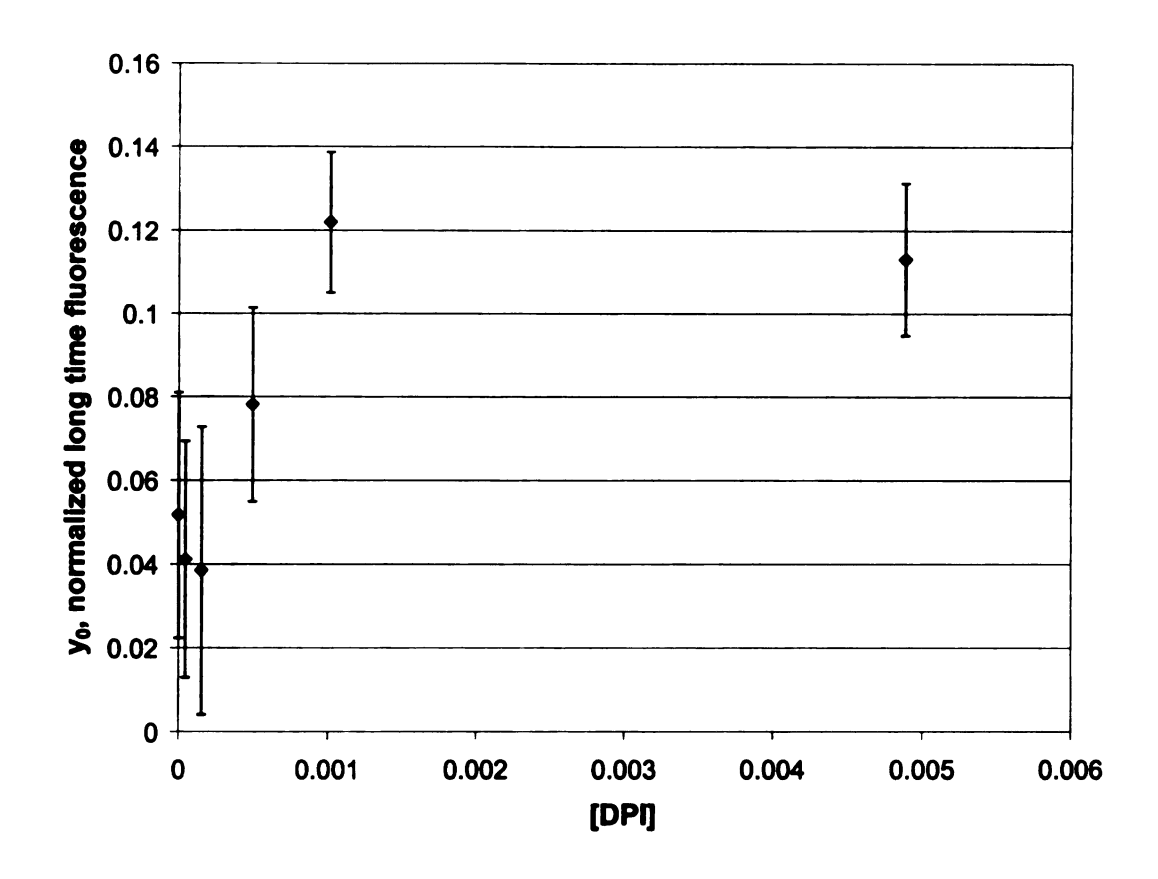


Figure 3.14: Effect of DPI concentration on predicted long time fluorescence. The parameter  $y_0$  in the exponential fit of the fluorescence decay reflects the predicted asymptotic or long time value of the fluorescence. As the DPI concentration is increased, this parameter rises due to regeneration of the MB dye. Data shown represent the average of three trials. The error bars represent one standard deviation. [MDEA] = 0.013 M, [MB] = 0.00011 M. I<sub>a</sub> at 647.1 nm = 40 mW/cm<sup>2</sup>, T=25°C.

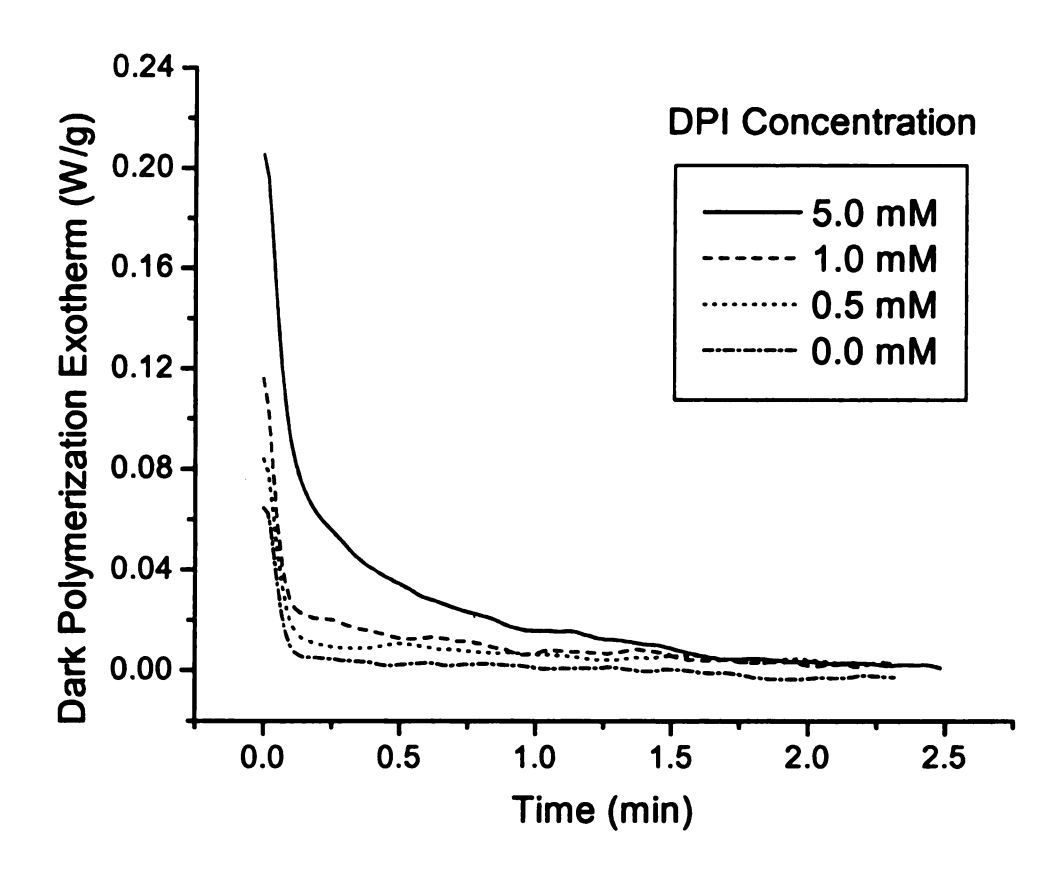


Figure 3.15: Dark polymerization exotherms for various DPI concentrations. Increasing DPI slows termination of the polymerization reaction. [MB] = 0.00010 M, [MDEA] = 0.013 M in EGDMA/HEMA 8:1 mass ratio. T = 25°C,  $I_a = 0.3$  mW/cm<sup>2</sup>. Each curve is the average of three replicate trials.

### 3.5. Conclusions

In this paper, we have offered experimental evidence for a proposed serial reaction mechanism by which active radical centers are produced by the three-component system comprised of methylene blue, N-methyldiethanolamine, and diphenyliodonium chloride. As summarized in Figure 3.16, the mechanism involves electron transfer/proton transfer from the amine to the dye as the primary photochemical reaction. The iodonium salt is an electron acceptor, acting to re-oxidize the neutral dye radical back to its original state and allowing it to re-enter the primary photochemical process. This reaction also generates phenyl radicals which can serve as initiating radicals. The iodonium has a double role: to regenerate the methylene blue and to replace the inactive, terminating dye radical with an active, initiating radical.

$$MB^{+}Ci^{-} \xrightarrow{h\nu} [MB^{+}Ci^{-}]^{*}$$

$$[MB^{+}Ci^{-}]^{*} + MDEA \xrightarrow{\longrightarrow} MB^{*} + MDEA^{*} + HCI$$

$$MB^{*} + DP[-CI \longrightarrow MB^{+}Ci^{-} + \phi - I + \phi^{*}]$$

Figure 3.16: Reaction mechanism for the three-component system MB/MDEA/DPI.

### 3.6. References

- 1. J.P. Fouassier, *Photoinitiation, Photopolymerization, and Photocuring*, Hanser-Gardner, Cincinnati (1995).
- 2. Fouassier, J. P., "Excited State Reactivity in Radical Polymerisation Photoinitiators," Radiation Curing in Polymer Science and Technology, Vol II: Photoinitiating Systems, J. P. Fouassier and J. F. Rabek (eds.), Elsevier, London, 1-61 (1993)
- 3. K. S. Anseth, D. C. Svaldi, C. T. Laurencin, and R. Langer. "Photopolymerization of Novel Degradable Networks for Orthopedic Applications," in *Photopolymerization: Fundamentals and Applications*, A. B. Scranton, C. N. Bowman, and R. W. Peiffer (eds.), ACS, 189-202 (1997).
- 4. Z. Kucybala, M. Pietrzak, J. Paczkowski, L.-Å. Lindén, and J. Rabek, "Kinetic Studies of a new photoinitiator hybrid systems based on camphorquinone-N-phenylglycine derivatives for laser polymerization of dental restorative and stereolithographic (3D) formulations," *Polymer*, 37, 4585-4591 (1996).
- Kathryn Sirovatka Padon and Alec B. Scranton, "Recent Advances in Three Component Photoinitiator Systems," in Recent Research Developments in Polymer Science, vol. 3, S. G. Pandalai (ed.), Transworld Research Network, Trivandrum, India, 369-385 (1999).
- 6. M. Kawabata, M. Harada, and Y. Takimoto, "Photoinitiation Systems Comprised of Dyes and Radical Precursors," J. Photopolym. Sci. Tech., 1, 222-227 (1988).
- 7. J. He and E. Wang, "Photoinitiated Polymerization by aryliodonium salt/benzophenone/tertiary amine binary photosensitization system," *Chin. J. Polym. Sci*, **8**, 44-50 (1990).
- 8. Joel D. Oxman, Andrew Ubel III, and Eric G. Larson. "Coated Abrasive Binder Containing Ternary Photoinitiator System," U.S. Patent 4,735,632 (1988).
- 9. J. P. Fouassier, D. Ruhlmann, B. Graff, Y. Takimoto, M. Kawabata and M. Harada, "A New Three-Component System in Visible Light Photo-Induced Polymerization," J. Imaging Sci. and Tech., 37, 208-210 (1993).
- A. Erddalane, J. P. Fouassier, F. Morlet-Savary and Y. Takimoto "Efficiency and Excited State Processes in a Three-Component System, Based on Thioxanthene Derived Dye/Amine/Additive, Usable in Photopolymer Plates," J. Polymer Sci., A: Polym. Chem., 34, 633-642 (1996).

- 11. J. P. Fouassier, D. Ruhlmann, Y. Takimoto M. Harada, and M. Kawabata, "New Three-Component Initiation Systems in UV Curing: A Time-Resolved Laser-Spectroscopy Investigation," J. Polymer Sci. A: Polym. Chem., 31, 2245-2248 (1993).
- 12. J. P. Fouassier and S. K. Wu. "Visible Laser Lights in Photoinduced Polymerization. VI. Thioxanthones and Ketocoumarins as Photoinitiators," *J. Appl. Polm. Sci.*, 44, 1779-1786 (1992).
- 13. J-H. He, M-Z Li, J-X Wang, and E-J Wang, "Synergetic effects of amines on the intra-ion-pair electron transfer dye photosensitization system Eo(IPh<sub>2</sub>)<sub>2</sub>," J. Photochem. Photobiol. A: Chem., 89, 229-234 (1995).
- 14. M. Harada, Y. Takimoto, N. Noma, and Y. Shirota. "A Mechanism for Photoinitiation of a Three-Component System Containing Thioxanthone Dye," J. Photopolym. Sci. Tech, 4, 51-54 (1991).
- 15. In fact, methylene blue is used medicinally to treat methemoglobinemia, a condition where the blood has reduced oxygen carrying capacity. See M. Cawein et. al., "Hereditary diaphorase deficiency and methemoglobinemia," Archives of Internal Medicine, April 1964.
- 16. S. H. Gehrke and P. I. Lee, "Hydrogels for Drug Delivery Systems," in *Specialized Drug Delivery Systems*, P. Tyle (ed.), Marcel Dekker, New York, 333 (1990).
- 17. Y. C. Lai, A. C. Wilson, and S. Z. Zantos, "Contact Lens," in *Kirk-Othmer Encyclopedia of Chemical Technology*, vol 7, 4th ed., J. I. Kroschwitz, (ed.), Wiley, New York, 192-218, (1993).
- 18. H. Sawada, "Thermodynamics of Polymerization. I.." J. Macromol. Sci.-Revs. Macromol. Chem., C3, 313-396 (1969).
- 19. H. Meier, "Photochemistry of Dyes," in *Chemistry of Synthetic Dyes*, vol IV, K. Venkatarman (ed.), Academic Press, New York, 389-515 (1971).
- 20. H. J. Hageman, "Photoinitiators for Free Radical Polymerization," *Prog. Org. Coat.*, 13, 123-150 (1985).
- 21. H. Block, A. Ledwith, and A. R. Taylor, "Polymerization of Methyl Methacrylate Photosensitized by Benzophenones," *Polymer*, 12, 271-288 (1971).

# **CHAPTER 4**

# THE EFFECT OF OXYGEN ON THE THREE-COMPONENT RADICAL PHOTOINITIATOR SYSTEM METHYLENE BLUE, N-METHYLDIETHANOLAMINE, AND

**DIPHENYLIODONIUM CHLORIDE:** 

## 4.1. Introduction and Motivation

In a previous paper,<sup>1</sup> we discussed the use of three-component systems to initiate free radical photopolymerization using visible light. In general, three-component initiation systems include a light absorbing moiety which is typically a dye, an electron donor which is almost always an amine, and a third component which is usually an iodonium salt. These systems are attractive photoinitiators because they are extremely sensitive and efficient in the visible region of the electromagnetic spectrum.<sup>2-5</sup> For a recent review of these systems, see reference 6.

### 4.1.1. Reaction Mechanism

In our previous contribution, we described a series of differential scanning calorimetry and time-resolved steady state fluorescence monitoring studies of the three-component initiator system comprised of 1) a methylene blue dye, 2) N-methyldiethanolamine as the electron donor, and 3) diphenyliodonium chloride. In these studies we found that adding the iodonium salt to the two-component dye/amine system

resulted in a significantly enhanced polymerization rate; however, the presence of the iodonium salt actually decreased the rate of consumption of the dye. From these results we proposed the reaction mechanism given in Figure 4.1. In this mechanism, the excited methylene blue dye first accepts an electron from the amine to produce a neutral methylene blue radical. The dye counterion (chloride) then accepts a proton from the amine cation-radical, finally forming a neutral amine radical and a molecule of hydrogen chloride. As in other dye/amine electron transfer systems, the amine radical is active for initiation, but the neutral dye radical is active only for termination.

In the mechanism shown in Figure 4.1, the iodonium salt participates in the reaction by accepting an electron from the dye radical. The newly re-formed dye cation is paired with the iodonium's chloride counterion and thus the original dye is regenerated. After accepting the electron, the iodonium rapidly fragments into a phenyl radical and a molecule of phenyl iodide. Therefore, the role of the iodonium salt is twofold: 1) the inactive, terminating dye radical is replaced with an active, initiating phenyl radical and 2) the dye molecule is regenerated to participate in another electron transfer reaction with the amine.

In our previous studies, we also observed that methylene blue dye itself could induce photopolymerization in the absence of an amine electron donor. We suggested the amine group present on the methylene blue structure acts as an electron donor and allows the methylene blue to undergo bimolecular self-reduction. Early research indeed suggested that photobleaching of MB could be attributed to the amine group in the absence of other reducing agents.<sup>8</sup>

$$MB^{+}CI^{-} \xrightarrow{h\nu} [MB^{+}CI^{-}]^{*}$$

$$[MB^{+}CI^{-}]^{*} + MDEA \xrightarrow{\longrightarrow} MB^{*} + MDEA^{*} + HCI$$

$$MB^{*} + DPI-CI \xrightarrow{\longrightarrow} MB^{+}CI^{-} + \phi-I + \phi^{*}$$

Figure 4.1: Reaction mechanism for the system methylene blue (MB), N-methyldiethanolamine (MDEA), and diphenyliodonium chloride (DPI).

### 4.1.2. Effect of Oxygen on the initiation reaction

In this contribution we use time-resolved steady state fluorescence monitoring to extend our study of the methylene blue (MB), N-methyldiethanolamine (MDEA), and diphenyliodonium chloride (DPI) three-component initiator system to investigate the effect of oxygen on the reaction mechanism. This technique allows us to observe the dye concentration in-situ as the dye is consumed via photoreaction. Two different sample cell geometries were used to complete these studies. The first set of experiments relied upon a thin-film geometry to provide a well-controlled atmosphere and a homogeneous, constant concentration of oxygen throughout the sample for the duration of the experiment (we estimate the diffusion time for oxygen through the thin film to be approximately 50 msec). The second set of experiments was performed using a capillary tube sample cell to model a sealed reactor. While the environment was not oxygen-free, surface diffusion of fresh oxygen into the reaction area was practically eliminated during the timescale of the experiment (the diffusion time from the darkened end of the capillary to the illuminated region is at least two orders of magnitude longer than the time to complete the experiment). This model of a sealed reactor is of interest since, in many

practical applications, an oxygen-impermeable layer (such as polyvinyl alchohol<sup>2.5</sup> paraffin oil,<sup>9</sup> or other materials<sup>10</sup>) may be added to the surface of a polymerizing liquid to inhibit the diffusion of atmospheric oxygen into the sample.

# 4.2. Experimental

The monomer 2-hydroxyethylmethacrylate was obtained from Polysciences. It was treated with DeHibit (Polysciences) to remove hydroquinone inhibitor and filtered prior to use. Methylene blue was obtained from Aldrich, and N-methyldiethanolamine (MDEA) and diphenyliodonium chloride (DPI) were obtained from Fluka. All three components of the initiating system were used as received.

Time-resolved steady state fluorescence monitoring experiments were performed using a Coherent Innova-90 Krypton ion laser (647.1 nm line) as the excitation source. The fluorescence was collected using a Spex Triplemate two stage triple monochromater equipped with a 1024-pixel OMA 4 liquid nitrogen cooled CCD detector. Fifty complete fluorescence spectra in the wavelength range 700-850 nm were taken at time intervals chosen to capture the entire decay of the methylene blue fluorescence. The intervals used ranged from every 200 msec to every 4.6 seconds, depending on the specific sample. The integration time was 200 or 167 msec in most cases. Both cell holders were equipped with a recirculating bath in order to maintain a consistent sample temperature.

The thin film fluorescence monitoring apparatus was fully described in an earlier publication, so only a brief description is provided here. The apparatus consists of an enclosed glass cell with a flat bottom upon which a thin film sample supported by a piece

of microporous polyethylene rests. A gas inlet port allows control of the atmosphere. In these experiments, the atmospheric composition was varied from 100% nitrogen to 50% nitrogen/50% air. The thin film sample is illuminated with the laser beam from beneath, and the fluorescence is collected from above. In these experiments, the absorbed light intensity was approximately 40 mW/cm<sup>2</sup>.

The capillary sample cell consists of a 1 mm diameter capillary tube held perpendicular to the laser beam. The fluorescence signal was collected perpendicular to both the capillary sample tube and the laser beam. The laser beam diameter was approximately 2 mm, and the laser power reaching the sample was 6.5 mW (as measured by a Scientech 362 Power meter). The incident power was therefore approximately 200 mW/cm<sup>2</sup>.

### 4.3. Results and Discussion

In order to investigate the effects of amine and iodonium salt on the consumption of the photosensitive component (methylene blue), we used steady state fluorescence monitoring experiments to observe the reduction of methylene blue fluorescence as a function of illumination time. The steady state fluorescence signal is directly proportional to the ground state concentration of the dye. Since the methylene blue dye is consumed during the photoinitiation reaction, observation of the dye fluorescence provides a direct measure of the progress of the photoinitiation reaction. A series of fifty complete fluorescence spectra was taken at time intervals chosen to capture the entire decay of the dye florescence. Slicing this three-dimensional spectrum at the peak of the

fluorescence signal (which appeared at approximately 710 nm for the capillary experiment and 724 nm for the thin film experiments) produces a trace corresponding to the decay of the fluorescence in time. Representative data are shown in Figure 4.2. The decay of the fluorescence peak was fit to a first order exponential function as shown in Equation 4.1:

$$y = y_0 + A_1 \exp \left[ -\frac{x}{t_1} \right]$$
 Equation 4.1.

In some cases, the presence of oxygen introduced a retardation period into the fluorescence decay. That feature was accounted for by introducing a delay time  $x_0$  and fitting the fluorescence decay to Equation 4.2:

$$y = y_0 + \exp\left[\frac{x - x_0}{t_1}\right]$$
 Equation 4.2.

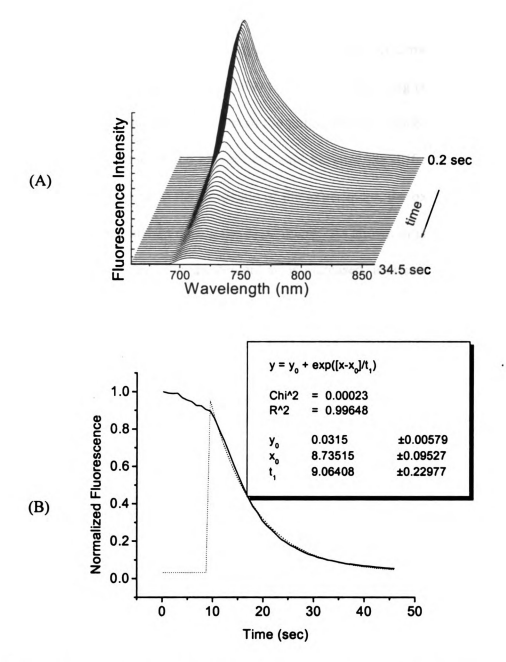


Figure 4.2: Steady state fluorescence monitoring. (A). The steady state dye fluorescence is monitored by taking a fluorescence spectrum approximately every 700 msec. (B). The three-dimensional plot is sliced parallel to the time axis to yield a single fluorescence w. time curve. The fit to an exponential decay is illustrated. For the representative data shown here, the concentrations of methylene blue, N-methyldiethanolamine, and diphenyliodonium chloride were 0.00011 M, 0.013 M, and 0.0010 M, respectively. The reaction temperature was 50°C and the capillary cell geometry was used.

### 4.3.1. Thin Film Experiments

To investigate the effect of oxygen on the consumption of the methylene blue dye, the first set of fluorescence monitoring experiments was performed using the thin film geometry. Figure 4.3 is a plot of methylene blue photobleaching constant (t<sub>1</sub> in Equation 4.1) as a function of the percentage air in the purge stream. Since the gas stream flowed steadily over the course of the experiment, and because the diffusion time through the thin film is small relative to the timescale of the experiment, the oxygen concentration in the sample remains constant during the experiment. As shown in the figure, the observed decay constant, t<sub>1</sub>, increases as the percent air is increased, indicating that the presence of oxygen inhibits the photobleaching reaction. This effect most likely arises from participation of the methylene blue triplet state in the photoreaction. Since triplet states are typically quenched by oxygen, the presence of oxygen limits the concentration of excited dye molecules available for participation in the dye-amine electron transfer reaction.

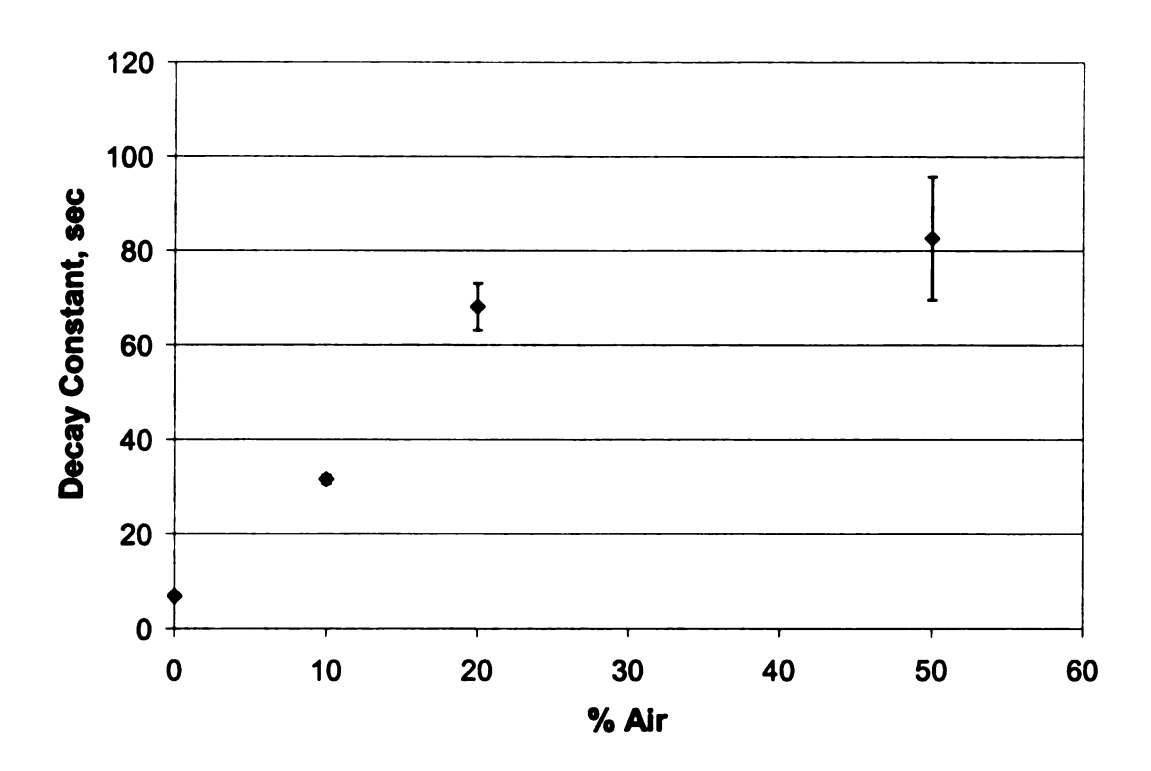


Figure 4.3: Characteristic decay constant of methylene blue fluorescence as a function of the percentage air. (The balance of the atmosphere is nitrogen.) The photobleaching rate is reduced (the decay time is increased) as the oxygen concentration is increased, suggesting a significant role for the methylene blue triplet state in the photobleaching reaction. Thin film geometry, [MB] = 0.00011 M, [MDEA] = 0.012 M, [DPI] = 0.0010 M. I<sub>a</sub> at 647.1 nm = 40 mW/cm<sup>2</sup>, T = 25°C. Error bars represent one standard deviation.

Figure 4.4 illustrates how the methylene blue fluorescence decay profile is affected by the presence of each component. The data in this figure demonstrate the photobleaching behavior in an environment containing 20% air/80% nitrogen (and thus an oxygen concentration of just over 4 mol%). Note that the methylene blue alone undergoes slow photobleaching with a relatively long time constant ( $t_1 = 154$  seconds). The addition of the iodonium salt to the methylene blue slows the photobleaching considerably, and the time constant increases to 268 seconds. This inhibition can be attributed to the dye-regeneration abilities of the diphenyliodonium chloride, as already outlined in Figure 4.1. In contrast, the addition of N-methyldiethanolamine to the methylene blue increases the photobleaching rate significantly, reducing the time constant from 154 seconds to 54 seconds. Finally, the addition of diphenyliodonium chloride to the two-component MB-MDEA system slows the photobleaching (again because of dve regeneration); the time constant when all three components are present is 68 seconds. The results of these experiments in a controlled air/nitrogen atmosphere further support to the mechanism proposed previously (Figure 4.1).

It is worth noting that oxygen itself can re-oxidize the reduced, colorless form of methylene blue back to its original state.<sup>12</sup> However, this oxygen-dye reaction affects all four trials mentioned above equally, so it has no impact on the overall conclusions.

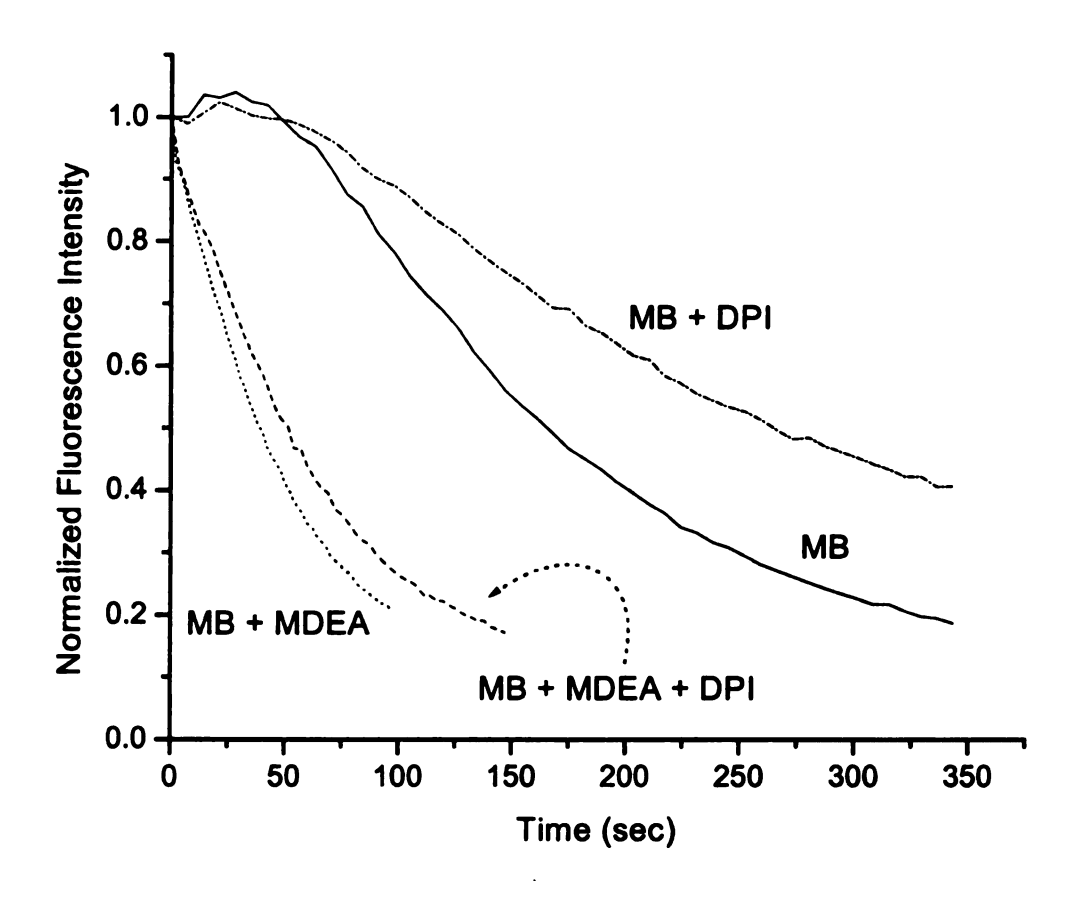


Figure 4.4: Effect of each component on decay of methylene blue steady state fluorescence in 20% air atmosphere. Thin film geometry, [MB] = 0.00011 M, [MDEA] = 0.012 M, [DPI] = 0.0010 M.  $I_a$  at 647.1 nm = 40 mW/cm<sup>2</sup>, T = 25°C. Each curve is the average of multiple trials.

### 4.3.2. Capillary tube experiments

The second set of experiments was performed using a capillary geometry. Since the capillary tubes were filled in ambient air, the samples were saturated with oxygen (organics typically contain  $\sim 2 \times 10^{-3}$  M oxygen at saturation 13). Figure 4.5 illustrates the effect of each of the three components on the photobleaching rate in the capillary geometry. In a previous study of the photobleaching of the MB/MDEA/DPI system in the absence of oxygen, any of the four possible component combinations (MB, MB/MDEA, MB/DPI, and MB/MDEA/DPI) exhibited bleaching of the methylene blue. In contrast, Figure 4.5 illustrates that, in the capillary geometry, samples containing methylene blue alone and the combination MB/DPI exhibit no photobleaching at all. However, the combinations MB/MDEA and MB/MDEA/DPI both show rapid consumption of the methylene blue dye, as evidenced by the decline in the dye fluorescence. These data indicate that, in oxygen-saturated solutions, amine is required for methylene blue photobleaching to occur. As we will discuss at more length later in the paper, we attribute this effect to the ability of the amine to consume the oxygen through a photo-activated chain reaction. Without this amine-mediated pathway to consume the oxygen, oxygen quenching of the methylene blue triplet excited state inhibits the photoinitiation reaction.

In Figure 4.5, note that that addition of DPI to the MB/MDEA mixture does not have a significant effect on the photobleaching of methylene blue. In contrast, Figure 4.6 shows that the rate of photobleaching is highly sensitive to the MDEA concentration. This effect is quantified in Figure 4.7 which illustrates that the characteristic fluorescence decay time decreases rapidly with increasing amine concentration. All of these results

support the conclusion that the primary photoreaction occurs between the MB dye and the MDEA. As mentioned previously, the DPI has a role in a secondary, non-photoinduced reaction.

Figure 4.8 contains a plot of the exponential decay constant, t<sub>1</sub>, as a function of the DPI concentration for experiments performed in the capillary geometry. Our previous results<sup>1</sup> for oxygen-free thin film systems showed that increasing the DPI concentration inhibited the consumption of methylene blue. In contrast, Figure 4.8 shows that the characteristic decay time for the methylene blue fluorescence decay actually decreases slightly when the DPI concentration is increased over the range 0 M to 0.005 M. This result is intriguing for two reasons. First, it appears to contradict the proposed role of the iodonium salt as a regenerator of the methylene blue dye. Secondly, recall that in Figure 4.5, the MB/DPI combination was shown to produce no photobleaching. It is surprising that increasing the onium salt concentration is able to affect the bleaching reaction at all.

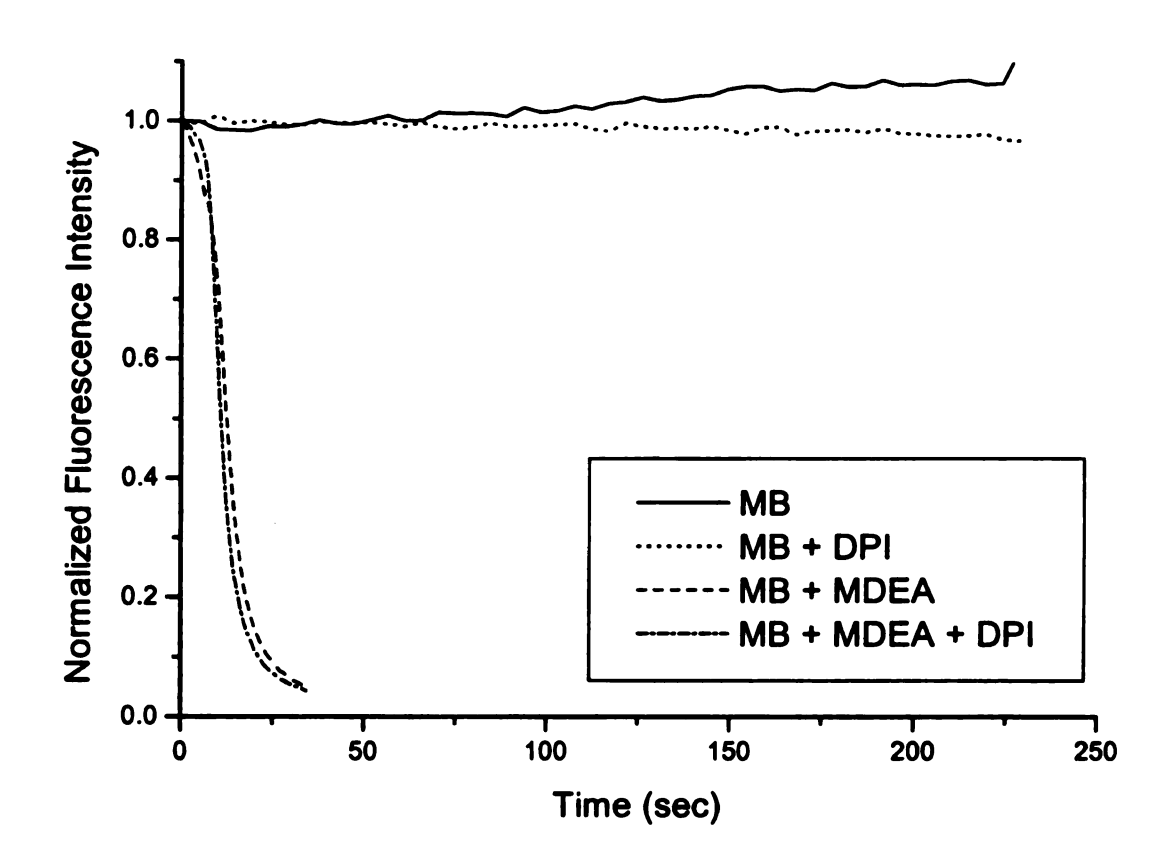


Figure 4.5: Decay of methylene blue fluorescence in the presence of amine and iodonium salt. Methylene blue alone (MB), and methylene blue with diphenyliodonium chloride (DPI) do not show any decay in fluorescence over 250 seconds. The addition of N-methyldiethanolamine (MDEA) to the system produces rapid consumption of methylene blue. Capillary geometry, methylene blue 0.00011 M, N-methyldiethanolamine 0.013 M, diphenyliodonium chloride 0.0010 M, 50°C.

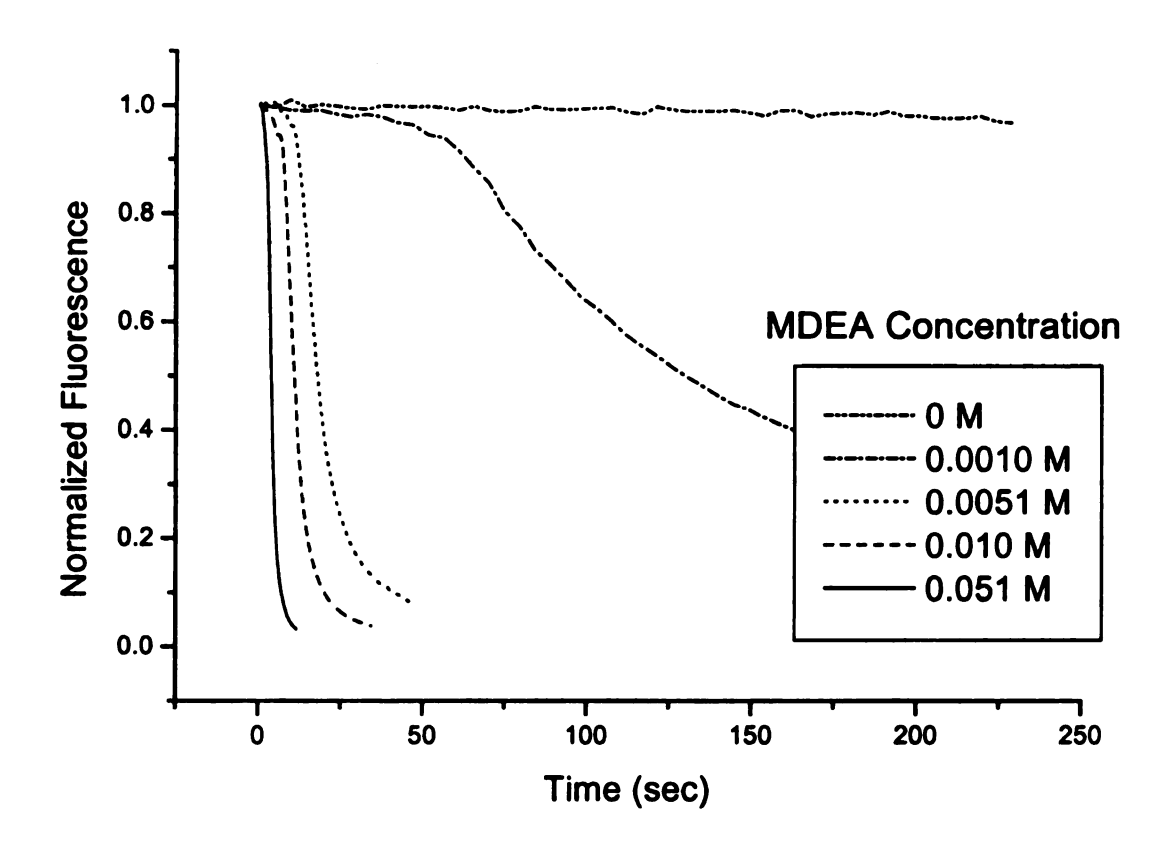


Figure 4.6: Effect of amine concentration on rate of methylene blue photobleaching. Increasing the amine concentration produces a dramatic increase in the rate of photobleaching. Capillary geometry, [DPI] = 0.001 M, [MB] = 0.00011 M, 50°C.

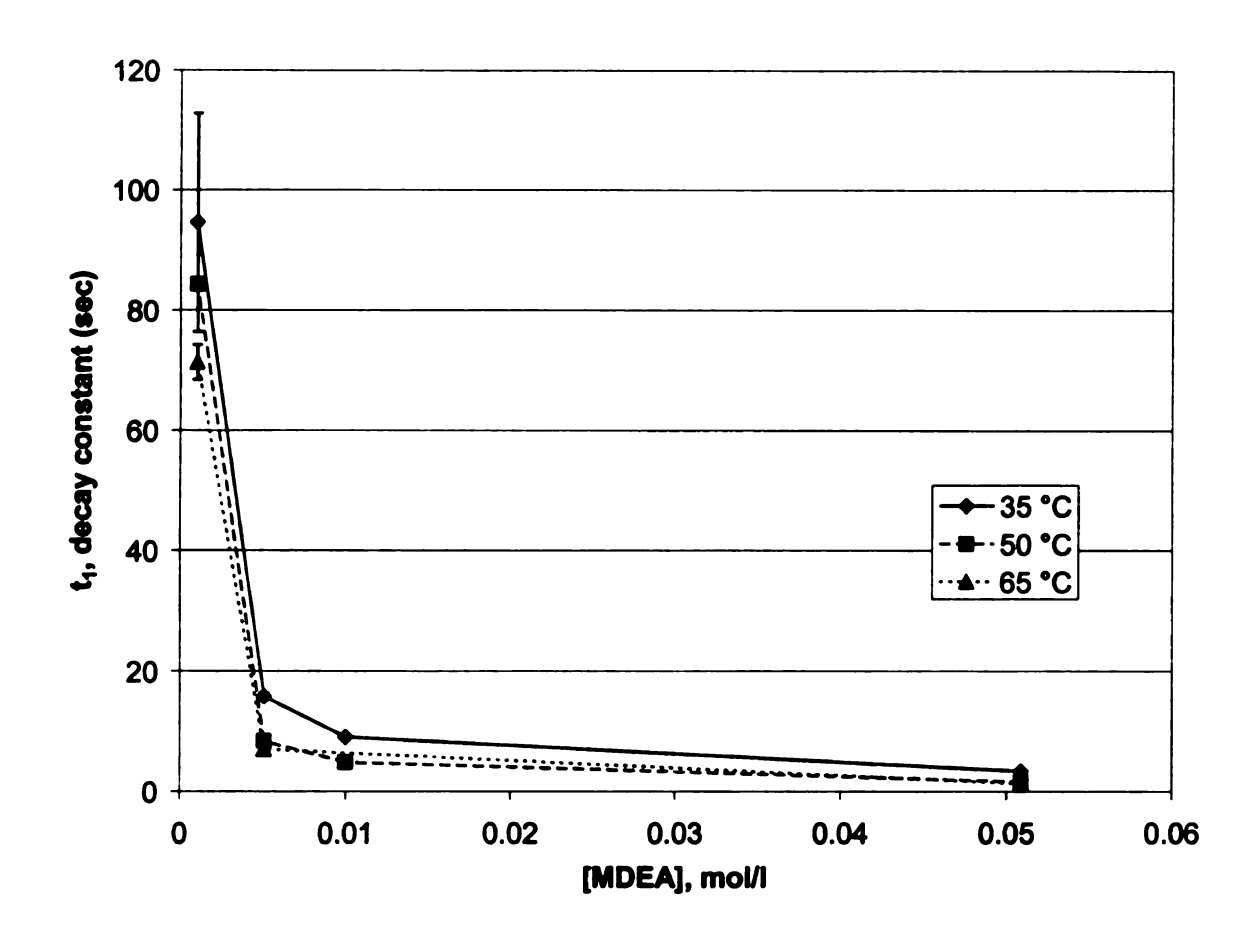


Figure 4.7: Effect of MDEA concentration on characteristic decay time. Increasing amine concentration produces a very dramatic decline in the exponential decay constant associated with the fluorescence bleaching. Capillary geometry, [MB] = 0.00011 M, [DPI] = 0.001 M.

The explanation for the effect of the DPI concentration illustrated in Figure 4.8 is rooted in complex factors affecting the shape of the decay curve. Notice that the exponential decay of the fluorescence in the capillary tubes (in Figure 4.2, for example) is preceded by a retardation period during which the fluorescence decreases only slightly. In the exponential fit, this retardation time was modeled as a pure inhibition—a period of time which must pass before the decay can begin (the timeshift factor  $x_0$  in Equation 4.2). Figure 4.9 illustrates how increasing the DPI concentration leads to a decrease in the retardation time. That is, the decay begins sooner (the timeshift factor  $x_0$  is reduced) as the DPI concentration is increased. Furthermore, Figure 4.10 reveals that for higher concentrations of DPI, although the retardation time is shorter, the overall fluorescence intensity remains higher during the retardation period.

We propose that the delay which precedes the exponential decay of the methylene blue fluorescence is caused by the presence of oxygen. Since the capillary tubes were filled in ambient air, the samples were saturated with oxygen. (It is revealing to note that the retardation period was virtually eliminated by purging the samples with nitrogen before filling the capillaries in a nitrogen environment.) Oxygen, a known triplet state quencher, can quench the excited triplet state methylene blue molecules and prevent reaction. This quenching explains the retarded decay observed at the beginning of the reaction. However, we believe that a photo-activated reaction that occurs during the retardation period consumes the oxygen, thereby allowing the rapid exponential decay of the methylene blue fluorescence after the retardation period.

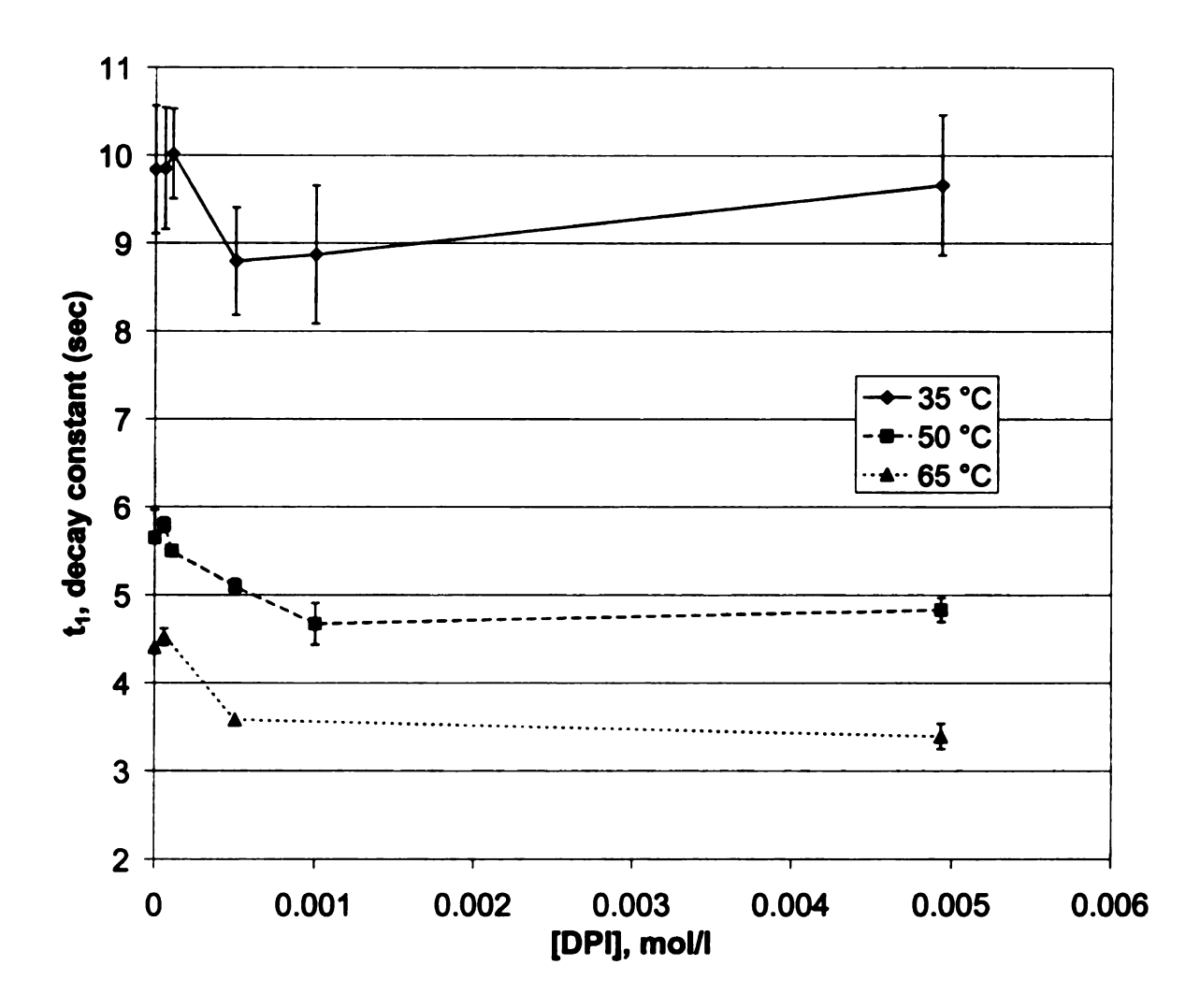


Figure 4.8: Effect of DPI concentration on  $t_1$ , the characteristic decay time for methylene blue fluorescence. Increasing DPI concentration produces a clear decrease in the characteristic decay time, indicating a faster rate of decay. The error bars shown represent one standard deviation. Capillary geometry, [MDEA] = 0.013 M, [MB] = 0.00011 M.

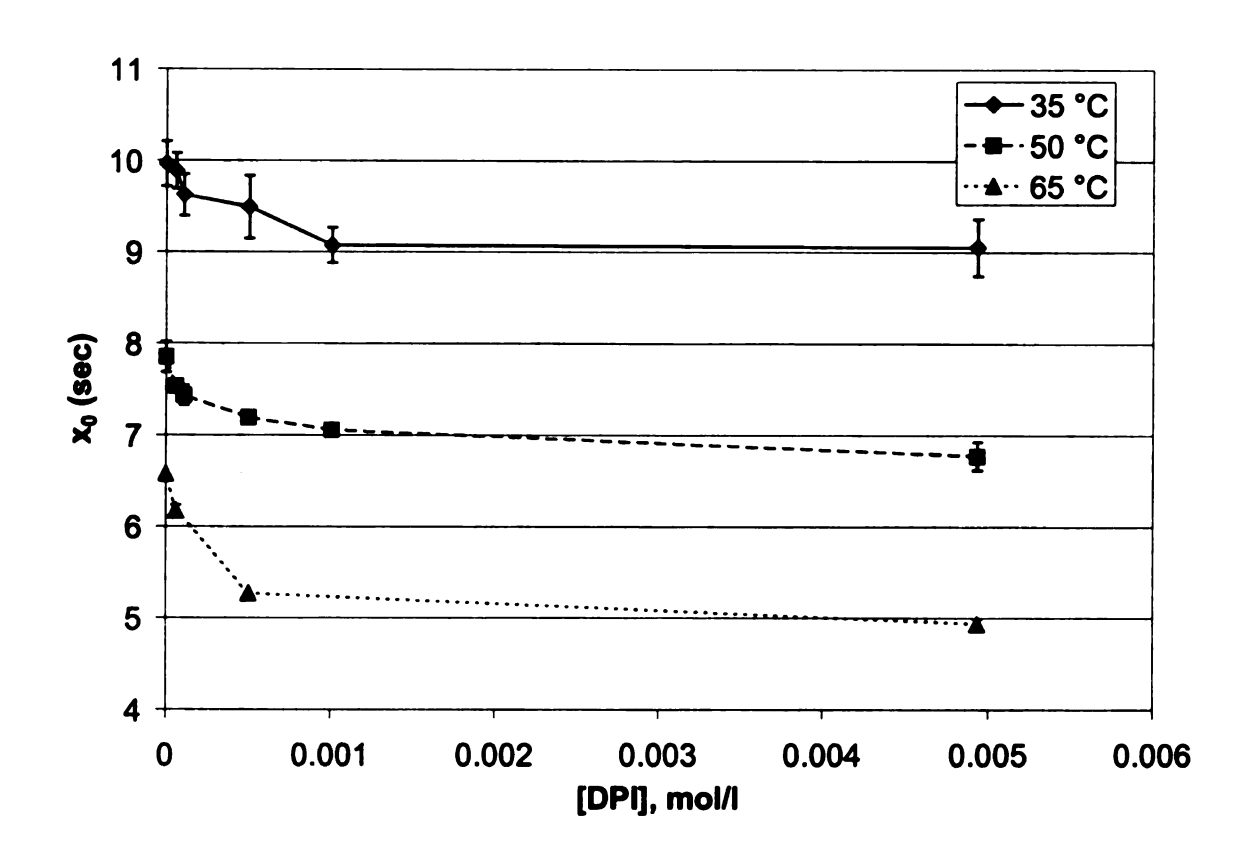


Figure 4.9: Effect of DPI concentration on  $x_0$ , a measure of the latent time before fluorescence decay. Increasing amounts of DPI cause the decay to begin slightly earlier. The error bars shown represent one standard deviation. The overall trend is not significantly affected by temperature. Capillary geometry, [MDEA] = 0.013 M, [MB] = 0.00011 M.

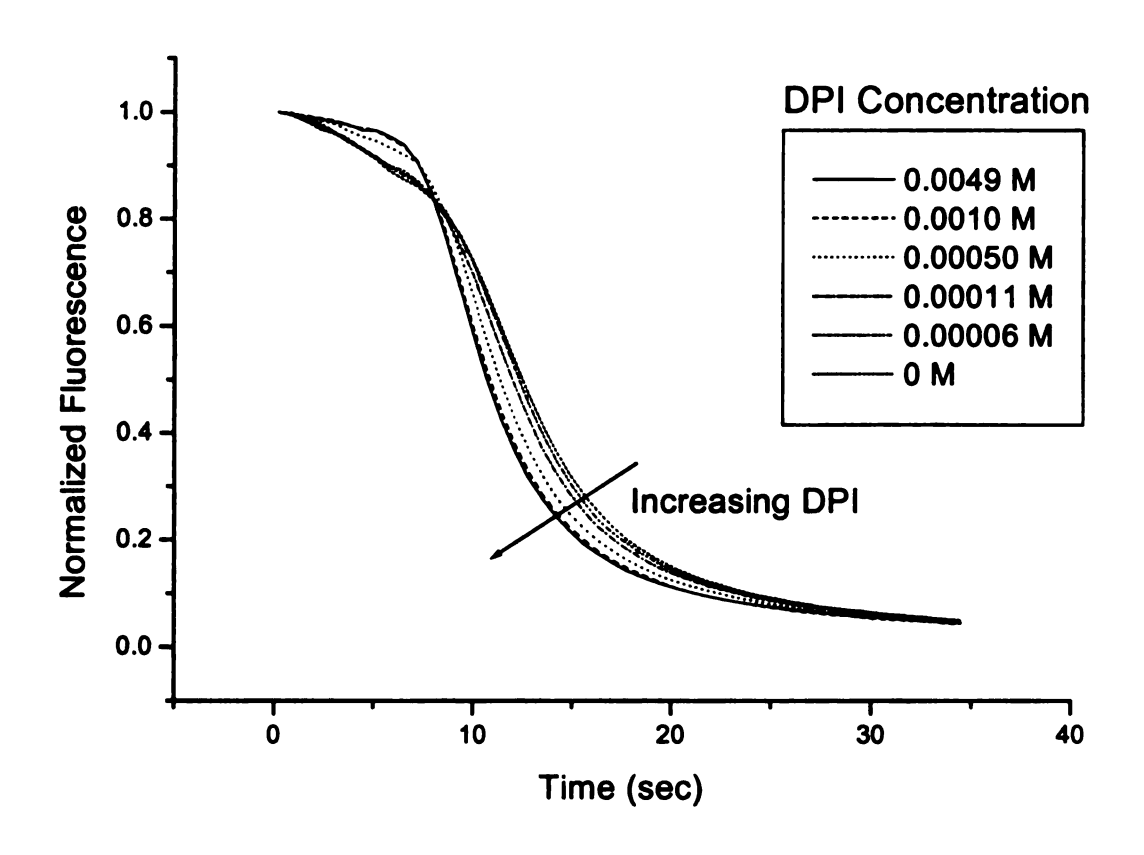


Figure 4.10: Effect of DPI concentration on rate of photobleaching. The arrow indicates the direction of generally increasing DPI concentration. Capillary geometry, 50°C, [MDEA] = 0.013 M, [MB] = 0.00011 M.

Oxygen can participate in a wide variety of reactions, and number of potential photo-induced oxygen-scavenging reactions could be envisioned. However, since tertiary amine radicals are known to be oxygen scavengers, <sup>14</sup> we believe that reduction of oxygen by a photo-generated tertiary amine radical is the most plausible explanation for the data. Our proposed oxygen-scavenging mechanism is shown in Figure 4.11. In this scheme, a tertiary amine radical is formed from electron transfer/proton transfer from the amine to the excited methylene blue cation/counterion (either a singlet state dye molecule or a triplet state which has escaped quenching). This amine radical undergoes an addition reaction with molecular oxygen, forming a peroxy radical. This radical undergoes subsequent electron transfer and proton transfer with a second amine molecule to form a peroxide and a new tertiary amine radical, which may cycle back to the beginning of the reaction. Once the oxygen is depleted via this rapid cyclic chain reaction, the triplet state methylene blue can react with the amine to produce active centers (with concomitant photobleaching of the dye).

Figure 4.11: Proposed oxygen-scavenging mechanism. The tertiary amine radical formed from reaction with the methylene blue initiates a cyclic electron transfer/proton transfer reaction which consumes molecular oxygen.

The importance of the MDEA in the oxygen-scavenging reaction is indicated by the effect of MDEA concentration on the length of the retardation time. Figure 4.6 gives an impression of the lengthening of the retardation time as the MDEA concentration is decreased. Figure 4.12 shows quantitatively how the length of the retardation time increases dramatically as the MDEA concentration is decreased. It is interesting to note that the oxygen concentration in many oxygen-saturated organic solvents is on the order of  $10^{-3}$  molar<sup>13</sup> and that the retardation times for samples with MDEA concentrations ranging from  $5 \times 10^{-3}$  M to  $5 \times 10^{-2}$  M show relatively brief retardation periods. In contrast, when the MDEA concentration is  $1 \times 10^{-3}$  M (on the same order of magnitude as the oxygen concentration), the retardation period is quite lengthy. Finally, when no MDEA is present, the retardation period is observed to be essentially infinite. As Figure 4.5 demonstrated previously, in the capillary tube geometry, no photobleaching whatsoever occurs when MDEA is absent.

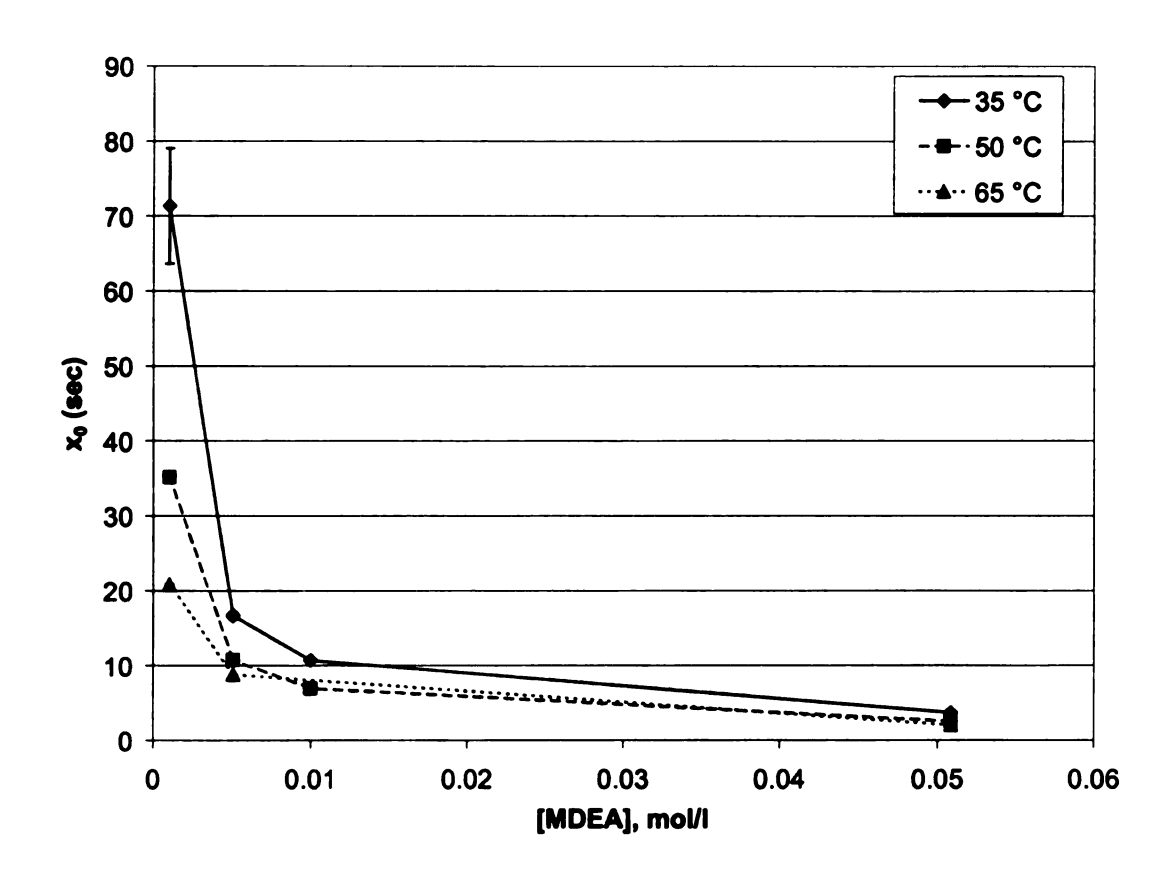


Figure 4.12: Effect of MDEA concentration on retardation time. Decreasing the MDEA concentration leads to an enormous increase in the retardation time associated with the MB photobleaching reaction, as measured by the timeshift factor  $x_0$ . Capillary geometry, [MB] = 0.00011 M, [DPI] = 0.001 M.

Recall that increasing the concentration of iodonium salt leads to both a slight increase in photobleaching rate and a decreased retardation time. These effects can be explained by the role for the iodonium salt proposed in Figure 4.1. As already discussed, one of the roles of iodonium salt is to re-oxidize the neutral methylene blue radical back to its original state. The dye-regeneration behavior of the DPI explains why the fluorescence intensity during the retardation period is higher while the retardation time itself is shortened as the DPI concentration is increased. During the retardation period, when significant amounts of oxygen are present, the methylene blue triplet state is largely quenched and the photobleaching reaction is dramatically inhibited. During this phase, the DPI regenerates the MB dye by reacting with the neutral MB radical produced in the slow photobleaching reaction. This reaction limits depletion of the MB concentration and thus maintains the MB fluorescence at a relatively high level. However, since the tertiary amine radicals which consume the oxygen are produced via reaction with methylene blue, samples with higher DPI concentrations (and thus higher effective MB concentrations) will exhibit an enhanced rate of oxygen consumption, so the retardation period will be shorter in duration.

The dye regeneration caused by the DPI also explains why the overall rate of photobleaching is enhanced with increasing concentrations of DPI. Since the amine is present in great excess in the experiments discussed here, the MB/MDEA electron transfer reaction is pseudo-first order in methylene blue. As just discussed, higher DPI concentrations lead to a greater degree of regeneration of the MB dye and thus a higher overall effective MB concentration. Therefore, those samples with higher effective initial

MB concentrations at the end of the inhibition period (the oxygen-scavenging step) will exhibit faster rates of photobleaching.

# 4.4. Summary and Conclusions

The relatively few papers published in the field of thee-component photoinitiators have advanced a number of hypotheses to explain the enhanced photoinitiation ability of these photoinitiator systems. This paper has focused on the photoinitiation ability of methylene blue, a cationic dye. This class of dyes has been virtually ignored in prior studies, and its behavior is slightly different than that of the better-studied anionic and neutral dyes. In this paper, we have offered further evidence for a proposed serial reaction mechanism for the action of the three-component system methylene blue, Nmethyldiethanolamine, and diphenyliodonium chloride. We have also provided some insight about the influence of oxygen on this system. As illustrated in Figure 4.13, the photoinitiation mechanism involves electron transfer/proton transfer from the amine to the dye as the primary photochemical reaction. The reaction occurs primarily from the triplet state of the dye. The triplet state reaction, however, is hindered by the presence of oxygen. Our proposed mechanism includes an oxygen-scavenging pathway in which the tertiary amine radicals formed in the primary photochemical process act to consume the oxygen via a cyclic reaction mechanism. The iodonium salt is an electron acceptor, acting to re-oxidize the neutral dye radical back to its original state and allowing it to reenter the primary photochemical process. This reaction also generates phenyl radicals capable of initiation. Therefore, the iodonium has a double role: to regenerate the

methylene blue and to replace the inactive, terminating dye radical with an active, initiating radical.

$$MB^{+}C\Gamma \xrightarrow{hv} [MB^{+}C\Gamma]^{1} \xrightarrow{-isc...} [MB^{+}C\Gamma]^{3}$$

$$MDEA^{0} + O_{2} \longrightarrow MDEA-OO^{0}$$

$$MDEA^{0} + MDEA$$

$$MDEA^{0} + MDEA$$

$$MDEA^{0} + MDEA-OOH$$

$$MB^{0} + DPI-CI \longrightarrow MB^{+}C\Gamma + \phi-I + \phi^{0}$$

Figure 4.13: Effect of oxygen on the proposed reaction mechanism for the three-component system MB/MDEA/DPI.

## 4.5. References and Notes

- 1. Kathryn Sirovatka Padon and Alec B. Scranton, "A Mechanistic Investigation of a Three-Component Radical Photoinitiator System Comprising Methylene Blue, N-Methyldiethanolamine, and Diphenyliodonium Chloride," J. Polym. Sci., A: Polym. Chem. 38, to appear (2000).
- 2. M. Kawabata, M. Harada, and Y. Takimoto, "Photoinitiation Systems Comprised of Dyes and Radical Precursors," J. Photopolym. Sci. Tech. 1, 222-227 (1988).
- 3. J. He and E. Wang, "Photoinitiated Polymerization by aryliodonium salt/benzophenone/ tertiary amine binary photosensitization system," *Chin. J. Polym. Sci.* 8, 44-50 (1990).
- 4. Joel D. Oxman, Andrew Ubel III, and Eric G. Larson. "Coated Abrasive Binder Containing Ternary Photoinitiator System." U.S. Patent 4,735,632, (1988).
- 5. J. P. Fouassier, D. Ruhlmann, B. Graff, Y. Takimoto, M. Kawabata and M. Harada, "A New Three-Component System in Visible Light Photo-Induced Polymerization," J. Imaging Sci. and Tech., 37, 208-210 (1993).
- 6. Kathryn Sirovatka Padon and Alec B. Scranton, "Recent Advances in Three Component Photoinitiator Systems," in *Recent Research Developments in Polymer Science*, vol. 3, S. G. Pandalai, ed. Transworld Research Network, Trivandrum, India, 369-385, (1999).
- 7. J. P Fouassier, *Photoinitiation, Photopolymerization, and Photocuring*, Hanser-Gardner, Cincinnati, (1995).
- 8. H. Meier, "Photochemistry of Dyes," in *Chemistry of Synthetic Dyes*, vol IV, K. Venkatarman, ed., Academic Press: New York, 389-515, (1971).
- 9. T. Lyubimova, S. Caglio, C. Gelfi, P. G. Righetti, and T. Rabilloud, "Photopolymerization of polyacrylamide gels with methylene blue," *Electrophoresis*, 14, 40-50, (1993).
- 10. E. Blot and C. Stock, "Road paint compositions containing an unsaturated polyester resin," U.S. Patent 5,907,003, (1999).
- 11. In the capillary experiments the maximum fluorescence was observed at 710 nm; in the thin film experiments the peak appears at 724 nm. The fluorescence peak of MB occurs at ~687 nm, but this wavelength is attenuated by the subtractive-dispersive filter stage of the spectrometer.

- 12. A. G. Cook, R. M. Tolliver, and J. E. Williams, "The Blue Bottle Experiment Revisited: How Blue? How Sweet?" J. Chem. Ed., 71, 160-161, (1994).
- 13. J. P. Fouassier, "Excited State Reactivity in Radical Polymerization Photoinitiators," in *Radiation Curing in Polymer Science and Technology, vol. II: Photoinitiating Systems*, J. P. Fouassier and J. F. Rabek, eds., Elsevier, (1993).
- 14. H. J. Hageman, "Photoinitiators and Photocatalysts for Various Polymerisation and Crosslinking Processes," in *Radiation Curing of Polymers II*, D. R. Randell, ed., Proc. 3rd annual symposium, Royal Soc. Chem., Sept. 12-14, 1990, 40-60.

## CHAPTER 5

# FUNDAMENTAL STUDIES OF THREE-COMPONENT PHOTOINITIATOR SYSTEMS CONTAINING EOSIN DYES

## 5.1. Introduction and Motivation

The preceding chapters have considered various mechanistic investigations of the three-component photoinitiator system methylene blue, N-methyldiethanolamine, and iodonium chloride. This choice of reactants simplifies the range of possible reactions in the three-component system because the positively charged methylene blue dye cannot directly react with the positively charged iodonium ion. In this chapter, this simplification is removed and studies are extended to anionic and neutral eosin dyes.

One goal of this research is to investigate the effects of dye structure on the behavior of three-component systems, particularly any differences arising from the dye charge. For this reason, the two dyes Eosin Y and Eosin Y, spirit soluble were chosen for study in the three-component system. As shown in Figure 5.1, the two dyes are essentially identical except for their charge. Eosin Y is an anionic dye (the dye moiety carries two negative charges balanced by sodium ions), while Eosin Y, spirit soluble is neutral. N-methyldiethanolamine and diphenyliodonium chloride were used as the electron donor and third components, respectively. Both of these compounds are relatively standard constituent choices for three-component systems.<sup>1</sup>

Figure 5.1: Eosin dyes

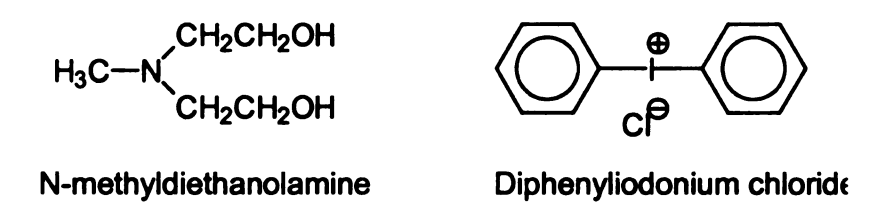


Figure 5.2: Electron donor and third component of photoinitiation system

# 5.2. Experimental

## 5.2.1. Materials

The monomer 2-hydroxyethylmethacrylate (HEMA) was obtained from Aldrich. It was treated with DeHibit (from Polysciences) to remove hydroquinone inhibitor and filtered prior to use. Eosin Y, 89%<sup>2</sup> (EY) and Eosin Y, spirit soluble, 99% (EYss) were obtained from Aldrich, and N-methyldiethanolamine (MDEA) and diphenyliodonium chloride (DPI) were obtained from Fluka. The structures are given in Figure 5.1 and Figure 5.2. All three photoinitiator components were used as received. All experiments were performed in neat monomer; no solvents were used.

The absorbance spectrum of Eosin Y is given in Figure 5.3. The spectrum for Eosin Y, spirit soluble is identical, indicating that the dye charge does not affect its absorption profile. The results below will show that the photoinitiation behavior of the two dyes is also quite similar, indicating that at least for Eosin Y, neutral and anionic dyes exhibit similar behavior.

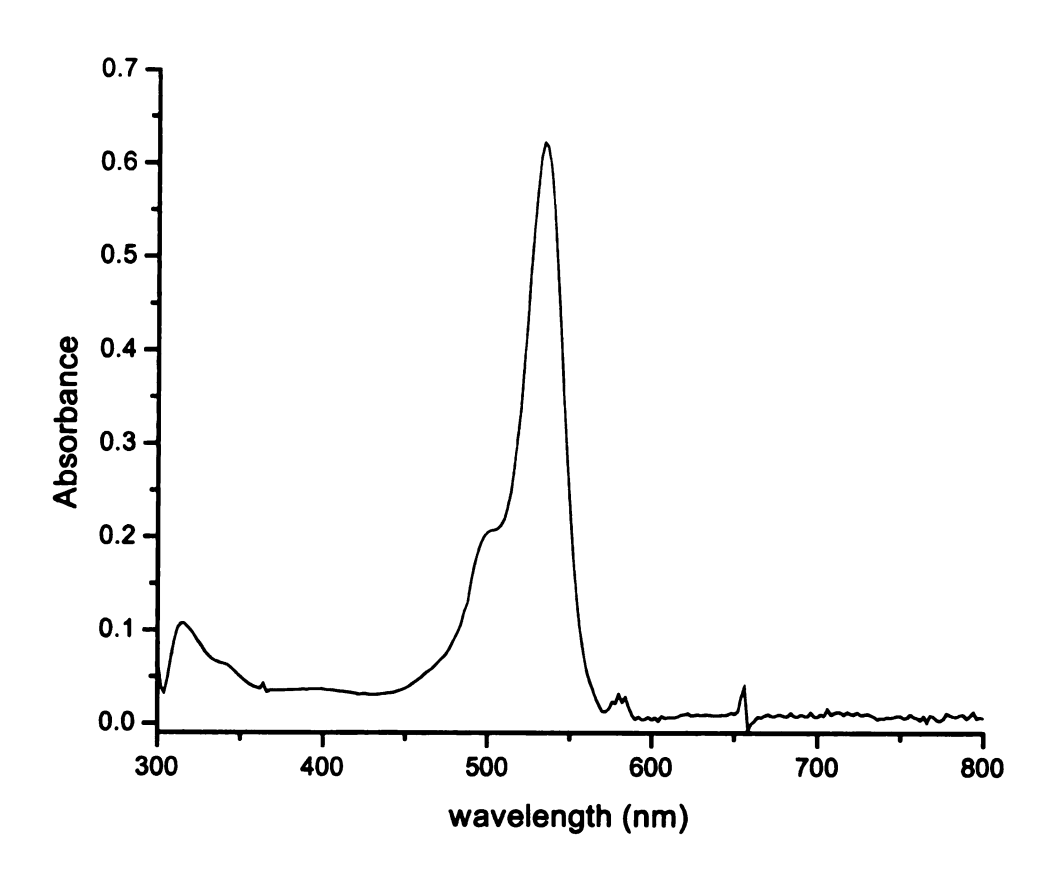


Figure 5.3: Absorbance spectrum of Eosin Y.  $1 \times 10^{-5}$  M Eosin Y in HEMA.

## 5.2.2. Photo-Differential Scanning Calorimetry

Photo-DSC was conducted using a Hewlett-Packard DSC 7 modified in-house for photo-experiments. The experimental setup is identical to that described in Chapter 3, so only a brief description will be given here. Initiation light from a 200 W Oriel mercury-xenon lamp was passed through a water filter to limit sample heating and through a glass filter to eliminate any ultraviolet-induced photoinitiation. The overlap of the lamp's spectral output and the absorbance profile of the dyes indicates that the effective incident radiant intensity was approximately 14.6 mW/cm² for the experiments with EY and 12.3 mW/cm² with EYss. (The absorption profiles of the two dyes are identical, but the lamp intensity varied slightly over time.) The average sample size was 4.4 mg. A nitrogen purge was used in the DSC to eliminate oxygen inhibition of the polymerization.

# 5.2.3. Time-Resolved Steady-State Fluorescence Monitoring

Time-resolved steady state fluorescence monitoring experiments were performed using a Coherent Innova-70 Argon ion laser (514.5 nm line) as the excitation source. The fluorescence was collected using a Spex Triplemate two stage triple monochromater equipped with a 1024-pixel OMA 4 liquid-nitrogen-cooled CCD detector. Fifty fluorescence spectra in the wavelength range ~450-700 nm were taken at time intervals chosen to capture the entire decay of the eosin fluorescence. The resulting pseudo-three-dimensional fluorescence profile was sliced at the peak of fluorescence to yield a profile of fluorescence intensity versus time. This profile can be fit to an exponential function to determine and compare the characteristic decay constants. As will be discussed later, the fluorescence decay is characterized by two very different time constants. For this reason,

decay profiles were observed over a period of about five seconds to capture the rapid decay characteristics as well as over a period of fifty seconds to observe the longer decay constants. (Since practical concerns about the size of the dataset generated limited us to fifty fluorescence spectra per experiment, this approach was necessary because fifty evenly-spaced spectra were not sufficient to capture all characteristics of the decay.) The integration time was 50 msec in all cases, but the time elapsed between individual spectra was varied to permit observation of different time scales.

Because two different reaction time scales operate in this system, in most cases the fluorescence profiles obtained were fit to a sum of exponential functions:

$$y = y_0 + A_1 \exp\left(\frac{x}{t_1}\right) + A_2 \exp\left(\frac{x}{t_2}\right)$$
 Equation 5.1.

In a few cases only one time scale was readily evident, so the fluorescence profiles were fit to a single exponential function:

$$y = y_0 + A_1 \exp\left(\frac{x}{t_1}\right)$$
 Equation 5.2.

Since the thin film fluorescence monitoring apparatus was also fully described in Chapter 3, again only a brief description is given here. The apparatus consists of an enclosed glass cell with a flat bottom upon which a thin film sample is supported by a piece of microporous polyethylene. The cell is equipped with a recirculating bath in order to maintain a consistent sample temperature. A nitrogen inlet port allows control of the atmosphere. The thin film sample is illuminated with the laser beam from beneath, and the fluorescence is collected from above. In these experiments, the intensity of laser light striking the sample was approximately 50 mW/cm<sup>2</sup>.

# 5.3. Results and Discussion

# 5.3.1. Photo-Differential Scanning Calorimetry

The DSC results reveal that the photopolymerization behavior for the eosin dyes is quite similar to that observed for methylene blue. As shown in Table 5.1, the fastest rate of cure, as measured by the time to reach the peak of the exotherm, is obtained when all three components are present. The next-fastest cure rate is obtained with the dye/amine combination, and the dye/iodonium pair exhibits the slowest overall rates. These results are consistent with the results from the methylene blue system, which also showed that the fastest rate was obtained in the presence of all three components and that the dye/amine pair was faster than the dye/iodonium pair.

The DSC results give some indication that EY may be a more effective initiator component than EYss. This is difficult to evaluate, however, due to variation in the intensity of the light source (14.6 mW/cm² versus 12.3 mW/cm² for EYss). In addition, the concentrations of amine are very slightly higher for the EY samples than for the EYss samples (the MDEA concentrations were 0.013 M and 0.012 M, respectively). For the dye/MDEA/DPI and dye/MDEA systems, the differences in photocuring behavior between the two dyes are relatively minor and are likely attributable to the slight variations in light intensity and component concentration just described. However, the sample initiated by EYss/DPI reaches its peak exotherm almost ten minutes after that initiated by the EY/DPI pair. This difference is probably significant; some possible reasons for the difference will be addressed in section 5.3.2.4.

Table 5.1: Time to reach exotherm peak for eosin initiator systems

Components	Eosin Y <sup>†</sup> 14.6 mW/cm <sup>2</sup>	Eosin Y, spirit soluble <sup>‡</sup> 12.3 mW/cm <sup>2</sup>
Dye + MDEA + DPI	11.0 min	13.7 min
Dye + MDEA	14.4 min	17.6 min
Dye + DPI	16.8 min	26.3 min

<sup>†: [</sup>EY] = 0.00010 M, [MDEA] = 0.013 M, [DPI] = 0.001 M

# 5.3.2. Time-Resolved Steady-State Fluorescence Monitoring

Since fluorescence intensity is generally directly proportional to fluorophore concentration, the fluorescence monitoring technique allows the dye concentration to be observed in real time as the dye is consumed during the photochemical reaction. Figure 5.4 shows the photobleaching behavior of Eosin Y, spirit soluble in all four possible component combinations. Notice first that illuminating EYss in HEMA in the absence of other components does result in very slow photobleaching of the dye fluorescence. Determining the mechanism of this photodegradation was not a goal of this work, but it may be caused by direct photoscission of bonds. The component combination EYss/MDEA results in relatively slow photobleaching. In contrast, the combination EYss/DPI produces extremely fast photobleaching. Finally, the combination of all three components produces a very interesting result: the early portion of the decay curve appears similar to the EYss/DPI curve, whereas the later section of the curve is similar in shape to the EYss/MDEA curve. The shape of the curve suggests that the MDEAmediated bleaching mechanism takes over after the DPI is mostly consumed. This apparent two-phase bleaching is discussed in further detail below.

The relative rates of photobleaching for the various component combinations are intriguing. Recall that the DSC photopolymerization results indicated that the fastest

<sup>\*: [</sup>EYss] = 0.00010 M, [MDEA] = 0.012 M, [DPI] = 0.0010 M

polymerization arose from the EYss/MDEA/DPI combination, followed successively by EYss/MDEA and EYss/DPI. The photobleaching results show a different trend. The EYss/MDEA couple shows very slow photobleaching compared to the dye/iodonium pair. This seemingly anomalous result suggests that while the iodonium salt rapidly bleaches the eosin dye, the reaction is rather inefficient in producing active radicals. A similar result was observed for the system ketocoumarin dye/MDEA/diphenyliodonium hexafluoroantimonate by Fouassier and coworkers.<sup>3</sup>

The results shown in Figure 5.4 suggest that the three-component initiation system displays two distinct time scales in photobleaching: a short time scale representing the EYss/DPI reaction and a long time scale representing the EYss/MDEA reaction. The data shown in Figure 5.4 come from an experiment with data points spaced ~1 second apart. In order to observe the short time scale, it was necessary to repeat the experiment with more closely spaced data points. The results are shown in Figure 5.5. The figure shows clearly that the on the rapid time scale, the rate of decay is faster for EYss/DPI than for EYss/DPI/MDEA. (This difference in photobleaching rate will be discussed below.) However, as Figure 5.4 shows, after about fifteen seconds, the overall amount of dye consumed is greater for the three-component system than for the dye/iodonium pair. This is probably due to additional photobleaching caused by reaction of the dye with the amine in the reaction in the sample containing all three components.

Each of the curves was fit to one of the exponential functions given in Equation 5.1 and Equation 5.2. Generally, data from the long experiments were used to determine the longer time constants, whereas data from the shorter experiments were more reliable in determining the shorter time constants. In most cases the results of three distinct trials

were averaged to determine the characteristic time constant of bleaching and its standard deviation. The time constants determined for the decay profiles shown in Figure 5.4 and Figure 5.5 are given in Table 5.2.

It is necessary to exercise discretion when interpreting the photobleaching data for the EYss/MDEA/DPI system. The sample containing EYss alone shows two bleaching constants: a significant long, slow reaction and an extremely rapid decay that is apparent in Figure 5.4 for only for a few milliseconds and which contributes only a small percentage to the overall bleaching. (In fact, this rapid decay is difficult to resolve from noise in the data.) This "shock" decay of a few dye molecules when the light is first turned on decay constant may arise from an impurity or may be inherent to the eosin dye, but it is so unimportant that it may be safely neglected. A similar short decay constant which appears in the EYss/MDEA sample is most likely also due to this rapid "shock" bleaching of the eosin dye. However, the short time constant which appears in the EYss/DPI sample is not attributable to this shock mechanism, since the weighting constants  $A_1$  and  $A_2$  for the two similar time constants are 0.47 and 0.30, respectively. Since the rapid 0.37 second decay constant contributes 60% of the overall bleaching, it cannot be assigned to the "shock" mechanism which is observed in the presence of EYss alone. Instead, it seems likely that two similar mechanisms with slightly different time constants work to consume the dye in the EYss/DPI system. As will be discussed below, the two slightly different time constants may arise from the asymmetric nature of the aromatic eosin structure.

The EYss/MDEA/DPI system shows two time constants:  $t_1 = 0.54 \pm 0.02$  seconds and  $t_2 = 24 \pm 6$  seconds. Since the short time constant was determined in this case from a

fit of a single exponential (Equation 5.2) to data obtained over a short observation time (a few seconds), the time constant observed most likely represents a combination of the two EYss/DPI time constants reported in Table 5.2. (This time constant is most likely also affected by the presence of MDEA, as will be discussed in section 5.3.2.3 below.) The long time constant is clearly attributable to the EYss/MDEA reaction. This analysis of the time constants confirms the initial conclusions made from visual inspection of Figure 5.4 and Figure 5.5: the bleaching of the three-component system displays characteristics of both the EYss/DPI reaction and the EYss/MDEA reaction.

Table 5.2: Average photobleaching constants for component combinations

Component Combination	Decay constant ± standard deviation (seconds)
Eosin Y, spirit soluble	$t_1 = 0.39^{\dagger}$ $t_2 = 28 \pm 8$
EYss/MDEA	$t_1 = 0.30 \pm 0.03$ $t_2 = 21 \pm 2$
EYss/DPI	$t_1 = 0.37 \pm 0.04$ $t_2 = 1.2 \pm 0.1$
EYss/DPI/MDEA	$t_1 = 0.54 \pm 0.02$ $t_2 = 24 \pm 6$

<sup>†:</sup> Only one data set had sufficiently low noise to fit this decay constant, so no standard deviation is available.

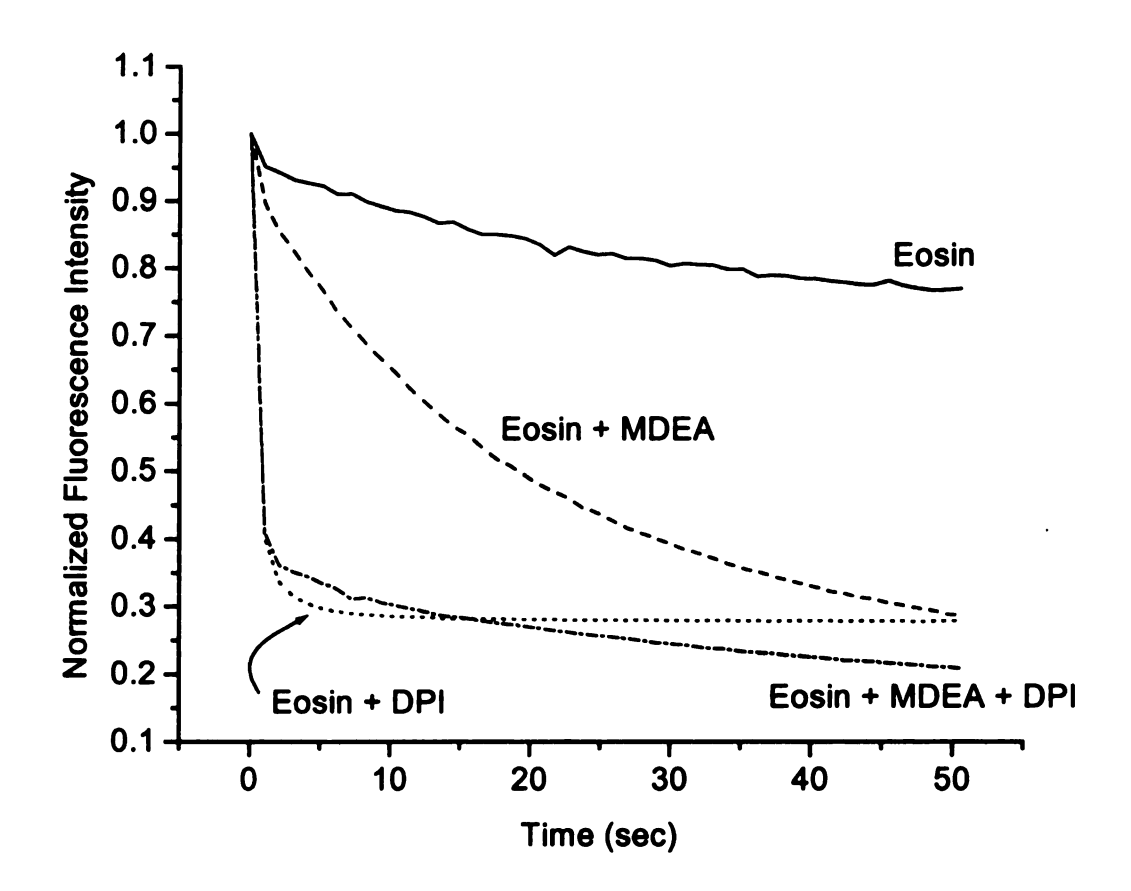


Figure 5.4: Decay of Eosin Y, spirit soluble steady-state fluorescence. [EYss] = 0.0001 M, [MDEA] = 0.012 M, [DPI] = 0.0010 M, all in HEMA, T =  $25^{\circ}$ C,  $I_a = 50$  mW/cm<sup>2</sup>. Long observation time. Each curve represents the average of three trials.

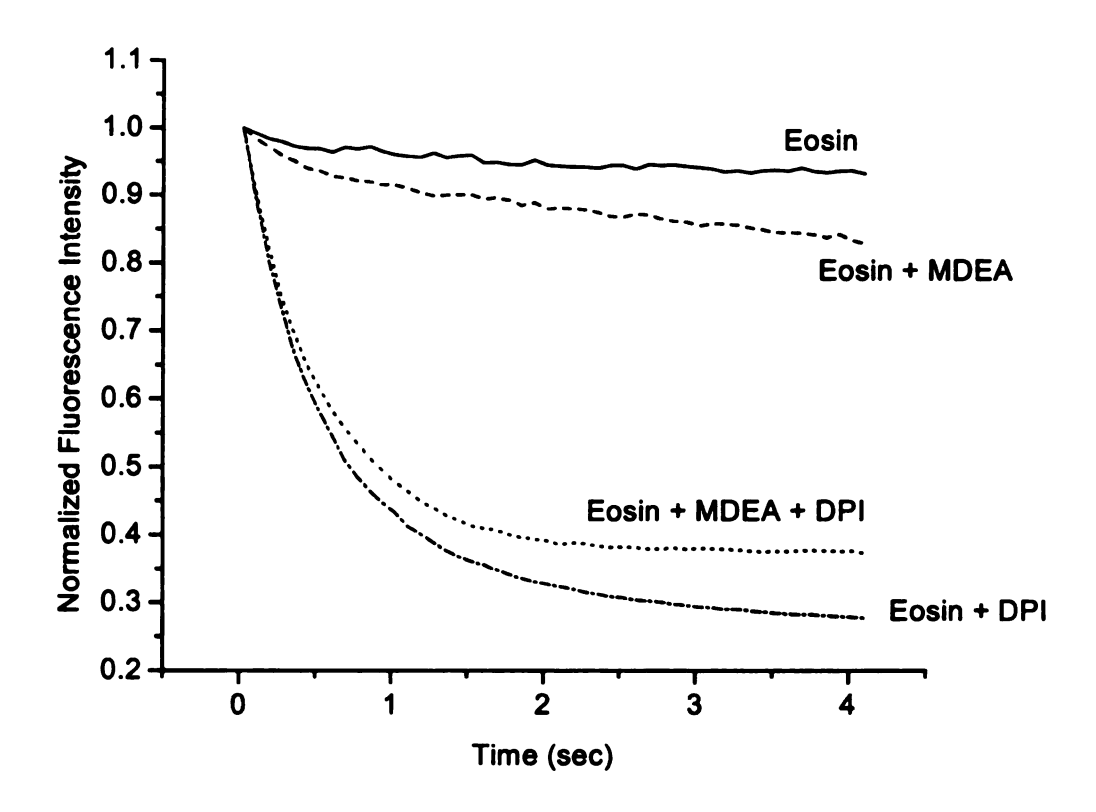


Figure 5.5: Decay of Eosin Y, spirit soluble steady-state fluorescence. [EYss] = 0.0001 M, [MDEA] = 0.012 M, [DPI] = 0.0010 M, all in HEMA, T =  $25^{\circ}$ C,  $I_a = 50 \text{ mW/cm}^2$ . Short observation time. Each curve represents the average of three trials.

#### 5.3.2.1. Mechanisms for Direct Reaction

The results presented above suggest that Eosin Y, spirit soluble is capable of direct photochemical reaction with both DPI and MDEA. The reaction with MDEA, an electron donor, most likely proceeds as illustrated in Figure 5.6 This is the well-known electron transfer/proton transfer reaction observed in a host of dye/electron donor pairs. In this reaction, the photoexcited dye (typically in its triplet state) forms an exciplex with the amine electron donor. An electron is transferred within the exciplex, and rapid subsequent proton transfer from amine to dye balances the charges. The amine radical is active for initiation, whereas the dye-based radical is generally a terminator. As shown in Figure 5.7, the dye-based radical may undergo disproportionation with a second dye molecule or may react with an additional amine molecule to form what is commonly termed the "leuco." or colorless form of the dye. 5.6

The process by which direct photooxidation reactions of dyes with iodonium salts occurs is not as well known as the photoreduction process just described. However, as illustrated in Figure 5.8, the reaction generally involves electron transfer from the photoexcited triplet dye to the iodonium cation, followed by rapid decomposition of the neutral iodonium radical. In the case of diphenyliodonium chloride, the end result is a phenyl radical and a molecule of phenyl iodide.

The photopolymerization results showed that the EYss/DPI system produced initiating radicals less effectively than the EYss/MDEA system. This seems unusual, since the relatively small, mobile phenyl radical might be expected to be fairly reactive. A possible explanation of this observation is that the phenyl radical may be able to

combine with the dye cation-radical, thus limiting the efficiency of this reaction as a photoinitiation route.

The origin of the electron transferred from dye to iodonium is not clear. However, in the cationic photoinitiation system anthracene/bis(4-dodecylphenyl) iodonium hexafluoroantimonate, Nelson *et al.*<sup>7</sup> suggest that an aromatic  $\pi$  electron from the excited anthracene aromatic ring structure is transferred to the iodonium salt. Delocalization of the electron stabilizes the resulting radical and makes it likely that an aromatic ring electron rather than an electron derived from a substituent would be donated in the eosin/iodonium system as well. Since the Eosin Y aromatic ring structure is asymmetrical, the cloud of shared  $\pi$  electrons in the aromatic system should also be asymmetrical. It is possible that the two slightly different time constants for EYss/DPI reaction described above may arise from electron donation from different points on the EYss ring structure, the influence of steric hindrance, or from non-superimposable molecular orientations during collision.

Eosin Y, spirit soluble 
$$\xrightarrow{hv}$$
 [EYss]\*

[EYss]\* + MDEA  $\longrightarrow$  [Exciplex]\*

Br

HO

Br

H3C

CH2CH2OH

CH2CH2OH

CH2CH2OH

Figure 5.6: Proposed direct reaction between Eosin Y, spirit soluble and MDEA

EYss—H
$$^{\bullet}$$
 + EYss—H $^{\bullet}$  — EYss—H $_2$  + EYss

EYss—H $^{\bullet}$  + RH — EYss—H $_2$  + R $^{\bullet}$ 

Figure 5.7: Formation of leuco dye

Figure 5.8: Proposed direct reaction between Eosin Y, spirit soluble and diphenyliodonium chloride

#### 5.3.2.2. Effect of Iodonium Concentration

Figure 5.9 is a plot of the short-time EYss fluorescence decay profiles at various concentrations of DPI. It shows the expected increase in rate of photobleaching with increasing DPI concentration, confirming that direct reaction occurs between the EYss dye and the iodonium salt.

Figure 5.10 illustrates how the long-time fluorescence decay profile changes as the iodonium salt concentration is varied with the MDEA concentration held constant at 0.01 M. At the highest iodonium concentration (5 mM), the EYss is completely consumed by reaction with the DPI, and the amine has virtually no effect. (In fact, the time constants for the sample with 5 mM DPI are almost identical to those cited in Table 5.2 for the EYss/DPI pair.) Conversely, at low iodonium concentrations, (0.06 mM and 0.11 mM) the photobleaching curves are almost indistinguishable from the curve for EYss/MDEA alone.

The shape of the curves offers support for the assignment of eosin bleaching to two distinct reactions, as suggested earlier. The iodonium salt is responsible for the rapid, early stages of the bleaching, and the amine produces the decay observed on longer time scales. Notice in Figure 5.10 that the amount of bleaching produced by the rapid reaction decreases as the iodonium concentration decreases. Furthermore, as illustrated in Figure 5.11, the long time constant observed in the decay profiles does not vary with iodonium concentration, indicating EYss/MDEA reaction is not influenced by DPI. With the exception of the highest-DPI sample, where the long time constant is not observed, the long time constant in the three-component systems is equal, within experimental error, to the time constant reported in Table 5.2 for the EYss/MDEA pair.

Prior work has suggested that in many cases, the role of the iodonium salt in three-component systems is to re-oxidize the dye radical formed from reaction with the amine, resulting in regeneration of the original dye and production of an active phenyl radical in place of the terminating dye radical. However, the data in Figure 5.11 show that this mechanism is not operative in this particular system. If it was, we would expect to see an increase in the time constant for EYss/MDEA reaction as the DPI concentration was increased. (Such a trend was observed with the methylene blue/MDEA/DPI system discussed in Chapter 3.) With the concentrations and component choices used in this work, the time scales of the EYss/DPI and EYss/MDEA photobleaching reactions are apparently so different that the DPI is consumed too rapidly to participate in this proposed iodonium-mediated dye regeneration reaction.

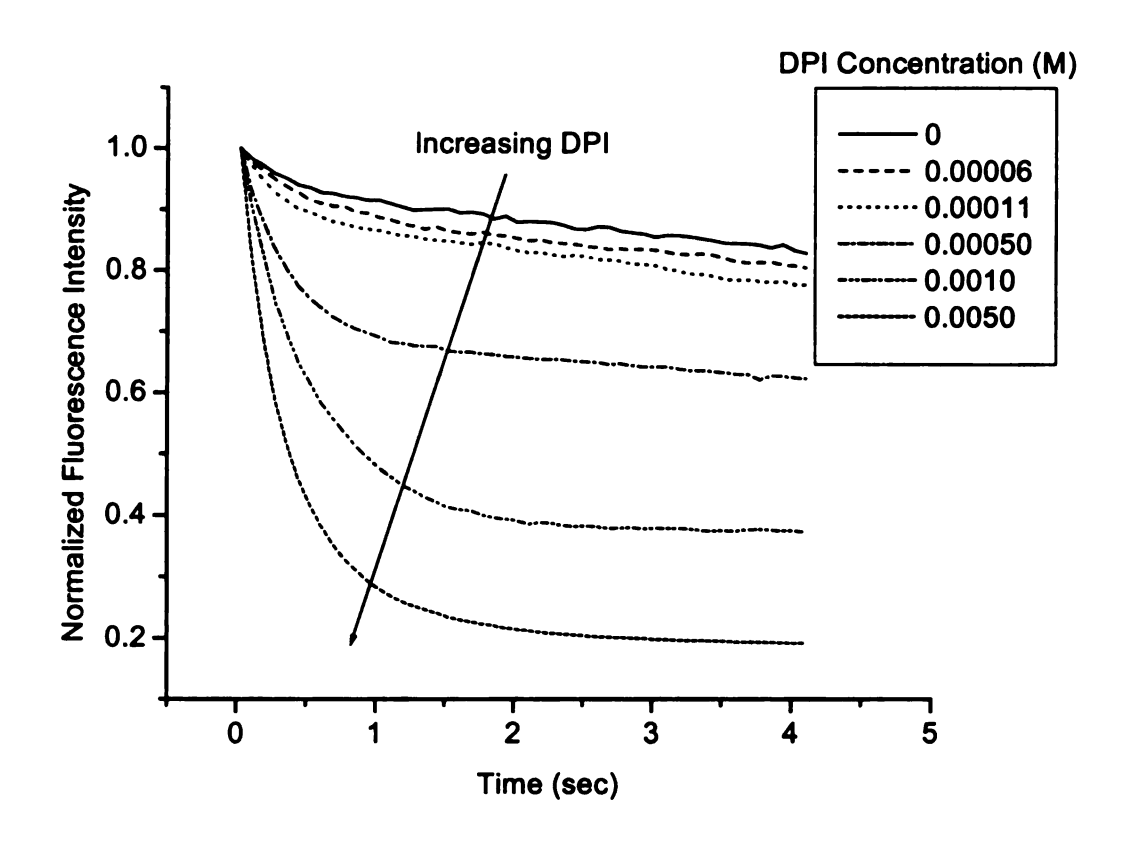


Figure 5.9: Effect of DPI concentration on Eosin Y, spirit soluble photobleaching. The rate of photobleaching increases as DPI concentration is increased. [EYss] = 0.0001 M, [MDEA] = 0.012 M, all in HEMA, T = 25°C,  $I_a = 50$  mW/cm<sup>2</sup>. Short observation time.

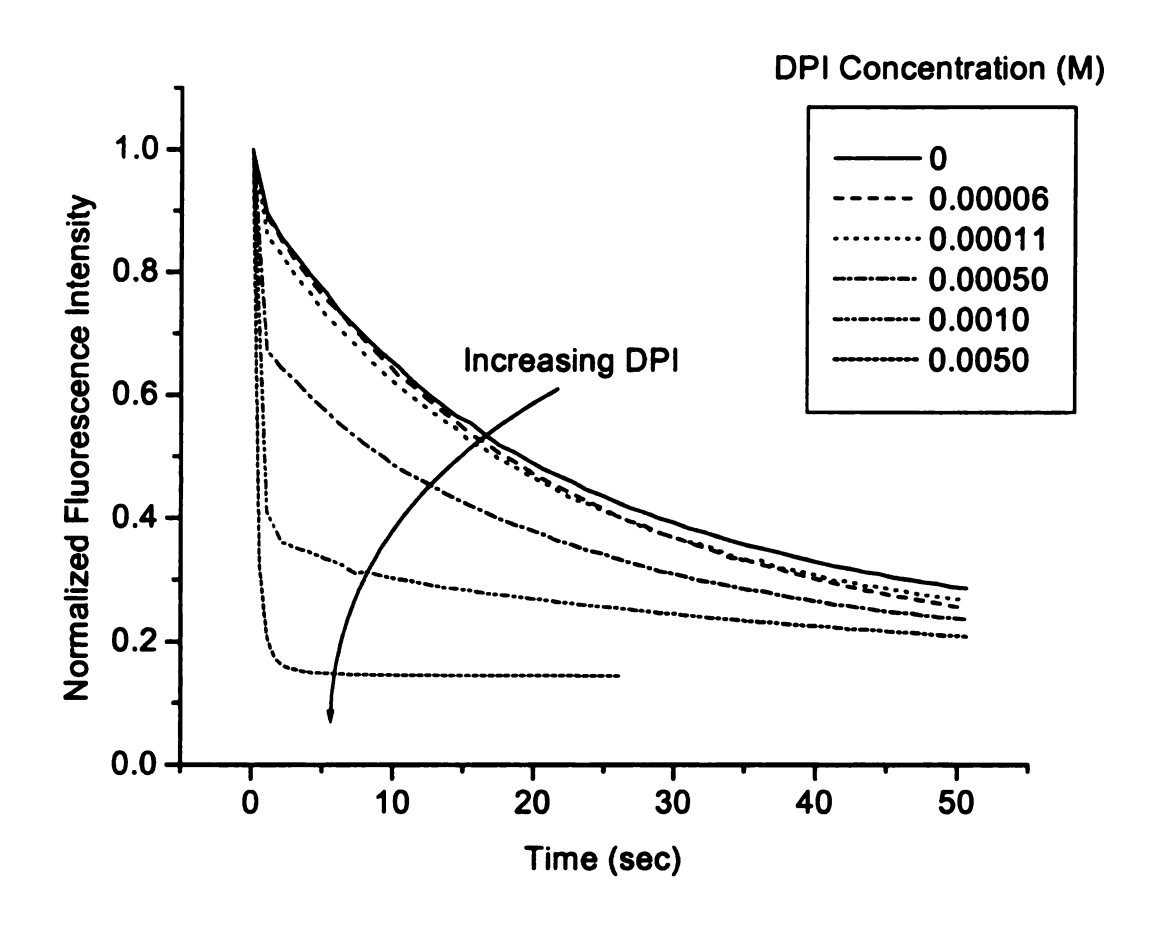


Figure 5.10: Effect of DPI concentration on Eosin Y, spirit soluble photobleaching. At high DPI concentrations, the photobleaching profile exhibits the characteristics of the EYss/DPI reaction, whereas at low DPI concentrations, the profile has the characteristics of the EYss/MDEA reaction. Both photobleaching mechanisms are apparent at intermediate DPI concentrations. [EYss] = 0.0001 M, [MDEA] = 0.012 M, all in HEMA, T = 25°C,  $I_a = 50$  mW/cm<sup>2</sup>. Long observation time.

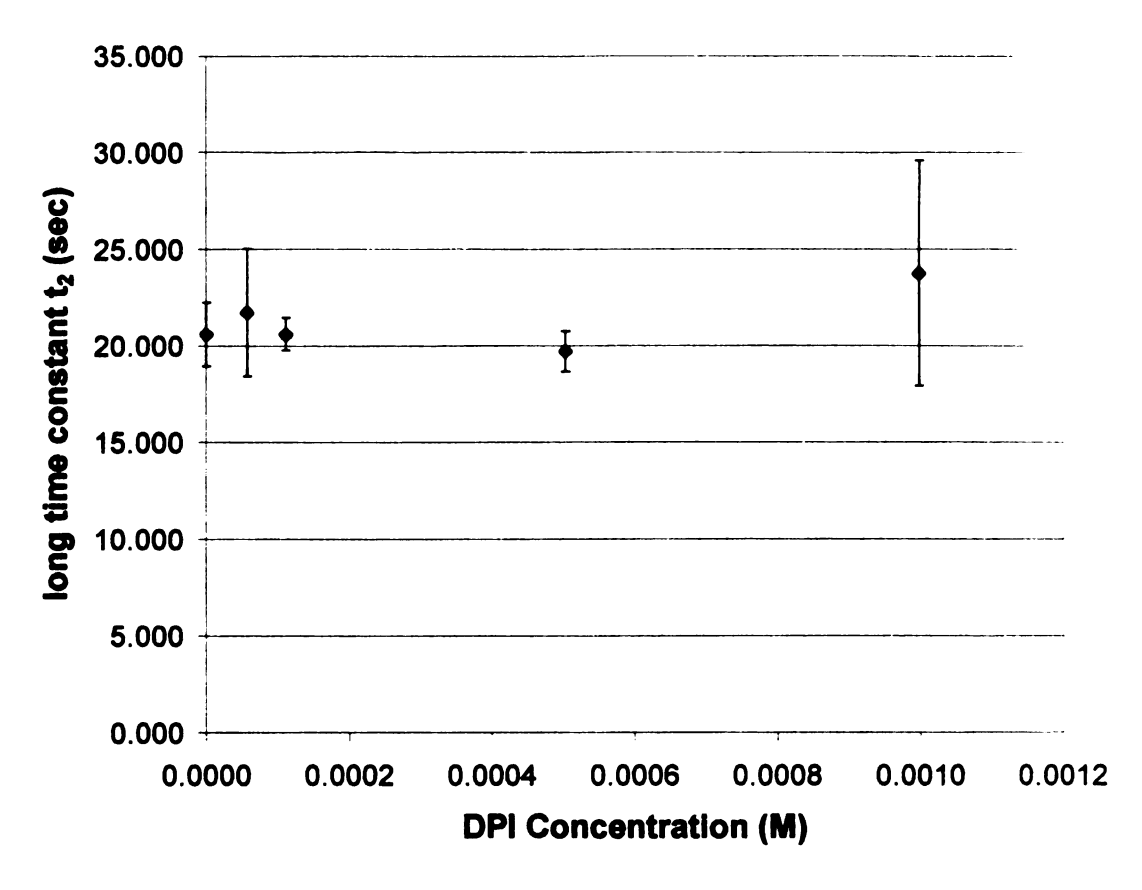


Figure 5.11: Long time constant (EYss/MDEA reaction) versus DPI concentration. The time constant for the EYss/MDEA reaction is not affected by the DPI concentration, indicating that iodonium-mediated dye regeneration does not occur in this system. [EYss] = 0.0001 M, [MDEA] = 0.012 M, all in HEMA, T = 25°C,  $I_a = 50$  mW/cm<sup>2</sup>. Long observation time. Error bars represent one standard deviation.

#### 5.3.2.3. Effect of Amine Concentration

Figure 5.12 shows the effect of varying the MDEA concentration on the fluorescence decay profiles of EYss. These data are difficult to interpret because at level of DPI present in the samples (0.0010 M), the appearance of the decay profiles is dominated by the EYss/DPI reaction. In fact, the behavior of the samples with the lowest concentrations of amine (0.00042 and 0.0010 M) is nearly identical to that of the zero amine sample (EYss/DPI alone), so only one of these three curves is shown in the figure.

Despite the significant impact of the DPI on the photobleaching behavior, the amine concentration does have some influence. At the highest concentration of amine shown in the figure (0.05 M), a curious shape in the decay profile is apparent. The rapid decay from the EYss/DPI reaction is evident, but then a very brief period of nearly stable fluorescence occurs before the slower decay characteristic of the EYss/MDEA reaction is evident. Furthermore, Figure 5.13 shows how increasing the concentration of MDEA appears to inhibit the EYss/DPI photobleaching reaction. Finally, it is worth noting that the concentration of DPI in these samples (0.001 M) is sufficient for nearly complete bleaching of the dye in the absence of amine (see Figure 5.4). In contrast, the data in Figure 5.12 show that at a constant DPI concentration, as the MDEA concentration is increased, a smaller amount of the EYss dye is consumed by the rapid dye/DPI reaction before the slow dye/MDEA reaction becomes evident. Since the time scales for the EYss/DPI and EYss/MDEA reactions are so different, the observations just described are interesting since changes in the slow MDEA reaction would not be expected to affect the fast DPI reaction.

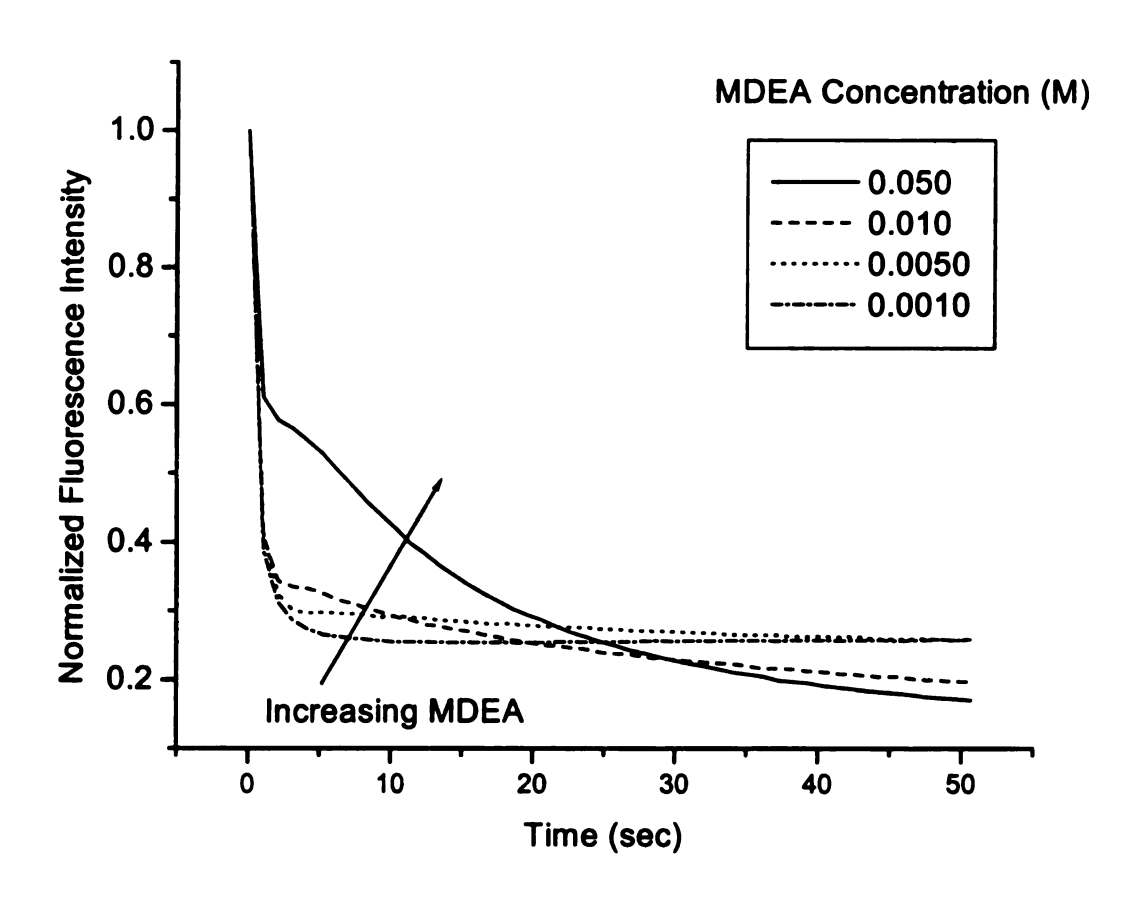


Figure 5.12: Effect of MDEA on Eosin Y, spirit soluble photobleaching. [EYss] = 0.0001 M, [DPI] = 0.0010 M, all in HEMA, T =  $25^{\circ}$ C,  $I_a = 50 \text{ mW/cm}^2$ . Each curve represents the average of three trials.

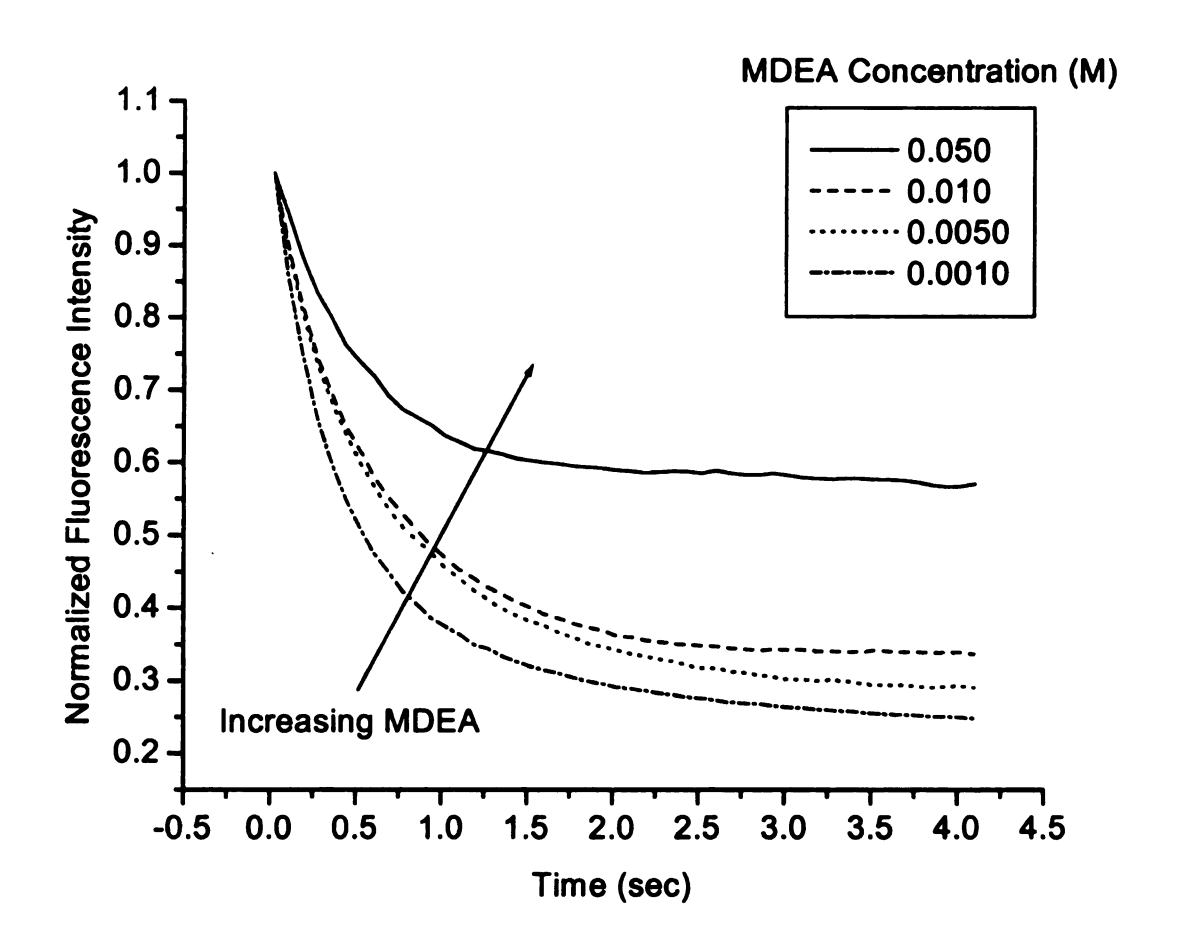


Figure 5.13: Effect of MDEA on photobleaching of Eosin Y, spirit soluble. Increasing MDEA concentration has a retarding effect on the rapid EYss/DPI reaction. [EYss] = 0.0001 M, [DPI] = 0.0010 M, all in HEMA, T = 25°C, I<sub>a</sub> = 50 mW/cm<sup>2</sup>. Short observation time. Each curve represents the average of three trials.

These observations suggest the occurrence of a secondary reaction between the oxidized dye and the amine. As outlined in Figure 5.14, we suggest that once the EYss is oxidized by the DPI, it may be reduced back to the original dye via reaction with amine. This reaction has a two-fold effect. First, it replenishes the eosin dye which may then undergo another direct reaction with DPI or MDEA, and second, it forms an active amine radical from a presumably less-active dye radical. In fact, such a reaction was proposed by He *et al.*<sup>8</sup> in a study of eosin bis(diphenyliodonium) salt and triethylamine. In that study, the eosin and DPI were counterions for each other, and as such were electrostatically linked.

The regeneration reaction also explains why, as illustrated in Figure 5.12, as the MDEA concentration is increased, the rapid EYss/DPI reaction phase consumes a smaller percentage of the eosin dye before the slow EYss/MDEA reaction takes over. During the EYss/DPI reaction, the MDEA is acting to regenerate the eosin dye. Therefore, a larger quantity of DPI must be consumed to bleach the same amount of eosin dye. The effect of MDEA on the short time scale bleaching of EYss is apparent from Figure 5.13. This set of curves clearly demonstrates how the short time scale bleaching of EYss (the DPI reaction) is slowed as the MDEA concentration is increased.

The curious shape of the decay curve noted at high concentrations of amine in Figure 5.12 (a brief period of stable fluorescence separating the obvious EYss/DPI and EYss/MDEA decay shapes) seems to imply that the dye regeneration reaction may not be as fast as the EYss/DPI photobleaching reaction. This phenomenon is even more apparent for the anionic Eosin Y dye, as will be discussed in the next section. (Note that this decay shape does not imply a pause between the exhaustion of the DPI and the

beginning of the EYss/MDEA reaction, but only that the EYss/MDEA reaction, which occurs throughout the illumination time, is camouflaged first by the rapid EYss/DPI reaction and then briefly by the slower regeneration reaction.)

Figure 5.14: Proposed amine-mediated dye regeneration scheme

#### 5.3.2.4. Behavior of Eosin Y salt

The behavior of Eosin Y is quite similar to that of Eosin Y, spirit soluble, but there are a few differences worth noting. First, as alluded to above, the slight lag time between the exhaustion of the DPI and the visible appearance of the characteristic dye/MDEA decay profile is exacerbated in the case of EY. In fact, as shown in Figure 5.15, at very high MDEA concentrations, the EY dye fluorescence actually rises for a short period of time before the EY/MDEA decay becomes obvious. This effect can be explained on the basis of differing reaction rates for the EY/DPI bleaching reaction and the MDEA-mediated regeneration reaction. For a short time after the EY fluorescence is mostly photobleached by reaction with DPI, the rate of dye regeneration is apparently slightly faster than the rate of consumption by reaction with MDEA. This difference in rates can account for the short rise in fluorescence intensity observed in the EY sample with the highest MDEA concentration as well as the short delay before continuation of EYss bleaching noted in Figure 5.12.

Another difference between EY and EYss, as was noted in section 5.3.1, is that the direct reaction between DPI and EY appears to be somewhat more efficient than that between DPI and EYss, since the rate of photocuring for the two-component EYss/DPI pair is significantly slower than that for the EY/DPI pair. This is most likely due to increased initiation efficiency of the radicals generated rather than a significant difference in the rate of the EY/DPI reaction, since the decay profiles for the EY/DPI and EYss/DPI pairs are essentially identical within experimental error, as shown in Figure 5.16. (The characteristic decay constants determined from the exponential fit are also equal within Furthermore, although Fouassier and Chesneau<sup>9</sup> report the experimental error.) formation of an eosin/diphenyliodonium complex under certain conditions, no spectroscopic evidence of a complex was observed in this system under experimental conditions. The visible absorption spectrum of EY was unchanged by the addition of DPI. 10 Therefore, while the DSC evidence suggests that the EY/DPI produces faster photocuring than EYss/DPI, it seems unlikely that this difference is due to ground-state pre-association of the negatively charged EY dye moiety and the positively charged DPI. Instead, it is likely that difference is due to an enhanced initiation efficiency of the radicals produced from the EY/DPI reaction as compared to the EYss/DPI pair.

The EY radical generated from reaction with DPI is apparently less readily regenerated by MDEA, since, as Figure 5.17 shows, the impact of the MDEA concentration on the short time scale bleaching of the EY with varying DPI concentration is less significant than for EYss. (Compare Figure 5.17 to Figure 5.13). This difference is probably attributable to the dye charge. After being oxidized by DPI, the charge on EY is reduced from -2 to -1. However, the charge on the EYss dye moiety changes from

neutral to +1. MDEA, being an amine, has a dipole moment due to the lone electron pair on the central nitrogen atom. This region of high electron density will experience a greater attraction to the positively charged EYss radical than the negatively charged EY radical. This is the most likely reason for the enhanced dye regeneration activity observed with EYss as compared to EY.

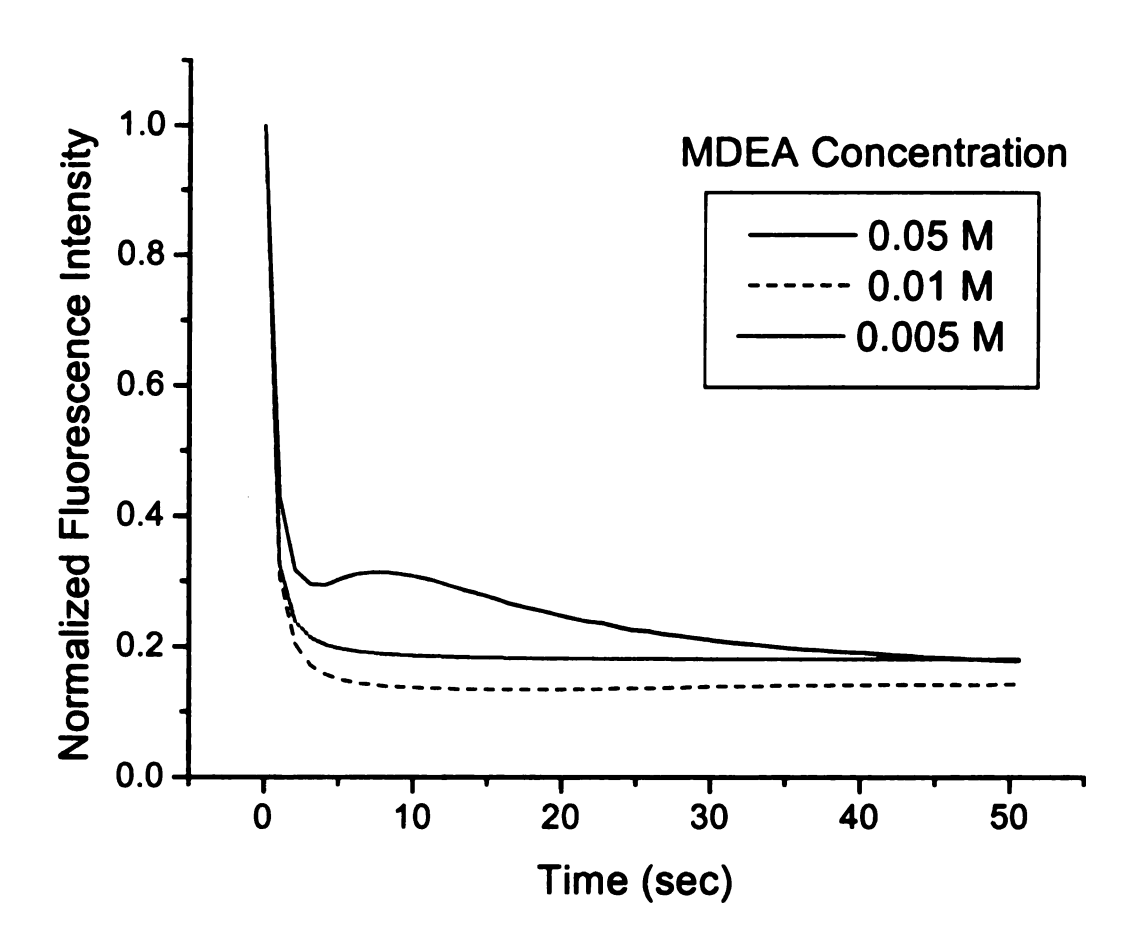


Figure 5.15: Effect of MDEA concentration on Eosin Y photobleaching. [EY] = 0.0001 M, [DPI] = 0.0013 M, all in HEMA, T =  $25^{\circ}\text{C}$ ,  $I_a = 50 \text{ mW/cm}^2$ . Each curve represents the average of three trials.

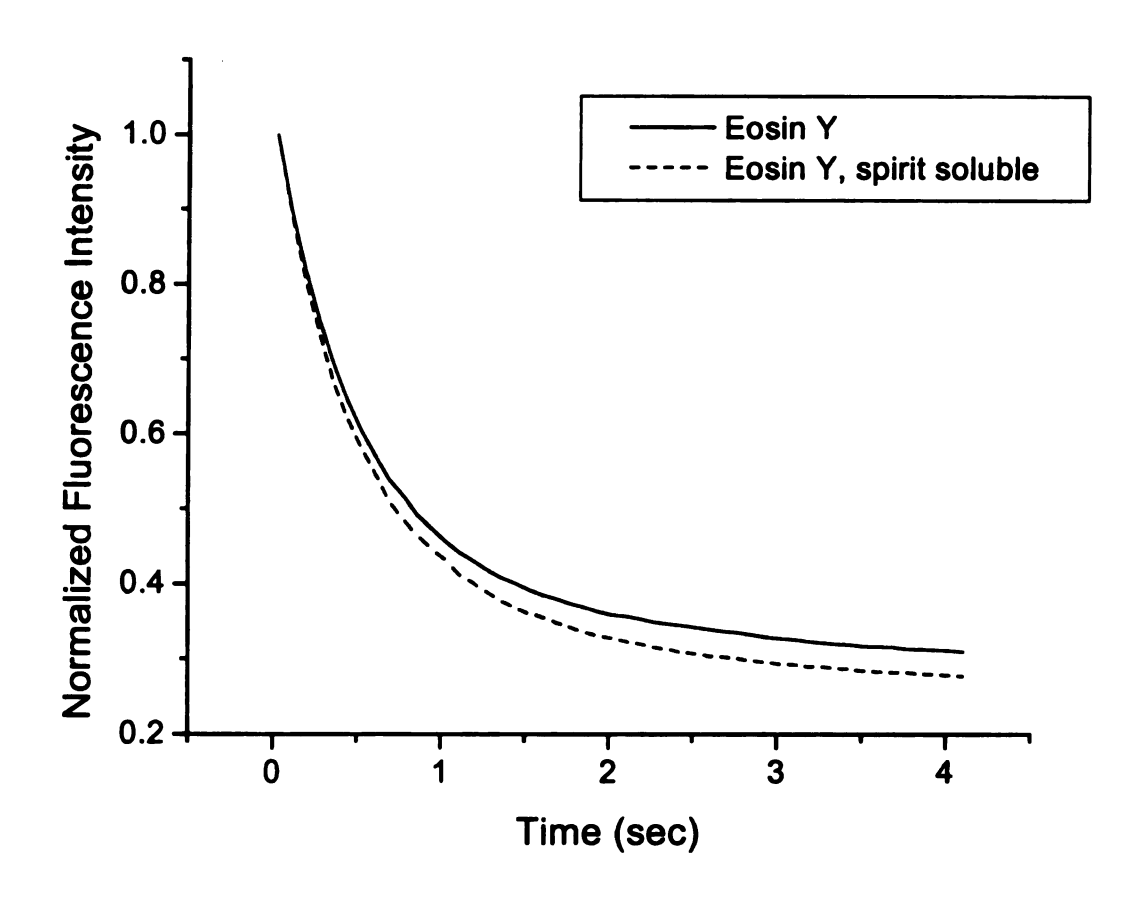


Figure 5.16: Comparison of Eosin Y and Eosin Y, spirit soluble photobleaching by DPI. [EY] = [EYss] = 0.0010 M, [DPI] = 0.001 M, all in HEMA,  $T = 25^{\circ}$ C,  $I_a = 50$  mW/cm<sup>2</sup>. No MDEA is present. Short observation time. Each curve represents the average of three trials

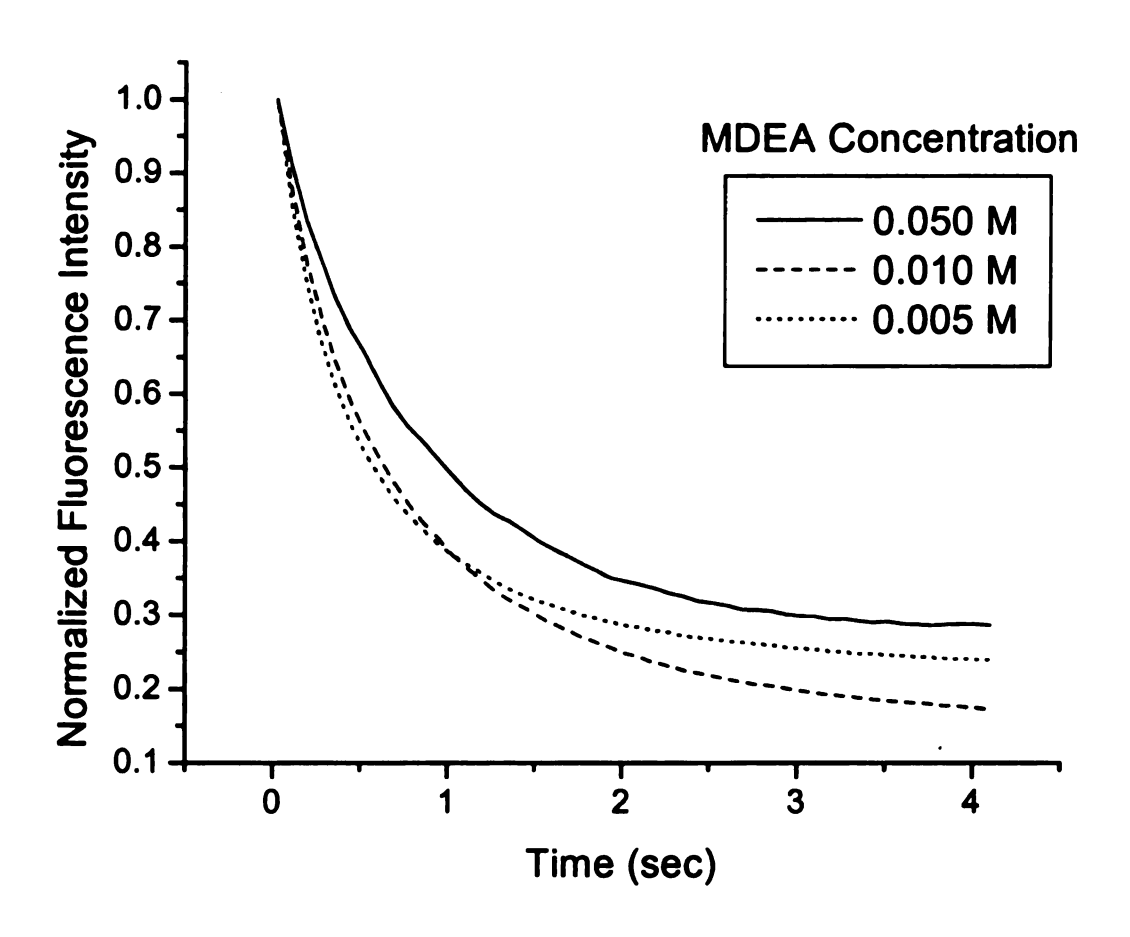


Figure 5.17: Effect of MDEA concentration on Eosin Y photobleaching. MDEA does not regenerate EY as efficiently as EYss. [EY] = 0.0001 M, [DPI] = 0.0013 M, all in HEMA, T = 25°C,  $I_a = 50 \text{ mW/cm}^2$ . Short observation time. Each curve represents the average of three trials

# 5.4. Summary and Conclusions

In this chapter, we have offered evidence for a proposed two-phase reaction mechanism for the consumption of eosin dyes in the three-component system eosin/MDEA/DPI. In this mechanism, the dye is rapidly oxidized by DPI, but for reasons which are not entirely clear, the reaction is not highly efficient at producing initiating radicals. The dye may also be reduced by MDEA in a somewhat slower electron transfer/proton transfer reaction which does, however, produce active initiating amine radicals. In a secondary reaction, another active radical can be produced if the reduced dye radical is further reduced to its leuco form by an additional molecule of amine. In the three-component system eosin/MDEA/DPI, a fourth reaction occurs: amine-mediated reduction of the bleached dye radical formed via reaction with DPI. This reaction apparently has a twofold effect: first, it regenerates the original eosin dye, and second, it produces an active amine radical in place of the presumably less active dye radical. The various reactions are summarized in Figure 5.18.

1) Eosin Y, spirit soluble 
$$\xrightarrow{hv}$$
 [EYss]\*

[EYss]\* + RH  $\longrightarrow$  [Exciplex]\*  $\longrightarrow$  EYss—H\* + R\*

EYss—H\* + EYss—H\*  $\longrightarrow$  EYss—H<sub>2</sub> + EYss

EYss—H\* + RH  $\longrightarrow$  EYss—H<sub>2</sub> + R\*

Figure 5.18: Summary of eosin reactions

### 5.5. References and Notes

- 1. Kathryn Sirovatka Padon and Alec B. Scranton, "Recent Advances in Three Component Photoinitiator Systems," in *Recent Research Developments in Polymer Science*, vol. 3, S. G. Pandalai (ed.), Transworld Research Network, Trivandrum, India, 369-385 (1999).
- 2. The primary contaminants in the commercial Eosin Y product are most likely fluorescein (the starting point for the commercial synthesis) and the free acid and lactone forms of Eosin. See F. J. Green, *The Sigma-Aldrich Handbook of Stains*, *Dyes, and Indicators*, Aldrich, Milwaukee, WI (1990).
- 3. J. K. Fouassier and S. K. Wu, "Visible Laser Lights in Photoinduced Polymerization. VI. Thioxanthones and Ketocoumarins as Photoinitiators," J. Appl. Polym. Sci., 44, 1779-1786, (1992).
- 4. H. J. Hageman, "Photoinitiators for Free Radical Polymerization," *Prog. Org. Coat.*, 13, 123-150 (1985).
- 5. H.-J. Timpe, S. Jockusch, and K. Körner, "Dye Sensitised Photopolymerisation," Radiation Curing Science and Technology, Vol, II: Photoinitiating Systems, J. P. Fouassier and J. F. Rabek (eds.), Elsevier, London, 575-601 (1993).
- 6. E. Chesneau and J. P. Fouassier, "Polymérisation Induite sous Irradiation Laser Visible. 2. Sensibilisation par les Colorants," *Angew. Makromol. Chem.*, 135, 41-64, (1985).
- 7. E. W. Nelson, T. P. Carter, and A. B. Scranton, "The Role of the Triplet State in the Photosensitization of Cationic Polymerizations by Anthracene," J. Polym. Sci., A: Polym. Chem., 33, 247-256 (1995).
- 8. J.-H. He, M.-Z. Li, J.-X. Wang, and E.-J. Wang, "Synergetic effects of amines on the intra-ion-pair electron transfer dye photosensitization system Eo(IPh<sub>2</sub>)<sub>2</sub>," J. Photochem. Photobiol. A: Chem., 89, 229-234 (1995).
- J. P. Fouassier and E. Chesneau, "Polymérisation induite sous irradiation laser visible.
   Le système éosine/amine/sel de iodonium," *Makromol. Chem.*, 192, 1307-1315, (1991).
- 1 O. Note that Fouassier and Chesneau used a singly-charged form of eosin. We did not observe spectroscopic evidence of complexation in the absorption spectra of either Eosin Y, spirit soluble, a neutral form, or Eosin Y, a doubly-charged form.

### **CHAPTER 6**

### CONCLUSIONS

This work has explored fundamental aspects of a few model three-component radical photoinitiation systems sensitive to visible light. Three-component systems typically consist of a dye that functions as the light-absorbing moiety, an electron donor such as an amine, and a third component that is most commonly an iodonium salt. The addition of an iodonium salt to the well-known bimolecular dye/amine system results in greatly enhanced sensitivity and cure speed. Three-component systems are also particularly attractive photoinitiators because of their flexibility. A wide range of dyes may be used in these systems, and by choosing a dye with the desired absorption characteristics, these systems may be "tuned" to any desired region of the ultraviolet or visible spectrum.

Although these systems have received limited fundamental study to date, research indicates that the iodonium salt functions as an electron acceptor, the amine is of course an electron donor, and the dye may either accept or donate an electron. This flexibility in the function of the dye makes a whole host of reactions possible in three-component initiation systems. In fact, the reactions that take place in three-component initiator systems seem to depend on the precise nature of the components chosen as well as the monomer and any solvent present.

### 6.1. Methylene Blue

The first system studied, methylene blue/N-methyldiethanolamine/diphenyliodonium chloride (MB/MDEA/DPI), is unique in that methylene blue is a cationic dye. Most fundamental research performed on these systems to date has involved anionic and neutral dyes. A cationic dye such as MB is of interest because the electrostatic repulsion between the dye and the iodonium cation precludes direct reaction between these two components. This choice of dye simplifies the list of possible reactions.

Differential scanning calorimetry and time-resolved steady-state fluorescence spectroscopy were used to deduce a mechanism for the MB/MDEA/DPI system. We concluded that the primary photochemical reaction was electron transfer from amine to dye, and that the role of the iodonium salt was to re-oxidize the neutral MB radical back to the original form of the dye, generating an active phenyl radical in the process. The addition of oxygen to this system complicates the mechanism, since oxygen is a triplet state quencher. The presence of oxygen limits the availability of excited triplet state MB for reactions and therefore slows consumption of the MB dye. However, in a closed system, the tertiary amine radicals produced from the MB/MDEA reaction can act to consume the oxygen in a cyclic mechanism. Only a few photonic events are required to produce enough tertiary amine radicals to consume a large quantity of oxygen molecules. Once the oxygen concentration is reduced, the MB/MDEA reaction can proceed more rapidly. The mechanism we propose is illustrated in Figure 6.1.

Figure 6.1: Proposed reaction mechanism for the three-component system MB/MDEA/DPI. The amine and phenyl radicals are active for initiation; the MB radicals is a terminator.

### 6.2. Eosin Dyes

The dyes Eosin Y and Eosin Y, spirit soluble (EY and EYss) were chosen as model anionic and neutral dyes with charges of -2 and 0, respectively. In contrast to the cationic methylene blue dye, the eosin dyes are able to react directly with both the amine and the iodonium components. In fact, the EY/DPI reaction might be expected to proceed more vigorously than the EYss/DPI reaction because of the possible electrostatic attraction between the negatively charged EY dye moiety and the positively charged iodonium cation. However, experimental results show that these two dyes function quite similarly in the three-component system eosin/MDEA/DPI, and no evidence of ground state pre-association of these two components was observed.

The reaction mechanism for three-component systems containing eosin dyes bears some similarity to the methylene blue mechanism. Electron transfer from amine to dye is still a feature of the mechanism. However, electron transfer from dye to iodonium salt is a prominent aspect of three-component systems containing eosin. In fact, the interaction of DPI with the eosin dyes bleaches the eosin fluorescence several times faster than does the eosin/MDEA interaction. In spite of this, photo-differential scanning calorimetry indicates that the eosin/DPI interaction does not produce active radicals as efficiently as does the eosin/MDEA interaction.

The eosin systems do not show evidence of the iodonium-mediated regeneration of amine-bleached dye observed in the methylene blue system. However, evidence was observed for the reverse mechanism: amine-mediated regeneration of iodonium-bleached dye. This reaction has two effects. First, generates an active amine radical in place of the

presumably less active dye-based radical. Second, it regenerates the eosin dye which can than participate in another direct reaction. The mechanism deduced for the eosin/MDEA/DPI system is given in Figure 6.2.

EYss  $^{+\bullet}$  + RH  $\longrightarrow$  EYss + R $^{\bullet}$  + H $^{+}$ 

Figure 6.2: Proposed mechanism for the three-component system EYss/MDEA/DPI.

### **CHAPTER 7**

### RECOMMENDATIONS FOR FUTURE WORK

While this work has answered some interesting fundamental questions about the initiation activity of three-component radical photoinitiators, it has also raised a number of questions. The following pages describe a number of possible areas for future work on three-component photoinitiator systems.

# 7.1. Identification of the Active Radical Species

Our mechanistic studies have identified the most likely reaction pathways and active radicals. A logical next step would be to test these hypotheses by attempting to positively identify the radicals. Several methods might be useful in this endeavor, as described below.

### 7.1.1. Electron Spin Resonance

Electron spin resonance, or ESR, is the most obvious means for attempting to identify radical species. This technique relies upon observations of the spin of electrons in as they orient themselves in a magnetic field. Determination of the structure of radical species is fairly straightforward with this technique, but it is not always applicable because it requires a high radical concentration and a significant radical lifetime. However, if a high concentration of the three initiator components was used in a non-reactive solvent, this technique could prove useful for identifying the various radicals

produced upon irradiation of a three-component system. In fact, Harada and collaborators used ESR to characterize the radical species produced by a three-component system in a 1991 publication.<sup>1</sup>

### 7.1.2. End Group Analysis

Another way to identify the active radicals produced in the three-component system is to identify the end groups on the polymer produced. Barring significant chain transfer activity, the initiating species will be found on at least one end of the polymer. (If termination is by combination, both end groups will be derived from the initiating species. If termination is by disproportionation, only one end group will be derived from the initiator.) Furthermore, if dye radicals function as terminators, as proposed in this work, end group analysis should reveal this as well.

### 7.1.2.1. Matrix-Assisted Laser Desorption Ionization Mass Spectrometry

Matrix assisted laser desorption/ionization time-of-flight mass spectroscopy, or MALDI, is an extremely powerful technique for structure elucidation. This technique, developed only about ten years ago, utilizes a matrix of small molecules to help carry large molecules such as polymers and biological molecules through the mass spectrometer. This so-called "soft" ionization technique is much less severe than traditional techniques, and generally allows the molecular ion to be desorbed intact.

MALDI TOF-MS is very attractive because it is highly sensitive and can provide a wealth of information about polymer structure. This technique has been used to characterize the molecular weight distribution in polymer samples<sup>2</sup> as well as for

identifying the polymer end groups.<sup>3</sup> Such studies could help clarify the mechanism operative in three-component systems by identifying the initiating radical as well as the termination mode.

The MALDI technique is not without problems. Since the method is relatively new, the selection of matrix (a critical choice) is often a trial-and-error process. In addition, although MALDI gives accurate molecular weights, molecular weight distributions determined by the technique are often skewed. Nonetheless, the technique is extremely powerful and could offer a great deal of information about three-component systems.

### 7.1.2.2. Nuclear Magnetic Resonance

Nuclear magnetic resonance (NMR) is a well-known technique for identifying the structures of organic compounds. It is based upon the spin of certain nuclei in a magnetic field. (The most common case is hydrogen NMR, since the hydrogen atom has two possible spin states.) The NMR spectrum of a molecule can be used to deduce its structure. This technique can be applied to polymers to identify the end groups. However, one disadvantage of this technique is that like ESR, a high concentration of analyte is required. For end group analysis to be successful, the requirement for high analyte concentration implies that the average polymer chain length must be short.

One method for obtaining short polymer chains is to conduct the polymerization with a very high concentration of initiator under "monomer starved" conditions. Another method which could prove extremely interesting is microemulsion polymerization. In a microemulsion, very tiny droplets of monomer are dispersed in a thermodynamically

stable emulsion. Since the monomer droplets are so tiny, each one can contain no more than one active radical. (The droplet is so tiny that if multiple radicals were present, they would terminate immediately.) For this reason, microemulsions produce polymer with a very narrow molecular weight distribution. Furthermore, if the droplets are sufficiently small, the polymer chain length can be quite short and thus amenable to end group analysis by NMR.

### 7.2. Luminescent Lifetime Studies

Luminescent lifetime studies can be used to determine the kinetic constants for reaction of the amine and iodonium components with the specific singlet and triplet states of the dye. This highly fundamental information is useful both for modeling of the initiation reaction as well as to determine the relative contributions of the dye singlet and triplet states to the initiation reaction.

A relatively simple method for studying the triplet lifetime is direct observation of the phosphorescence. A pulsed laser is used to excite the dye. After the triplet state is formed via intersystem crossing, it can relax in several ways, one of which is phosphorescence. Observation of this transient phosphorescence provides a way to measure the triplet state lifetime during a single experiment. Some molecules do not phosphoresce appreciably, and for these, transient absorption can be used to measure the lifetime. However, transient absorption is a very labor-intensive experiment requiring hundreds of thousands of laser shots and multiple experiments to determine a single lifetime, so phosphorescence measurements are preferred wherever possible.

Similarly, fluorescence lifetime measurements can be used to assess the interaction of the dye singlet state with the various components of the initiating system. Because fluorescence lifetimes are typically very short (on the order of nanoseconds), lifetime measurements require fast picosecond pulsed lasers and instrument response times. The typical method for obtaining such fast response times is time-correlated single photon counting. In this method, the time interval between arrival of the laser pulse at the sample and emission of the first fluorescent photon is measured. Many repetitions of this experiment can be completed in seconds, and a histogram which represents the fluorescence decay is generated very rapidly from a single sample.

### 7.3. Kinetic studies

In this work photo-differential scanning calorimetry has been used to study the photopolymerizations. A disadvantage to the use of DSC is its relatively slow response time (a few seconds). An alternate method for characterizing the propagation reaction is Raman spectroscopy. By observing a characteristic band of the monomer that is destroyed upon polymerization, the reaction rate and conversion can be monitored throughout the reaction. For instance, for acrylate systems, the C=C bond stretch of vinyl acrylate monomers that appears around 1640 cm<sup>-1</sup> can be used to monitor polymerization without use of an internal reference for normalization.<sup>4,5</sup> Since the same initiation laser can be used for Raman spectroscopy as in the laser fluorescence bleaching experiments described in chapters 3-5, this method is particularly attractive because it is easy to compare the polymerization rate data to the photobleaching data.

# 7.4. Biological Applications of Three-Component Systems

One of the most exciting aspects of visible-light photoinitiation is its potential for use *in situ* in biological systems which would be damaged by ultraviolet initiation or traditional thermal initiation. However, biocompatible initiation systems are vital for this application. In addition, nontoxic initiation systems would be useful for photocurable coatings and packaging with direct food contact. Nontoxic, biocompatible light-absorbing moieties for three-component initiators are readily available. Methylene blue, as discussed in Chapter 3, is one example. Riboflavin-induced polymerization has also been demonstrated. Camphorquinone is already used in photocurable dental composites.

Amine toxicity is a potential issue in three-component initiator systems. Many aliphatic amines common in three-component systems, such as triethylamine, are highly toxic. N-methyldiethanolamine, which was used in this work, is lower in toxicity. N-phenyl glycine is particularly interesting, since its toxicity is significantly lower than that of aliphatic amines and it is an amino acid derivative. Another approach to the amine toxicity issue is to use light absorbing moieties which contain their own reducing group. Methylene blue and riboflavin are two examples of this class of molecules.

Diphenyliodonium salts are viewed by some as an environmental problem because of their potential to produce benzene, a known carcinogen. Several possible solutions to this problem exist. One is to replace the iodonium salt altogether through use of an alternative third component such as a bromo compound.<sup>8-10</sup>. Another possibility is to use substituted aryliodonium salts rather than phenyliodonium salts. In addition, the

aryliodonium component could be replaced with a non-aryl compound such as an alkyl iodonium salt.

#### 7.5. New Directions

### 7.5.1. Cationic photoinitiation

Although this work has focused on the use of three-component systems as radical photoinitiators, with very few modifications, three-component systems have also been shown to be useful for cationic photoinitiation. 11-13 Essentially, two modifications are needed. First, a non-nucleophilic counterion for the iodonium salt such as hexafluoroantimonate is generally required. (Oxman and Jacobs report that simple iodonium salts such as chlorides are acceptable, but also report that diaryliodonium hexafluorophosphate and diaryliodonium hexafluoroantimonate are preferred. 13) The second modification to the three-component system generally described in this work is to the electron donor (amine) component. Bi and Neckers report that basic amines such as the trialkylamines common in three-component radical photoinitiators will terminate the cationic chains and must be replaced with less-basic aromatic amines that possess alpha hydrogens. 11,12

Three-component photoinitiation systems for cationic photopolymerization are even newer than the radical systems discussed in this work, and future work to address the initiation mechanism of these system would be extremely useful and interesting.

# 7.5.2. Combination of two dyes plus amine

In 1965, Chen reported that the rate of polymerization initiated by a dye/electron donor system could be enhanced by combining anionic and cationic dyes (she used cationic methylene blue and anionic eosin dyes).<sup>14</sup> This different sort of three-component system has not been well studied, and addition of a fourth component (an iodonium salt) could also prove a fruitful area for study.

### 7.6. References

- 1. M. Harada, Y. Takimoto, N. Noma, and Y. Shirota, "Mechanism of photoinitiation of a three component system containing thioxanthene dye," *J. Photopolym. Sci. Tech.*, 4, 51-54 (1991).
- 2. H. S. Creel, "Prospects for the Analysis of High Molar Mass Polymers Using MALDI Mass Spectrometry," *Trends in Polymer Science*, 1, 336-342 (1993).
- 3. G. Montaudo, M. S. Montaudo, C. Puglisi, and F. Samperi, "Characterization of end groups in Nylon 6 by MALDI-TOF Mass Spectrometry," J. Polym. Sci, A: Polym. Chem., 34, 439-447 (1996).
- 4. J. Clarkson, S. M. Mason, and K. P. J. Williams, "Bulk radical homopolymerization studies of commercial acrylate monomers using near infrared Fourier transform Raman Spectroscopy," *Spectrochemica Acta*, 47A, 1345-1351, (1991).
- 5. E. Gulari, K. McKeigue, and K. Y. S. Ng, "Raman and FTIR Spectroscopy of Polymerization" Bulk Polymerization of Methyl Methacrylate and Styrene," *Macromolecules*, 17, 1822-1825, (1984).
- 6. G. K. Oster, G. Oster, and G. Prati, "Dye-sensitized photopolymerization of acrylamide," J. Am. Chem. Soc., 79, 595-598 (1957).
- 7. Z. Kucybala et al. "Kinetic studies of a new photoinitiator hybrid systems based on camphorquinone-N-phenylglycine derivatives for laser polymerization of dental restorative and stereolithographic (3D) formulations," *Polymer*, 37, 4585-4591, (1996).
- 8. A. Erddalane, J. P. Fouassier, F. Morlet-Savary and Y. Takimoto "Efficiency and Excited State Processes in a Three-Component System, Based on Thioxanthene Derived Dye/Amine/Additive, Usable in Photopolymer Plates," J. Polymer Sci., A: Polym. Chem., 34, 633-642 (1996).
- 9. J. P. Fouassier, A. Erddalane, F. Morlet-Savary, I. Sumiyoshi, M. Harada, and M. Kawabata "Photoinitiation Processes of Radical Polymerization in the Presence of a Three-Component System based on Ketone-Amine-Bromo Compound," *Macromolecules*, 27, 3349-3356 (1994).
- 10. M. Harada, M. Kawabata, and Y. Takimoto, "Photoinitiation systems containing bromo compounds," J. Photopolym. Sci. Tech., 2, 199-204, (1989).

- 11. Y. Bi and D.C. Neckers, "A visible light initiating system for free radical promoted cationic polymerization," *Macromolecules*, 27, 3683-3693 (1994).
- 12. Y. Bi and D.C. Neckers, "Photopolymerization of cyclohexene oxide a visible light initiating system and mechanistic investigations," Proc. RadTech, Orlando, Florida, 180-186 (1994).
- 13. J. D. Oxman, D. W. Jacobs, "Ternary Photoinitiator System for Curing of Epoxy/Polyol Resin Compositions," U.S. Patent 5,998,495 (1999).
- 14. C. S. Hsia Chen, "Dye Sensitized Photopolymerization. II. Enhanced Sensitization by Combination of a Cationic and an Anionic Dye," J. Polym. Sci. A, 3, 1127-1136 (1965).

**APPENDIX** 

## A.1. Concentration Effects of Methylene blue

#### A.1.1. Dimerization

At high concentrations, methylene blue can dimerize. In water, the single or monomeric form of methylene blue absorbs around 665 nm, whereas the dimer absorbs around 610 nm. Figure A.1 is a plot of the extinction coefficients for the methylene blue monomer and dimer in 2-hydroxyethylmethacrylate at concentrations ranging from 4 × 10<sup>-6</sup> M to 6 × 10<sup>-5</sup> M. As shown on the plot, the data were linearly extrapolated to higher concentrations. While extrapolated data should be interpreted with great care, it is reasonable to conclude from the data that at the concentrations used in Chapters 3 and 4, (0.0001 M) the methylene blue dye was present primarily in its monomeric form.

### A.1.2. Polymerization inhibitor

Prior work has shown that the methylene blue dimer is a terminator or chain transfer agent.<sup>1,2</sup> In fact, methylene blue been used as a polymerization inhibitor at concentrations ranging from 0.1 to 10%.<sup>1</sup> For this reason, at high methylene blue concentrations at which the dimer is the dominant form of the dye, slow rates of photopolymerization (or no reaction at all ) would be expected. For example, Figure A.2 gives the polymerization exotherm for a sample with amine and iodonium concentrations similar to those used in Chapter 3, but with a concentration of methylene blue ten times higher. The polymerization is a great deal slower in this scenario. (Compare Figure A.2 to Figure 3.4). At a methylene blue concentration of 0.0001 M, the polymerization reaches its peak rate in only about 10 minutes. However, under very similar experimental

conditions with a methylene blue concentration of 0.001 M, the polymerization does not reach its peak rate until 40 minutes of illumination.

### A.1.3. Photobleaching

High concentrations of methylene blue also have an effect on the photobleaching behavior of methylene blue, as shown in Figure A.3. (Compare this figure to Figure 4.5 in Chapter 4). Two features of Figure A.3 are readily apparent. First, an extremely high light intensity is required to bleach the methylene blue dye. Second, the samples containing amine show a very marked increase in fluorescence intensity before the fluorescence level begins to decline. The increase in fluorescence intensity is probably attributable to quenching of the singlet-state methylene blue dye by amine molecules. In a study of thionine (a dye that is structurally very similar to methylene blue), Neumann and Rodrigues<sup>3</sup> suggest that when an amine molecule interacts with the thionine singlet state, the dye is deactivated to its ground state and photo-production of radicals does not occur. This radiationless deactivation of the singlet state also implies that the amine interaction will reduce the fluorescence emitted by the sample. At the extremely high concentrations of methylene blue used in Figure A.3, singlet dye molecules would be expected to be abundant and more likely to encounter amine molecules within their short lifetimes. Therefore, it is reasonable to suspect that as amine is consumed by reaction with triplet methylene blue, less amine would be available to quench the triplet state, resulting in increased methylene blue fluorescence. Thus, consumption of the amine tends to increase the fluorescence intensity, while consumption of the dye tends to decrease fluorescence. These two competing phenomenon exactly balance each other at

the peak of the fluorescence level observed at about twelve seconds in Figure A.1. After that time, the fluorescence level is observed to decrease as the consumption of the methylene blue dye by reaction becomes the most important phenomenon.

The importance of the amine concentration in this singlet state quenching mechanism is demonstrated in Figure A.4. In the figure, the amine concentration is varied from 0 to 0.005 M while the methylene blue and diphenyliodonium chloride concentrations are held constant at 0.001 M each. Notice that the relative height of the fluorescence peak decreases noticeably with amine concentration.

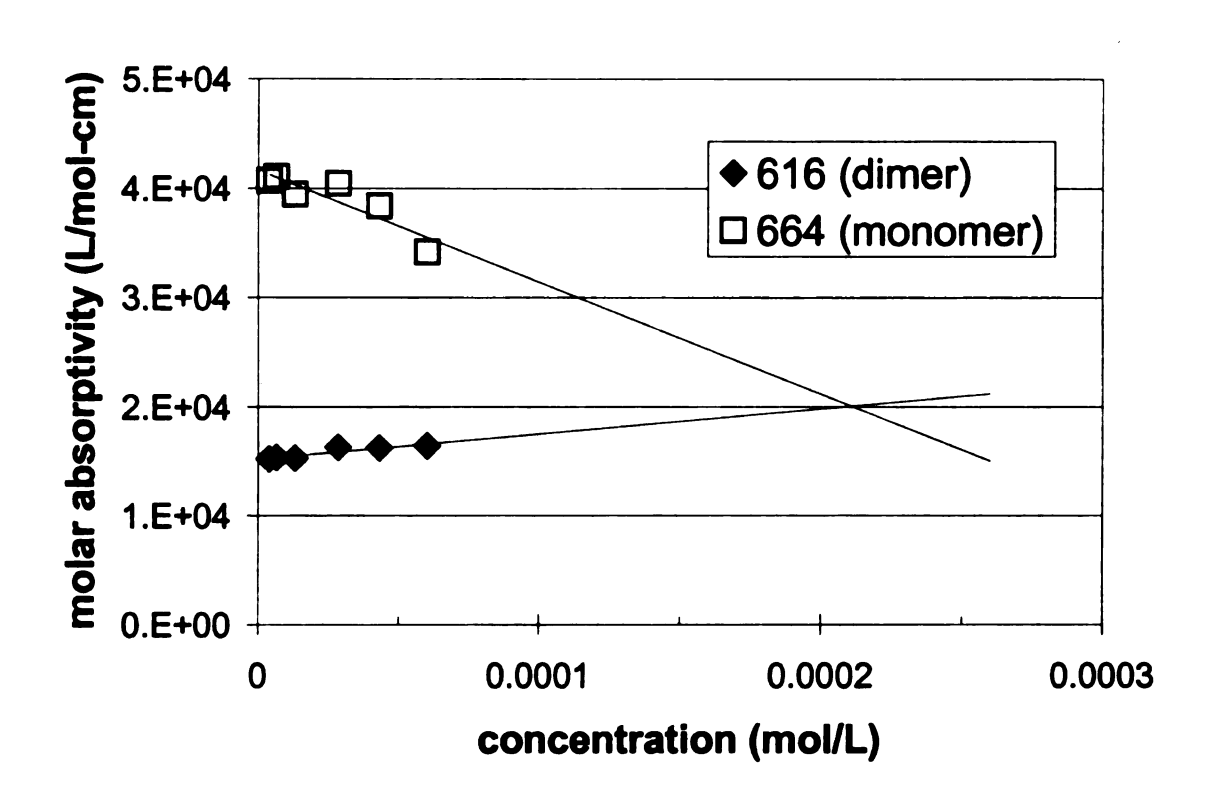


Figure A.1: Molar absorptivity of methylene blue monomer and dimer peaks as a function of concentration.

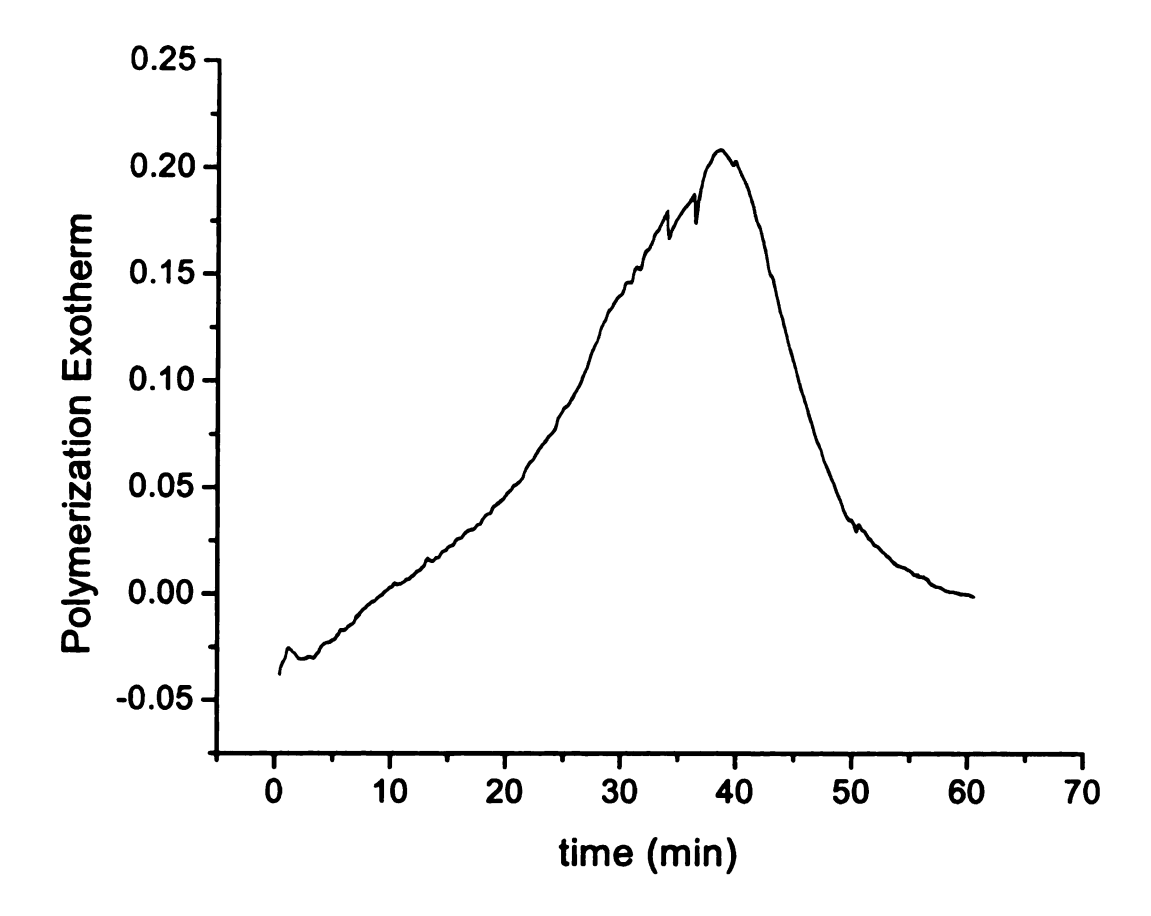


Figure A.2: Polymerization exotherm for sample with high methylene blue concentration. [MB] = 0.0010 M, [MDEA] = 0.0018 M, [DPI] = 0.0010 M. T = 35 °C.

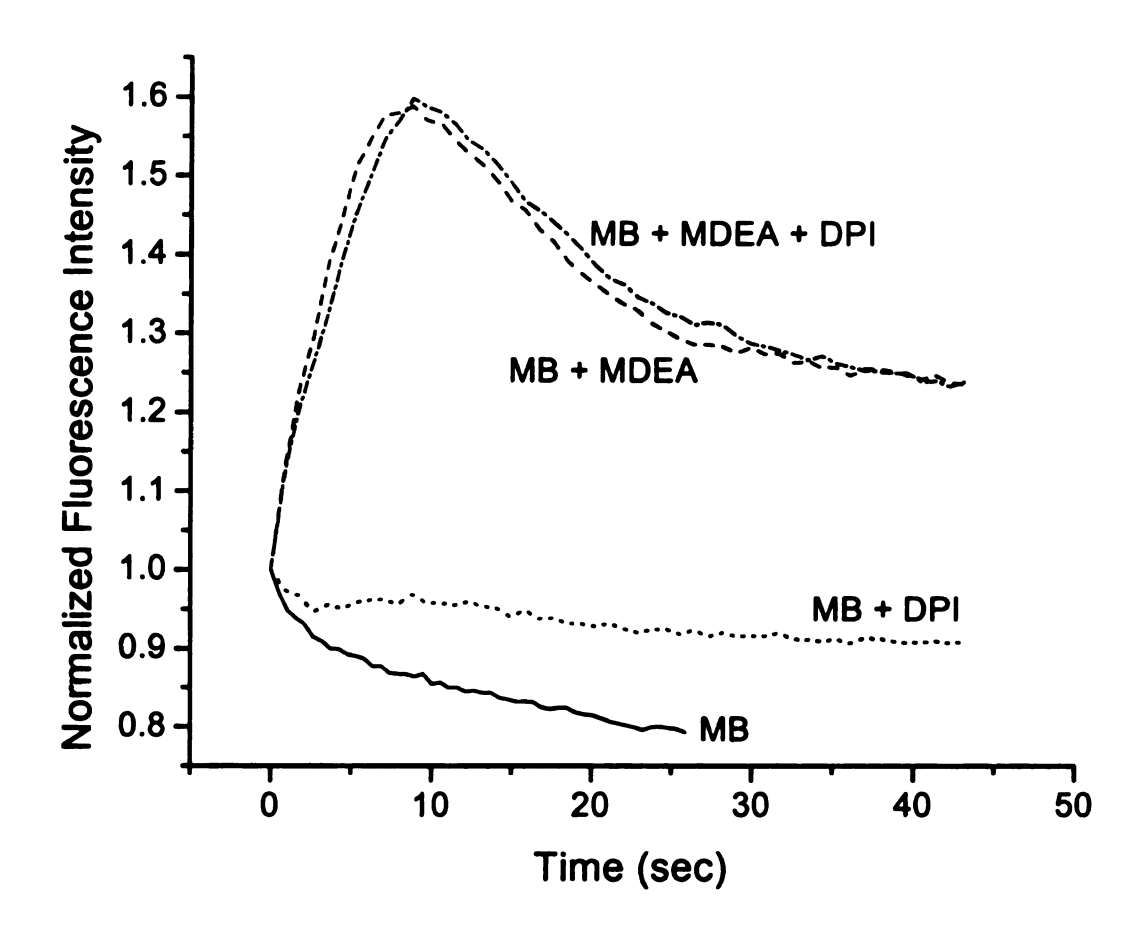


Figure A.3: Photobleaching of methylene blue at high dye concentration. [MB] = 0.001 M, [MDEA] = 0.0018 M, [DPI] = 0.001 M,  $I_a = \sim 5.3$  W/cm<sup>2</sup>, T= 25 °C, capillary geometry as described in Chapter 4.

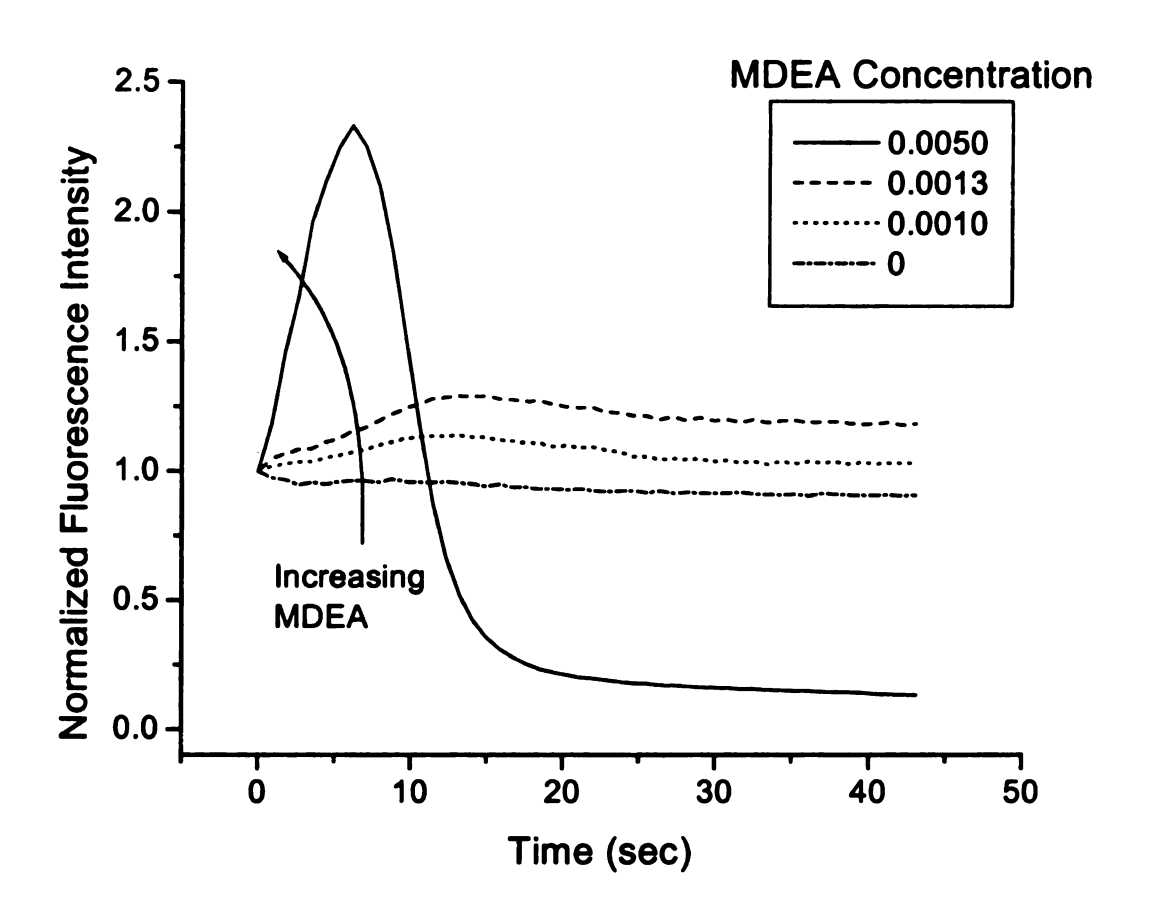


Figure A.4: Effect of amine concentration on pre-bleaching fluorescence peak. [MB] = 0.001 M, [DPI] = 0.001 M,  $I_a = \sim 5.3$  W/cm<sup>2</sup>, T= 25 °C, capillary geometry as described in Chapter 4.

# A.2. Ground State Complexes

#### A.2.1. Literature

Several authors have suggested the participation of a ground state complex in the reaction mechanism for two-component systems; such a complex could affect the corresponding three-component mechanism. For example, in a study of a two component system containing diphenyliodonium chloride and triethylamine, authors He and Wang observed the formation of a charge-transfer complex between these two molecules with an absorption peak centered around 500 nm.<sup>4</sup> They report that illumination of this charge transfer peak was effective for initiating polymerization of methyl methacrylate. However, the complex requires polar solvents (they used CH<sub>3</sub>CN and water in a 14:1 ratio by volume) to promote its formation. Since the studies reported in this dissertation were all carried out in neat 2-hydroxyethylmethacrylate and/or ethylene glycol dimethacrylate, formation of an iodonium-amine complex was not expected.

Based on a kinetic analysis carried out in aqueous solutions of acrylamide, Feng et al. suggest the participation of a methylene blue-triethanolamine complex in the two-component dye-amine reaction.<sup>2</sup> The authors do not report any special conditions required for formation of this complex. Finally, Fouassier and Chesneau report the formation of an eosin/diphenyliodonium complex under certain conditions, but they also report that this complex is destroyed in the presence of amine.<sup>5</sup>

### A.2.2. Looking for Complexes

Because the formation of complexes often causes changes in the electronic structure of the molecules involved, complex formation can often be detected from changes in the ultraviolet-visible absorption spectra. For this reason, ultraviolet-visible absorption spectroscopy was used to look for evidence of complexation in the system methylene blue/N-methyldiethanolamine/diphenyliodonium chloride. The experimental protocol was as follows: Solutions of each component were prepared in methanol. For each pair of components, a reference scan was carried out using two cuvettes sandwiched together, each containing one of the components. The samples were then mixed and placed in a 20 cm pathlength cuvette for scanning. In this way, any signal observed in the sample can be attributed to the effect of mixing the two components. However, for each of the three pairs of components (dye/amine, dye/onium, and onium/amine), no absorption due to complexation was observed. For this reason, we concluded that component complexes did not play a significant role in the three-component system methylene blue/N-methyldiethanolamine/diphenyliodonium chloride. In addition, as mentioned in Chapter 5, no spectroscopic evidence of complexes was observed in the system eosin/N-methyldiethanolamine/diphenyliodonium chloride.

# A.3. Three-Component Systems Containing Camphorquinone

#### A.3.1. Motivation

Camphorquinone, shown in Figure A.5, is a neutral light-absorbing molecule that has found some use in three-component systems and also has well-known applications in

photocurable dental composites.<sup>6-11</sup> For this reason, we chose to apply the tools developed in this work to the system camphorquinone/N-methyldiethanol-amine/diphenyliodonium chloride.

Camphorquinone is unique among visible light photoinitiators because it does not have a strong absorption profile in the visible spectrum, as shown in Figure A.6. However, its absorption spectrum overlaps well with the output of the Hg-Xe lamp used in the photo-DSC experiments. Furthermore, the low extinction coefficient in the visible region is preferred for some thick-cure applications because the light will not be strongly attenuated by the camphorquinone absorption and thus can pass through the a thick sample.

Figure A.5: Camphorquinone

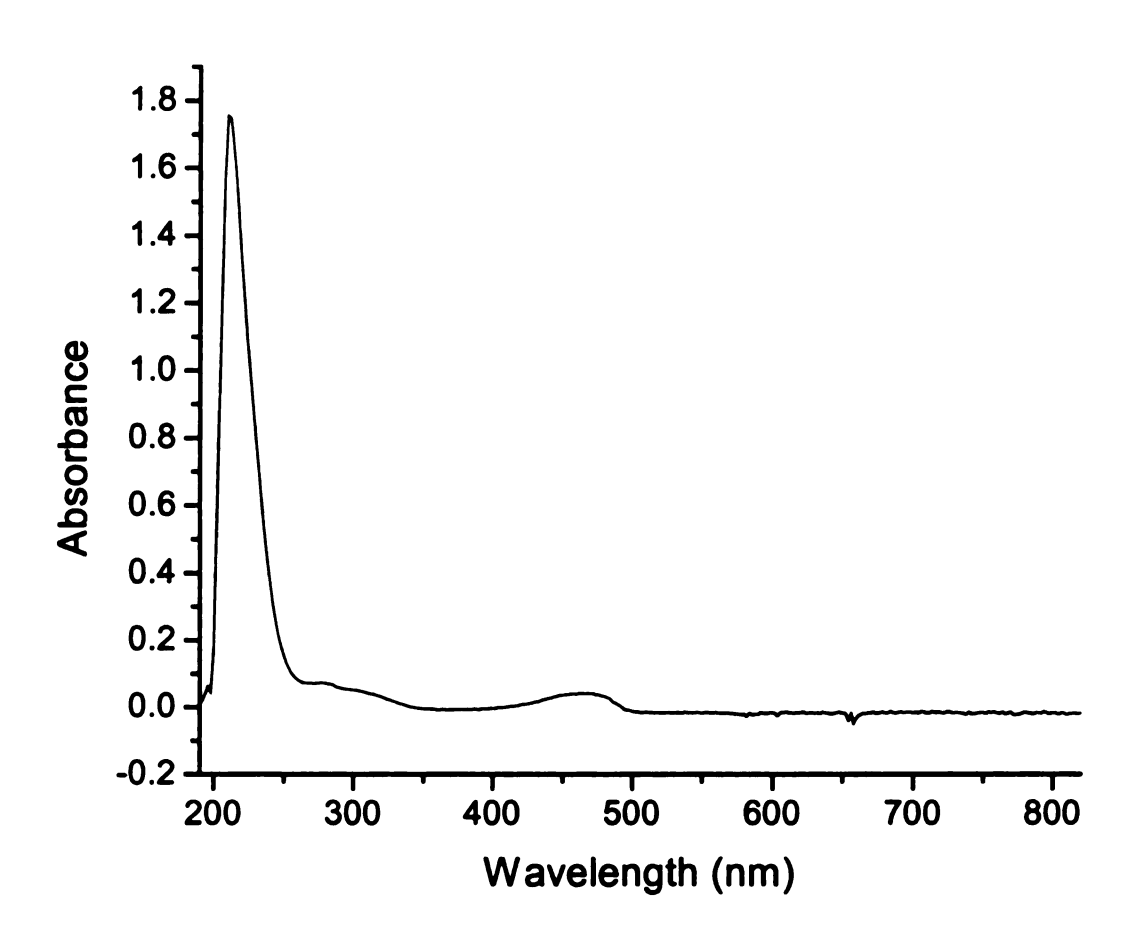


Figure A.6: Absorbance spectrum for camphorquinone. 0.051 wt.% in methanol.

#### A.3.2. DSC results

The polymerization exotherms for photopolymerization with camphorquinone are shown in Figure A.7. The results are quite similar to those seen for methylene blue and eosin: the fastest polymerization occurs when all three components are present, the next-fastest with dye and amine, and the slowest with dye and iodonium salt.

### A.3.3. Photobleaching

Unfortunately, the photobleaching results with camphorquinone were not very useful. It appears that camphorquinone, upon reaction, does not undergo significant photobleaching. Sample results are given in Figure A.8. Camphorquinone itself does not have a very intense fluorescence emission. This results in a very noisy, weak fluorescence profile, as illustrated in the figure. Furthermore, unlike eosin and methylene blue, camphorquinone not an aromatic molecule. Based on its structure, it seems unlikely that electron-transfer reaction with either amine or iodonium salt would disturb the camphorquinone structure enough to cause photobleaching.

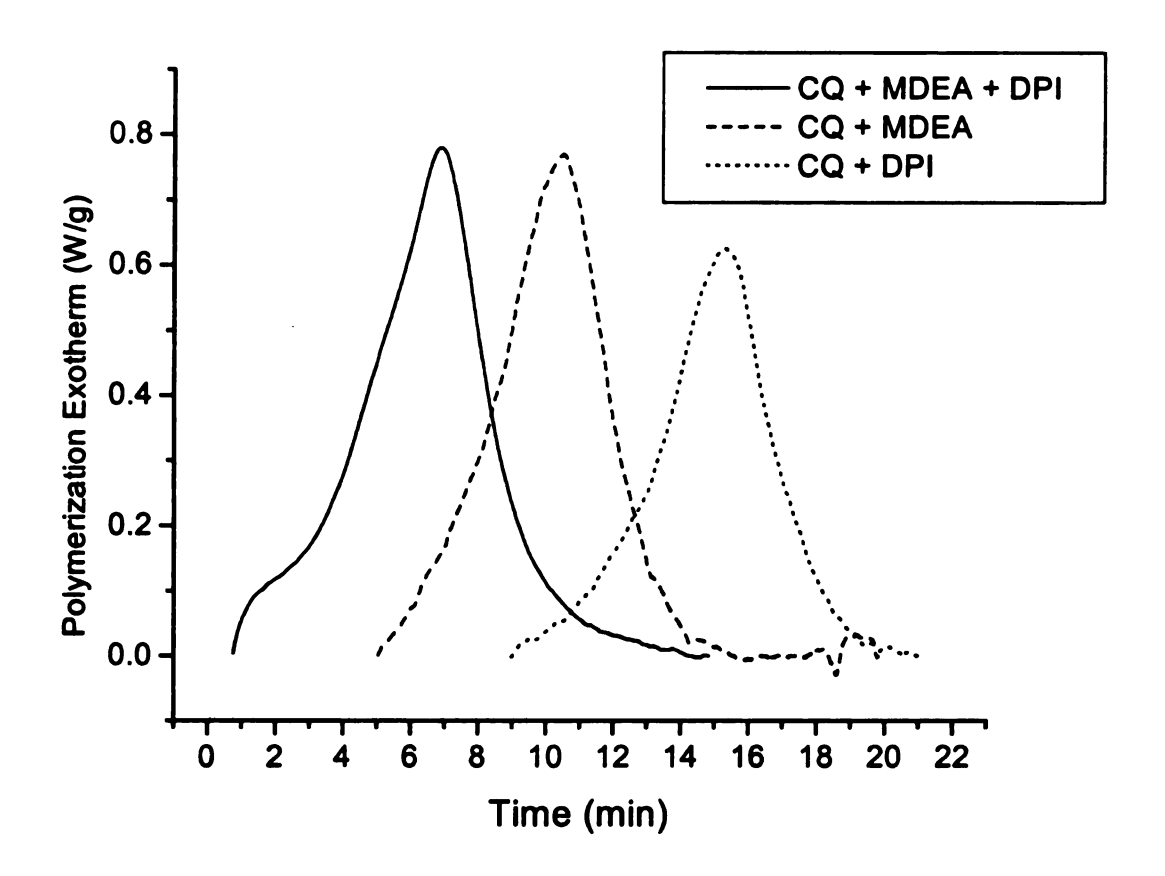


Figure A.7: Polymerization exotherm for camphorquinone/N-methyldiethanol-amine/diphenyliodonium chloride system. [CQ] = 0.0012 M, [MDEA] = 0.013 M, [DPI] = 0.001 M, T = 50 °C,  $I_a \sim 27$  mW/cm<sup>2</sup>.

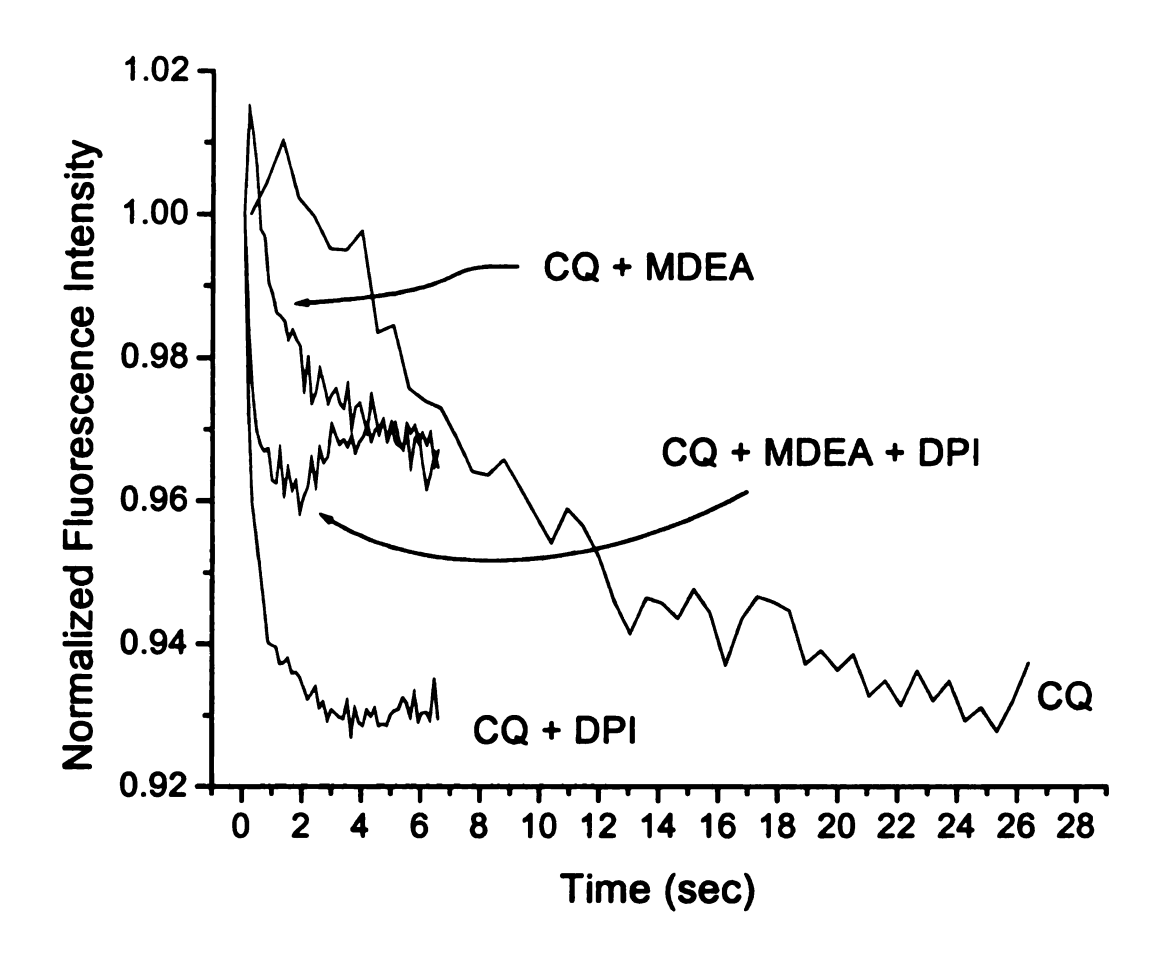


Figure A.8: Camphorquinone fluorescence bleaching. [CQ] = 0.0012 M, [MDEA] = 0.013 M, [DPI] = 0.001 M, T = 25 °C,  $I_a \sim 800 \text{ mW/cm}^2$ .

#### A.4. References

- 1. C. S. Hsia Chen, "Dye-Sensitized Photopolymerization. I. Polymerization of Acrylamide in Aqueous Solution Sensitized by Methylene Blue-Triethanolamine System," J. Polym. Sci. A, 3, 1101-1125 (1965).
- 2. M. Feng, Z. Liang, and Y. Chen, "The photopolymerization kinetics of photosensitized acrylamide system induced by He-Ne laser," *Chin. J. Polym. Sci.*, 9, 24-30 (1991).
- 3. M. G. Neumann and M. R. Rodrigues, "The mechanism of the photoinitiation of the polymerization of MMA by the thionine-triethanolamine system," *Polymer*, 39, 1657-1661 (1998).
- 4. J. He and E. Wang, "Radical Photopolymerization Using Aryliodonium Salt/ Tertiary Amine Complex System as the Photoinitiator," *Chin. J. Polym. Sci.*, **8**, 36-43 (1990).
- J. P. Fouassier and E. Chesneau, "Polymérisation induite sous irradiation laser visible.
   Le système éosine/amine/sel de iodonium," *Makromol. Chem.*, 192, 1307-1315, (1991).
- 6. J. D. Oxman, A. Ubel III, and E. G. Larson, "Coated Abrasive Binder Containing Ternary Photoinitiator System," U.S. Patent 4,735,632 (1988).
- 7. J. P. Fouassier, A. Erddalane, F. Morlet-Savary, I. Sumiyoshi, M. Harada, and M. Kawabata, "Photoinitiation Processes of Radical Polymerization in the Presence of a Three-Component system based on Ketone-Amine-Bromo Compound," *Macromolecules* 27, 3349-3356 (1994).
- 8. J. P. Fouassier, D. Ruhlmann, Y. Takimoto, M. Harada, and M. Kawabata, "New Three-Component Initiation Systems in UV Curing: A Time-Resolved Laser-Spectroscopy Investigation," J. Polymer Sci. A: Polym. Chem. 31, 2245-2248 (1993).
- 9. M. Harada, M. Kawabata, and Y. Takimoto, "Photoinitiation Systems Containing Bromo Compounds," J. Photopolym. Sci. Tech., 2, 199-204 (1989).
- 10. M. Kawabata, M. Harada, and Y. Takimoto, "Photopolymerizable composition highly sensitive to visible light," US Patent 4,868,092 (1989).
- 11. T. Nakahara, K. Kusumoto, and S. Yuasa, "Photochemical polymerization catalysts for dental materials," JP 62, 22,804 (1987).

